

**Preparation of Polymer Nanoparticles by Ring Opening Metathesis  
Polymerization in Aqueous Dispersed Systems with Water-Soluble  
Ruthenium-based Catalyst**

by

Chunyang Zhu

A thesis submitted to the Department of Chemical Engineering  
in conformity with the requirements for  
the Degree of Doctor of Philosophy

Queen's University  
Kingston, Ontario, Canada  
September, 2016

Copyright ©Chunyang Zhu, 2016

## Abstract

Ring opening metathesis polymerization (ROMP) is a variant of olefin metathesis used to polymerize strained cyclic olefins. Ruthenium-based Grubbs' catalysts are widely used in ROMP to produce industrially important products. While highly efficient in organic solvents such as dichloromethane and toluene, these hydrophobic catalysts are not typically applied in aqueous systems. With the advancements in emulsion and miniemulsion polymerization, it is promising to conduct ROMP in an aqueous dispersed phase to generate well-defined latex nanoparticles while improving heat transfer and reducing the use of volatile organic solvents (VOCs). Herein I report the efforts made using a PEGylated ruthenium alkylidene as the catalyst to initiate ROMP in an oil-in-water miniemulsion.  $^1\text{H}$  NMR revealed that the synthesized PEGylated catalyst was stable and reactive in water. Using 1,5-cyclooctadiene (COD) as monomer, we showed the highly efficient catalyst yielded colloiddally stable polymer latexes with  $\sim 100\%$  conversion at room temperature. Kinetic studies demonstrated first-order kinetics with good livingness as confirmed by the shift of gel permeation chromatography (GPC) traces. Depending on the surfactants used, the particle sizes ranged from 100 to 300 nm with monomodal distributions. The more strained cyclic olefin norbornene (NB) could also be efficiently polymerized with a PEGylated ruthenium alkylidene in miniemulsion to full conversion and with minimal coagulum formation.

## Co-Authorship

The bulk of the research was carried out independently by myself, under the supervision of Prof. Michael F. Cunningham. Guidance was also provided by Prof. Cathleen M. Crudden for catalysis and experimental design. The preparation and editing of this thesis was conducted under the supervision of Prof. Michael F. Cunningham.

Chapter 4 has been prepared for submission and will be co-authored by Michael F. Cunningham, Cathleen M. Crudden, Xiaowei Wu, and Matt T. Zamora. Xiaowei Wu provided the metathesis catalyst used in this project. Matt T. Zamora provided advice on experimental design. I performed all the laboratory experiments. Guidance was provided by Prof. Cunningham and Prof. Crudden.

Chapter 5 is being prepared for submission and will be co-authored by Michael F. Cunningham, Cathleen M. Crudden, and Xiaowei Wu. Xiaowei Wu provided the metathesis catalyst used in this project. I performed the laboratory experiments. Guidance was provided by Prof. Cunningham and Prof. Crudden.

## **Acknowledgements**

I would like to thank my supervisor Prof. Michael Cunningham for his kind guidance and support in working towards my PhD degree at Queen's University. I would also like to thank Prof. Cathleen Crudden who has played formative roles in my development as a researcher. They are remarkable people from whom I have learned a lot.

I have had the privilege of working with an amazing group of talented researchers at Queen's. Each member of the Cunningham group, Hutchinson group and Crudden group has had an impact on me and my work. I am particularly grateful to Sean George, Dawn Free, Xin Su, Omar Garcia, Joaquin Arredondo, Kevin Payne, Ali Darabi, Matt Zamora, Olena Zenkina, Thomas Rooney, and Jan Schier, who have been like older brothers or sisters to me, offering advice and sharing their experiences.

I would like to thank my parents Dr. Enhou Zhu and Yongying Xu for their devotion, patience, understanding and encouragement when I am studying abroad. I would like to thank all my friends for their help during my study.

Last but not least, I would like to thank myself because I made myself a better man.

## **Statement of Originality**

I hereby certify that all of the work described within this thesis is the original work of the author.

Any published (or unpublished) ideas and/or techniques from the work of others are fully acknowledged in accordance with the standard referencing practices.

Chunyang Zhu

September 2016

## Table of Contents

Abstract.....	ii
Co-Authorship.....	iii
Acknowledgements.....	iv
Statement of Originality.....	v
List of Schemes.....	ix
List of Figures.....	x
List of Tables.....	xii
List of Abbreviations.....	xiii
Chapter 1 Introduction.....	1
1.1 Overview.....	1
1.2 Research Objectives.....	2
1.3 Research significance and original contributions.....	2
1.4 References.....	3
Chapter 2 Literature review.....	5
2.1 Olefin metathesis.....	5
2.2 Metathesis catalysts.....	6
2.3 Solvent effect in olefin metathesis.....	7
2.4 Metathesis catalysts in aqueous phase.....	9
2.5 Ring Opening Metathesis Polymerization.....	12
2.6 ROMP monomers.....	15
2.7 Applications of ROMP.....	15
2.8 Polymerization in dispersed systems.....	16
2.9 Emulsion polymerization.....	17
2.10 Miniemulsion polymerization.....	21
2.11 Polymer latexes and nanoparticles.....	24
2.11.1 Particle Size and Particle Size Distribution.....	24
2.12 Conclusion.....	26
2.13 References.....	27
Chapter 3 Ring opening metathesis polymerization in homogeneous systems.....	32
3.1 Ring opening metathesis polymerization in DCM.....	33
3.2 Kinetic study of ring opening metathesis polymerization in solution.....	33
3.2.1 Controlled character.....	34

3.2.2 Number average molecular weight ( $M_n$ ) and molecular weight distribution (MWD)..	35
3.3 ROMP in unconventional solvents .....	36
3.4 ROMP of 1,5-cyclooctadine (COD) in <i>N,N</i> -Dicyclohexylmethylamine (DCHMA) .....	37
3.5 Experimental Procedures for ROMP in SHS.....	38
3.6 Catalyst reactivity and reaction kinetics .....	39
3.7 Molecular weight and molecular weight distribution .....	41
3.8 Removal and recycling of SHS.....	43
3.9 Conclusion .....	45
3.10 References.....	46
3.11 Supporting Information.....	49
Chapter 4 Ring opening metathesis polymerization in miniemulsion using PEGylated ruthenium- based metathesis catalyst .....	54
4.1 Preface.....	54
4.2 Abstract.....	54
4.3 Introduction.....	54
4.4 Experimental section.....	56
4.4.1 Materials .....	56
4.4.2 Characterization .....	57
4.4.3 Synthesis of PEGylated Ru-based metathesis catalyst .....	57
4.4.4 The influence of air and moisture on catalytic performance of complex 3 .....	58
4.4.5 ROMP of 1,5-cyclooctadiene (COD) and norbornene (NB) in miniemulsion .....	59
4.5 Results and discussion .....	59
4.5.1 Catalyst design.....	59
4.5.2 Monomer miniemulsion.....	62
4.5.3 Miniemulsion polymerization.....	64
4.5.4 Kinetic study .....	65
4.5.5 Molecular weight .....	66
4.5.6 Catalyst loading and solid content .....	69
4.5.7 Surfactants.....	70
4.6 Conclusion .....	70
4.7 Acknowledgements.....	71
4.8 References.....	71
4.9 Supporting Information.....	76

Chapter 5 Ring opening metathesis polymerization of norbornene in miniemulsion using PEGylated ruthenium-based metathesis catalyst .....	89
5.1 Preface.....	89
5.2 Abstract.....	89
5.3 Introduction.....	90
5.4 Experimental section.....	91
5.4.1 Materials .....	91
5.4.2 Characterization .....	92
5.4.3 ROMP of norbornene (NB) in miniemulsion .....	92
5.5 Results and discussion .....	93
5.5.1 Monomer miniemulsion.....	93
5.5.2 Miniemulsion polymerization.....	95
5.5.3 Kinetic study .....	97
5.5.4 Molecular weight .....	98
5.5.5 Particle size distribution.....	100
5.5.6 Effect of surfactants .....	101
5.6 Conclusion .....	102
5.7 Acknowledgements.....	102
5.8 References.....	103
5.9 Supporting Information.....	106
Chapter 6 Conclusions and Recommendations for Future Work .....	112
6.1 Conclusions.....	112
6.2 Recommendations for future work .....	113
6.3 References.....	115
Appendix A Preparation of monomer miniemulsion.....	116
Appendix B Experimental results for ROMP with the new catalyst.....	118



## List of Schemes

Scheme 2.1 Proposed early stage mechanism of metathesis. ....	6
Scheme 2.2 Mechanism of olefin metathesis proposed by Chauvin. ....	6
Scheme 2.3 Grubbs catalysts: first generation (G1), second generation (G2), and third generation (G3). ....	7
Scheme 2.4 Early water-soluble ruthenium catalysts developed by Grubbs and co-workers. ....	10
Scheme 2.5 Examples of hydrophilic metathesis catalysts for aqueous olefin metathesis. ....	11
Scheme 2.6 pH-responsive catalysts. ....	12
Scheme 2.7 Different types of olefin metathesis reactions. ....	12
Scheme 2.8 Mechanism of ring opening metathesis polymerization. ....	13
Scheme 3.1 (a) Mechanism of ROMP; (b) The formation of a ruthenium-amine complex; (c) The catalyst (2 <sup>nd</sup> generation Grubbs' catalyst) and SHS ( <i>N,N</i> -dicyclohexylmethylamine) employed in this study. ....	38
Scheme 3.2 Protonation and deprotonation of <i>N,N</i> -dicyclohexylmethylamine (DCHMA). ....	43
Scheme 4.1 Synthesis of PEGylated Ru-based metathesis catalyst. ....	60
Scheme 4.2 Procedure for ROMP in miniemulsion with air-free conditions. ....	64
Scheme 5.1 Procedure for ROMP in miniemulsion with air-free conditions. ....	97

## List of Figures

Figure 2.1 Intervals in emulsion polymerization. ....	18
Figure 2.2 Micellar, homogeneous and droplet nucleation in free radical emulsion polymerization. .....	20
Figure 2.3 Preparation of monomer miniemulsion: (a) a general procedure, (b) homogenization by sonication. ....	22
Figure 3.1 Conversion ( $x$ ) and $\ln[1/(1-x)]$ plots for ROMP of 1,5-cyclooctadiene (COD) using PEGylated Grubbs Catalyst as catalyst. ....	34
Figure 3.2 Molecular weight distribution (MWD), molecular weight ( $M_n$ ) and dispersity profiles for ROMP of COD. ....	35
Figure 3.3 Conversion ( $x$ ) and $-\ln(1-x)$ plots for ROMP of 1,5-cyclooctadiene (COD) in DCHMA. .....	40
Figure 3.4 $M_n$ vs conversion profile for entry 1 (left) and entry 2 (right). The dot lines indicate the theoretical values of molecular weights. ....	42
Figure 3.5 Evolution of normalized SEC traces for entry 1 .....	42
Figure 3.6 Removal and recycling of SHS by biphasic extraction. ....	45
Figure 4.1 Conversion vs time plots for ROMP in different solvents with 0.1 wt % PEGylated catalyst (complex 3). ....	61
Figure 4.2 Conversion vs time curves for COD ROMP in different solvents with 0.2 wt % PEGylated catalyst. ....	62
Figure 4.3 Droplet size (●) vs time and PDI (▲) vs time for monomer miniemulsion. ....	63
Figure 4.4 Size distribution by intensity for polymer latex obtained from ROMP of 1,5- cyclooctadiene in miniemulsion. ....	65
Figure 4.5 Conversion ( $x$ ) and $\ln[1/(1-x)]$ plots for ROMP of 1,5-cyclooctadiene (COD) in miniemulsion catalyzed by complex 3. ....	66
Figure 4.6 Number average molecular weight ( $M_n$ ) and dispersity ( $\mathcal{D}$ ) plots for ROMP of 1,5- cyclooctadiene (COD) in miniemulsion using complex 3 as catalyst. ....	67
Figure 4.7 The evolution of GPC traces (normalized height) with conversion for ROMP of 1,5- cyclooctadiene (COD) in miniemulsion using complex 3 as catalyst. ....	67
Figure 5.1 Droplet size (●) vs time and PDI (▲) vs time for NB monomer miniemulsion. ....	94
Figure 5.2 Conversion ( $x$ ) and $\ln[1/(1-x)]$ plots for ROMP of norbornene (NB) in miniemulsion using PEGylated metathesis catalyst. ....	97

Figure 5.3 Number average molecular weight ( $M_n$ ) and dispersity ( $\mathcal{D}$ ) plots for ROMP of norbornene (NB) in miniemulsion using PEGylated water-soluble metathesis catalyst. ....	99
Figure 5.4 The evolution of GPC traces (normalized height) with conversion for ROMP of NB in miniemulsion using PEGylated water-soluble catalyst.....	100
Figure 5.5 Size distribution by intensity for polymer latex obtained from ROMP of norbornene (NB) in miniemulsion (Exp 1). Z-average parameter: 107 nm, PDI: 0.092. ....	101
Figure 6.1 Functional cyclic olefins for ROMP.....	114

## List of Tables

Table 2.1 Solvent selection for olefin metathesis. ....	8
Table 2.2 Comparison among emulsion, miniemulsion, and microemulsion polymerization. ....	17
Table 3.1 Experimental conditions of ROMP of COD in DCHMA at 25 °C initiated by 2 <sup>nd</sup> generation Grubbs' catalyst .....	40
Table 4.1 Experimental conditions and results for ROMP in miniemulsion .....	69
Table 5.1 Experimental conditions and results for ROMP of NB in miniemulsion .....	95
Table 5.2 Molecular weight and particle size data for each experiment in this study. ....	96

## List of Abbreviations

CLRP	Controlled/living radical polymerization
CMC	Critical micelle concentration
COD	1,5-Cyclooctadiene
CTAB	Cetyl trimethylammonium bromide
CTAC	Cetyl trimethylammonium chloride
DCHMA	<i>N,N</i> -dicyclohexylmethylamine
DLS	Dynamic light scattering
EVE	Ethyl vinyl ether
FRP	Free radical polymerization
G1	Grubbs' catalyst, 1st generation
G2	Grubbs' catalyst, 2nd generation
G3	Grubbs' catalyst, 3rd generation
HD	Hexadecane
Mo	Molybdenum
NB	Norbornene
NHC	<i>N</i> -heterocyclic carbene
NMR	Nuclear magnetic resonance
PB	Polybutadiene
PCy <sub>3</sub>	Tricyclohexylphosphine
PEG	Polyethylene glycol
PNB	Polynorbornene
ROMP	Ring-opening metathesis polymerization
Ru	Ruthenium
SDS	Sodium dodecyl sulfate
SEC	Size exclusion chromatography
SHS	Switchable hydrophilicity solvent
THF	Tetrahydrofuran
Ti	Titanium
VOC	Volatile organic compound
W	Tungsten

# Chapter 1

## Introduction

Ring opening metathesis polymerization (ROMP) is recognized as a versatile strategy to synthesize polymers with well-defined chain lengths, architectures and functionalities. ROMP shares some common features (e.g. good livingness, narrow molecular weight distributions) with reversible-deactivation radical polymerizations (RDRP) including atom transfer radical polymerization (ATRP),<sup>1</sup> nitroxide mediated polymerization (NMP),<sup>2</sup> reversible addition-fragmentation chain transfer (RAFT)<sup>3</sup> and catalytic chain transfer (CCT).<sup>4</sup> But the mechanism of ROMP is quite distinct from radical polymerizations, and transition metal-based catalysts are normally introduced to catalyze the chain propagation. The wide use of volatile organic compounds (VOCs) in ROMP has remained as a common practice to minimize the solvent effect on catalysis.<sup>5</sup> As an alternative approach, this work aims to introduce ROMP into a dispersed system using water as the continuous phase to prepare well-defined polymer latexes.

### 1.1 Overview

The main challenges of implementing metathesis chemistry in dispersed systems consist of several aspects. Firstly, most of the existing metathesis catalysts are not compatible with emulsion or miniemulsion polymerization. It has been a long time since Ru-based or W-based catalysts were first introduced in ROMP; but they cannot be readily dissolved in water because of the hydrophobic groups attached to the transition metal. The first half of Chapter 2 provides a brief overview of olefin metathesis with an emphasis on the mechanism and catalyst development. Secondly, the rational design of polymerization processes in dispersed phase is sophisticated. Depending on the different nucleation mechanisms used in the polymerization, the chain initiation process could occur in micelles, the water phase or monomer droplets. The second half of Chapter 2 presents a historic background of dispersed-phase polymerizations with a discussion of various dispersed systems and nucleation mechanisms.

The study of ROMP was initiated via conducting polymerizations in a homogeneous phase, as described in Chapter 3. The purpose of running homogeneous polymerization is to eliminate the effect of water and surfactant, so that the performance of a metathesis catalyst can be more scientifically evaluated. Using the customized water-soluble metathesis catalyst, Chapter 4 is dedicated to applying the miniemulsion technique to ROMP to make polybutadiene (PB) nanoparticles from 1,5-cyclooctadiene (COD). Chapter 5 demonstrates the feasibility of the miniemulsion technique by using norbornene (NB) to prepare well-defined polynorbornene (PNB) latex particles. A summary of this PhD thesis and some recommendations for future work are listed in Chapter 6.

## **1.2 Research Objectives**

- To propose an appropriate structure and synthetic route for metathesis catalysts customized for dispersed-phase ROMP.
- To design and formulate a dispersed-phase polymerization process for ROMP.
- To characterize and assess the quality of polymer nanoparticles in terms of monomer conversion, molecular weight and particle size.
- To establish general strategies to control the key properties (molecular weight and particle size) of polymer nanoparticles.

## **1.3 Research significance and original contributions**

This work represents the first comprehensive exploration in combining transition-metal mediated ROMP and dispersed-phase polymerizations. The significance of this work lies in the potential to extend our results to a large scale manufacturing of ROMP polymers with lower environmental impact. Some major achievements are listed below.

- Identified a synthetic strategy of using a water-soluble catalyst that can be efficiently dispersed in a continuous phase at the beginning of polymerization and then migrates to the particles once polymerization commences. The catalyst exhibited high tolerance towards water.
- Ring opening metathesis polymerization (ROMP) of 1,5-cyclooctadiene (COD) in miniemulsion was conducted utilizing a water-soluble ruthenium alkylidene as catalyst. The highly efficient catalyst yielded stable polymer latexes with nearly 100% conversion in 1 hour and minimal coagulation was observed.
- Kinetic studies were conducted for both homogeneous and heterogeneous polymerizations. The studies revealed similar first-order kinetics to bulk ROMP with an excellent livingness as confirmed by the shift of gel permeation chromatograph (GPC) traces.
- A well-established strategy to make stable polymer latexes with monomodal distributions was formulated. Depending on the surfactants used (ionic and non-ionic surfactants), the particle sizes were found to range from 100 to 300 nm.
- Low catalyst loading (0.1 mol% to monomer) and a higher solid content (20 wt% to water) latexes were tested to assess the system suitability for potential industrial implementation.
- Norbornene (NB), a more strained cyclic olefin, could also be efficiently polymerized by the water-soluble catalyst in miniemulsion with full conversion in the absence of coagulum.

## 1.4 References

- (1) Matyjaszewski, K. Atom Transfer Radical Polymerization (ATRP): Current Status and Future Perspectives. *Macromolecules* **2012**, *45* (10), 4015–4039.
- (2) Georges, M. K.; Veregin, R. P. N.; Kazmaier, P. M.; Hamer, G. K. Narrow Molecular Weight Resins by a Free-Radical Polymerization Process. *Macromolecules* **1993**, *26* (11), 2987–2988.
- (3) Chiefari, J.; Chong, Y. K. B.; Ercole, F.; Krstina, J.; Jeffery, J.; Le, T. P. T.; Mayadunne, R. T. A.; Meijs, G. F.; Moad, C. L.; Moad, G.; Rizzardo, E.; Thang, S. H. Living Free-Radical



Polymerization by Reversible Addition–Fragmentation Chain Transfer: The RAFT Process.

*Macromolecules* **1998**, *31* (16), 5559–5562.

- (4) Gridnev, A. A.; Ittel, S. D. Catalytic Chain Transfer in Free-Radical Polymerizations. *Chem. Rev.* **2001**, *101* (12), 3611–3660.
- (5) Demel, S.; Schoefberger, W.; Slugovc, C.; Stelzer, F. Benchmarking of Ruthenium Initiators for the ROMP of a Norbornenedicarboxylic Acid Ester. *J. Mol. Catal. A Chem.* **2003**, *200* (1-2), 11–19.

## Chapter 2

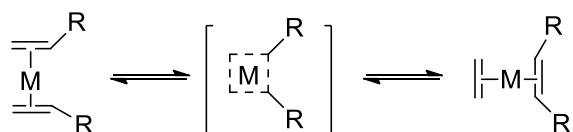
### Literature review

The last decades have seen a remarkable progress in olefin metathesis with a deep understanding of the metathesis mechanism and rapid advancement of metathesis catalysts. There have been tremendous articles and reviews in olefin metathesis; and the majority of them have been focused on the development of metathesis catalysts.<sup>1-4</sup> Ring opening metathesis polymerization (ROMP) is a variant of olefin metathesis in which the cyclic olefins can be polymerized into unsaturated polymers. The typical reaction steps of a polymerization still apply for ROMP such as initiation, propagation, and termination. However, in ROMP the monomer is “inserted” into the propagating chains via coordination by the transition-metal center, which is distinct from free radical polymerizations. The first half of this chapter provides the fundamentals of ROMP as well as some related topics such as catalysts, solvents, and monomers used in ROMP.

Dispersed-phase polymerizations are the proposed strategies to prepare ROMP polymer nanoparticles. The second half of this chapter provides the fundamentals of dispersed-phase polymerization that were originally developed from free radical polymerization. Both the mechanism and applications of dispersed-phase polymerizations like emulsion and miniemulsion polymerization are briefly reviewed.

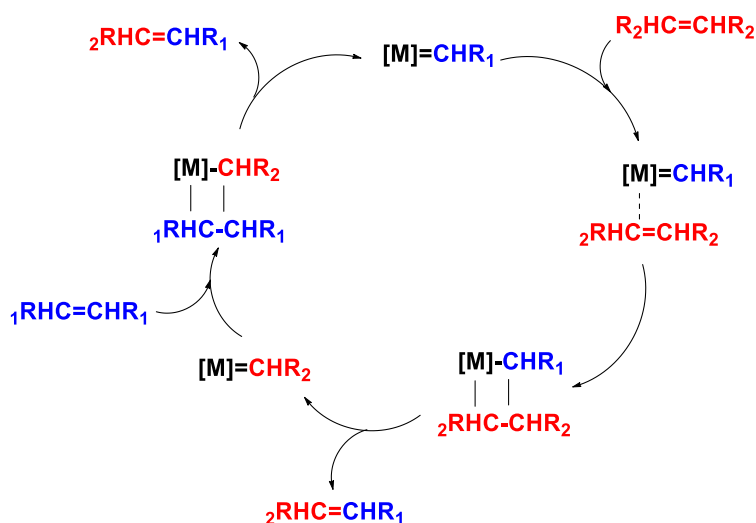
#### 2.1 Olefin metathesis

Olefin metathesis has been recognized as a concise and elegant method to achieve the redistribution of fragments of olefins, and was first recognized in the mid-1950s.<sup>5</sup> With the advancement in modern metathesis catalysts, olefin metathesis now can be used for various substrates in many fields such as the synthesis of pharmaceutical products, the production of high-strength materials, and the manufacturing of consumer products from renewable plant-based feedstocks.<sup>1</sup>



**Scheme 2.1 Proposed early stage mechanism of metathesis.<sup>6</sup>**

Early on, olefin metathesis was believed to be a “pair-wise” exchange of alkylidenes coordinated by the transition metals (Scheme 2.1).<sup>6</sup> However, Katz published a mechanistic study and showed that the ratios of observed products in his experiment were inconsistent with the pair-wise mechanism.<sup>7</sup> Herisson and Chauvin proposed a new metathesis mechanism (Scheme 2.2).<sup>8</sup> They suggested that an intermediate species was involved in the reaction of a metal carbene and an olefin, which was also known as the “carbene” mechanism or “non-pairwise” mechanism. The new mechanism suggested the fragmentation of olefins was involved in the reaction.<sup>8</sup>

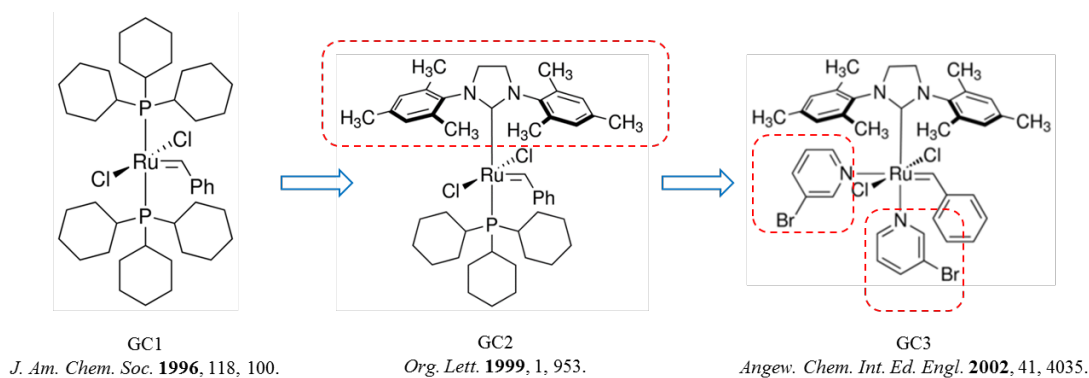


**Scheme 2.2 Mechanism of olefin metathesis proposed by Chauvin.<sup>8</sup>**

## 2.2 Metathesis catalysts

Transition metal-based catalysts play key roles in metathesis research and much progress has been made in the development of well-defined metal-carbene (alkylidene) complexes. A “well-defined” catalyst

refers to a complex that can generate stable and controlled propagating species during the reaction. The first examples of well-defined catalysts for ROMP were based on titanium, although they were not very active.<sup>9</sup> Since then, many species of active catalysts have been employed based on Ti, W, Mo, and Ru.<sup>10</sup> After the popularization of ruthenium-based Grubbs catalysts, much attention shifted toward modifying and isolating well-defined Ru alkylidenes. As illustrated in Scheme 2.3, the prototype of a well-defined ruthenium catalysts (first generation Grubbs' catalyst, G1) was successfully developed in 1996.<sup>11</sup> Now G1 is widely known as a precursor to other modified Grubbs-type catalysts. In 1999, the same group reported the second generation Grubbs' catalyst (G2) bearing a saturated *N*-heterocyclic carbene (NHC) that promoted a higher reactivity.<sup>12</sup> The initiation rate of the catalyst could further be increased by replacing the tricyclohexylphosphine (PCy<sub>3</sub>) with more labile pyridine ligands.<sup>4</sup> This modified catalyst (third generation Grubbs' catalyst, G3) is especially beneficial in ROMP that generally requires a high ratio of the rate of initiation to the rate of propagation ( $k_i \gg k_p$ ).



**Scheme 2.3 Grubbs catalysts: first generation (G1),<sup>11</sup> second generation (G2),<sup>12</sup> and third generation (G3).<sup>4</sup>**

### 2.3 Solvent effect in olefin metathesis

Various organic solvents such as benzene, toluene, and dichloromethane have been employed for ROMP. The effect of different solvents on the polymerization rates are significant. For example, when polymerizing a norbornene derivative using Grubbs' third generation catalyst (G3), the kinetic study

revealed a dramatic change in polymerization rates in various solvents like C<sub>6</sub>D<sub>6</sub>, CDCl<sub>3</sub>, or deuterated tetrahydrofuran. The half-life for the reaction (the time required for the initial concentration of a reactant to be reduced to one-half its initial value) was 550 s in CDCl<sub>3</sub>, 60 s in deuterated THF, and 110 s in C<sub>6</sub>D<sub>6</sub>.<sup>10</sup>

CH<sub>2</sub>Cl<sub>2</sub> is believed to be a good solvent for metathesis because as a polar solvent it can promote the ligand dissociation but it also acts as a non-coordinating solvent to allow for olefin binding. In addition, the reactions need to be run dilute to reduce the effect of intermolecular reactions. However, it is not always the best practice to use CH<sub>2</sub>Cl<sub>2</sub> in every case of olefin metathesis. In general, the phosphine-bound ruthenium pre-catalysts initiate faster in polar solvents than in non-polar solvents (Table 2.1).<sup>24</sup>

**Table 2.1 Solvent selection for olefin metathesis.**<sup>24</sup> •

<b>Preferred Solvents (non-coordinating)</b>	<b>Tolerated Solvents (coordinating/nucleophilic)</b>	<b>Avoid if Possible (strongly coordinating)</b>
pentane, hexane, etc.	MeOH, <i>i</i> PrOH, etc.	acetonitrile
benzene, toluene, etc.	acetone	DMSO
TBME	Et <sub>2</sub> O, THF, etc.	DMF
CH <sub>2</sub> Cl <sub>2</sub> , ClCH <sub>2</sub> CH <sub>2</sub> Cl, PhCl, etc.	neutral/acidic water	pyridine
EtOAc, HOAc, <i>i</i> PrOAc, etc.		free amines
		basic water

Grubbs *et al.* conducted a more quantitative examination of catalyst initiation in various solvents by UV-vis spectroscopy and <sup>1</sup>H NMR spectroscopy.<sup>24</sup> They found that the rate coefficient, *k*<sub>init</sub>, was approximately proportional to the dielectric constant of the solvent used. For example, the initiation rate of both first and second generation Grubbs' Catalysts increased by 30% upon moving from toluene ( $\epsilon =$

2.38) to dichloromethane ( $\epsilon = 8.9$ ).<sup>25</sup> These solvent effects are extremely important when highly polar or charged substrates are also involved in the reactions.

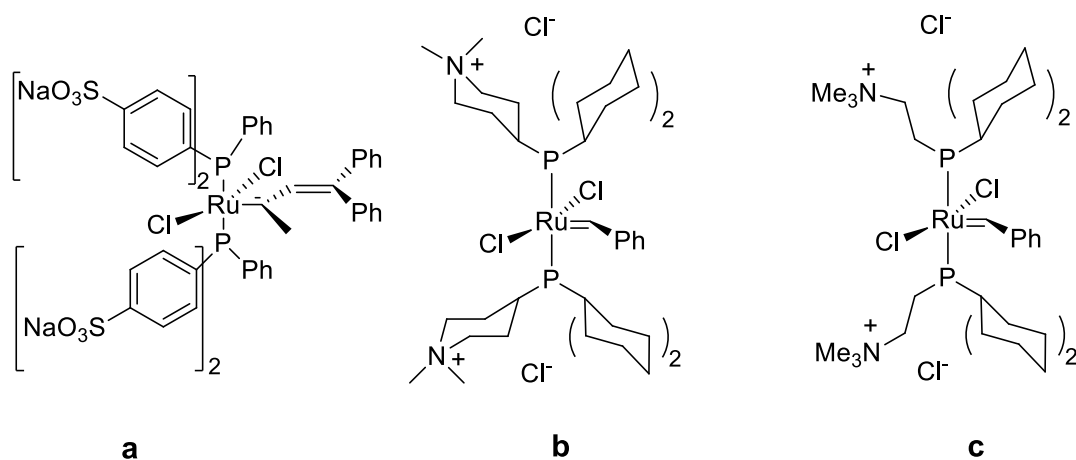
## 2.4 Metathesis catalysts in aqueous phase

The majority of polymerizations in this work were conducted in the presence of water. This section will review recent progress in the development of metathesis in the aqueous phase. The environmental impact of volatile organic compounds (VOCs) has raised researchers' interest in choosing water as a continuous phase to conduct organometallic reactions including olefin metathesis. Besides the environmental concerns, aqueous olefin metathesis opens opportunities to fabricate hydrophilic polymers that are usually impossible to obtain via olefin metathesis in hydrophobic organic solvents.

The early attempts to apply ROMP in water were reported in the 1960s by introducing hydrates of Ru or Ir chlorides as catalysts in the aqueous phase.<sup>13</sup> Despite the inadequate polymerization rate and low level of control, an emulsion polymerization of norbornene was reported for the first time. Further progress was then achieved by Claverie *et al.* by using a hydrophilic Ru alkylidene in emulsion to polymerize norbornene (NB).<sup>14</sup> Polynorbornene nanoparticles (50 ~ 100 nm) were reported with high yield but the resulting latex was prone to flocculation. The same group also applied first generation Grubbs' catalyst to miniemulsion polymerization of 1,5-cyclooctadiene to generate polybutadiene nanoparticles (250 ~ 650 nm) with a moderate yield, although organic solvent (toluene) was used in this case to dissolve the catalyst.<sup>14</sup>

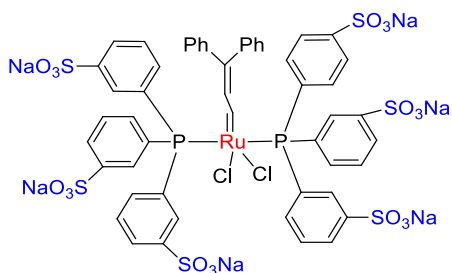
A better practice might be the modification of certain ligands or functional groups on the metathesis catalysts that are already commercialized. Many "tagged" ruthenium catalysts have been prepared by introducing hydrophilic functional groups. Early attempts to prepare water-soluble metal alkylidene complexes were made by Grubbs *et al.*. The first approach they used was to introduce the water-soluble ligands  $\text{PhP}(p\text{-C}_6\text{H}_4\text{SO}_3\text{Na})_2$  into the first generation Grubbs Catalyst (Scheme 2.4 a).<sup>15</sup> The obtained

catalyst was soluble in water but failed to initiate ROMP in the aqueous phase. Later, two active catalysts (Scheme 2.4 b and c) were also developed for the metathesis polymerization in both water and methanol. It turned out the propagating species decomposed before polymerization was complete and the final conversions were low.<sup>16</sup>

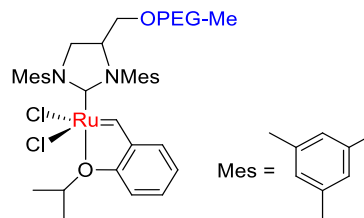


**Scheme 2.4 Early water-soluble ruthenium catalysts developed by Grubbs and co-workers.<sup>15</sup>**

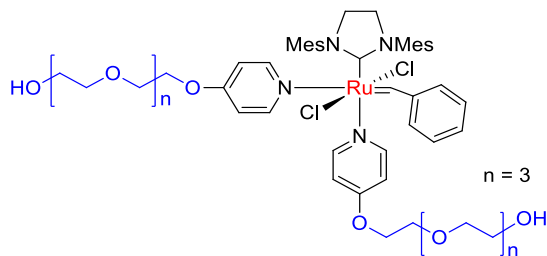
Shortly afterwards, Grubbs *et al.* reported a water-soluble catalyst bearing a poly(ethylene glycol) conjugated NHC to catalyze ROMP in the aqueous phase with a high yield in 24 hours.<sup>17</sup> An improvement was made by the same group with a similar modification on a Hoveyda-type catalyst.<sup>18</sup> The modified complex showed high reactivity to polymerize a hydrophilic derivative of endo-norbornene monomer in water. Hence the benefits of well-defined ruthenium NHC catalysts can be extended to the aqueous phase by solubilizing the catalysts with appropriate hydrophilic functional groups. As an indication of this, another promising approach was reported by Breitenkamp and Emrick<sup>19</sup> using poly(ethylene glycol)-tagged pyridines to substitute the tricyclohexylphosphine (PCy<sub>3</sub>) group on G2. Some other alternative approaches were also reported including a “macro-initiator” method<sup>20</sup> which introduced self-stabilized copolymers incorporated with hydrophilic PEG-tagged NB derivatives.



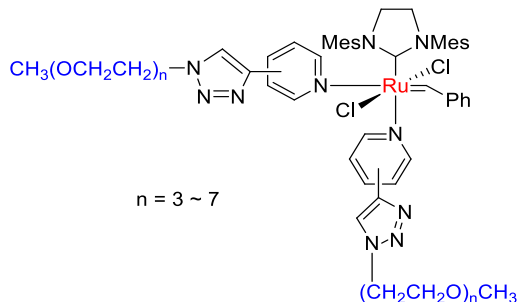
[14] *Macromolecules* **2001**, 34, 382.



[18] *J. Am. Chem. Soc.* **2006**, 128, 3508.



[19] *J. Polym. Sci. Part A Polym. Chem.* **2005**, 43, 5715.

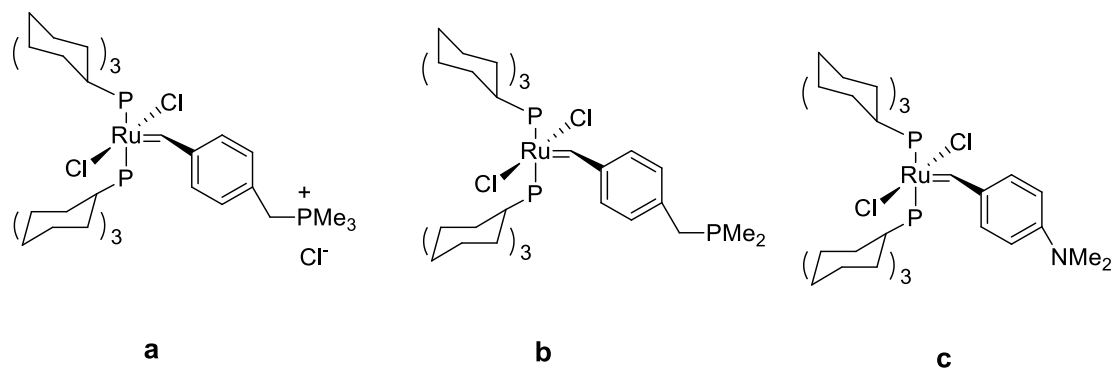


[21] *Macromolecules* **2008**, 41, 530.

### Scheme 2.5 Examples of hydrophilic metathesis catalysts for aqueous olefin metathesis.<sup>14,18,19,21</sup>

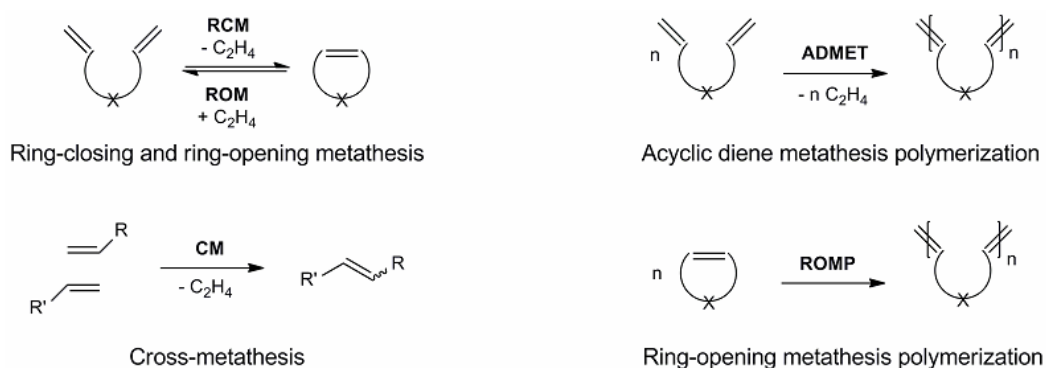
Scheme 2.5 highlights part of the previous efforts on catalyst design in an aqueous phase. It is clear that the proper modifications on NHC groups or labile ligands does endow solubility and stability of metathesis catalysts in an aqueous phase.<sup>22</sup> More interestingly, Schanz and coworkers reported a series of pH-responsive catalysts in order to promote ROMP in protic acidic media (Scheme 2.6).<sup>23</sup> Catalyst in Scheme 2.6 was the first example of Ru complexes that were used for ROMP in protic acidic media although no polymerization was observed without the addition of HCl. When HCl was used, the NMe<sub>2</sub> group in catalysts b and c could enhance the dissociation of the PCy<sub>3</sub> ligand for a more efficient initiation of polymerization. Thus, the reactivity of catalysts can be adjusted based on the pH of the aqueous phase.





**Scheme 2.6** pH-responsive metathesis catalysts that can be used in aqueous phase.<sup>23</sup>

## 2.5 Ring Opening Metathesis Polymerization

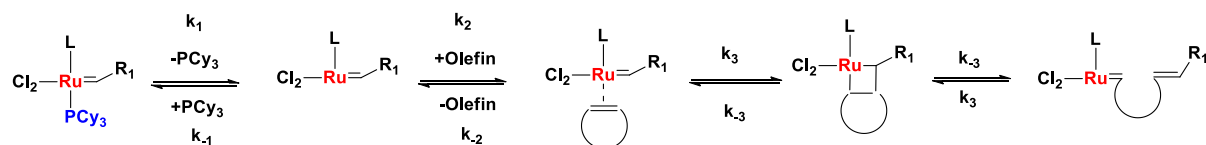


**Scheme 2.7** Different types of olefin metathesis reactions.<sup>1</sup>

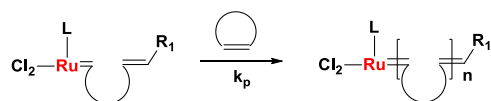
Olefin metathesis (OM) can further be classified into various subfields (Scheme 2.7) including cross metathesis (CM), ring closing metathesis (RCM), ring opening cross metathesis (ROCM), ring opening metathesis polymerization (ROMP), and acyclic dienemetathesis polymerization (ADMET).<sup>1</sup> Ring opening metathesis polymerization (ROMP), in particular, has been widely applied to build well-defined macromolecular architectures due to its superiority to preserve the functionalities of the polymer chains

without damaging the double bonds of the monomers. For example, poly(norbornene), a commercialized product with the trade name “Norsorex” since 1976, can be polymerized by ROMP from norbornene. With the successful commercialization of some of the metathesis catalysts, polymer chemists are now able to prepare a huge number of polymers via ROMP. Typical monomers range from norbornenes, norbornene-based monomers, to cyclooctenes, cyclooctadienes, etc.. Cyclic olefins with functional groups are also used to build advanced functional polymers, and they all follow a similar mechanism as shown in Scheme 2.8.

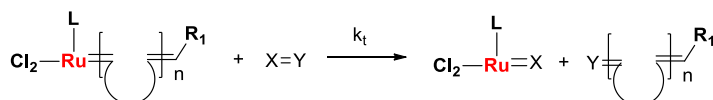
### Initiation:



### Propagation:



### Termination:



### **Scheme 2.8 Mechanism of ring opening metathesis polymerization.**

Ring opening metathesis polymerization (ROMP) is a chain growth process where cyclic olefins (monomers) are converted to polymer chains. The main difference from the free radical mechanism is that any double-bonds in the monomer are preserved after the polymerization. Generally, the initiation starts with the reaction between transition metal alkylidene complex and a cyclic olefin. This process involves the formation of a four-membered metallacyclobutane intermediate which yields a primary growing

chain. Since the reactivity of the primary chain is high, more cyclic olefins are added to the growing chains until a reaction equilibrium is achieved. Also, the chain growth process can be quenched deliberately through the addition of a termination agent which can deactivate the transition metal and insert a functional group at the end of the polymer chain.

Assuming a fast initiation and a stable propagation that is not chain-length-dependent, the rate of propagation can be simply estimated as shown below:

$$R_p = -\frac{d[M]}{dt} = k_p[Ru][M] \quad \text{Equation 2.1}$$

Where  $R_p$  ( $\text{mol}\cdot\text{L}^{-1}\cdot\text{min}^{-1}$ ) is the rate of propagation,  $k_p$  ( $\text{L}\cdot\text{mol}^{-1}\cdot\text{min}^{-1}$ ) is the rate coefficient of propagation,  $[Ru]$  ( $\text{mol}\cdot\text{L}^{-1}$ ) is the concentration of the growing chains, and  $[M]$  ( $\text{mol}\cdot\text{L}^{-1}$ ) is the concentration of the monomer. Assuming a constant concentration of growing chains ( $[Ru]$ ) with minimum catalyst decomposition, it's not surprising to expect the propagation to follow first order kinetics under appropriate conditions.<sup>24</sup>

Metathesis reactions are generally reversible and the propagation illustrated in Scheme 2.8 may occur in the opposite direction. However, the release of strain associated with the cyclic olefin can drive the equilibrium to a high monomer conversion. In other words, the driving force of ROMP is the release of strain energy,<sup>1</sup> denoted by the enthalpy term in thermodynamic terms. The monomers commonly used in ROMP like cyclobutene, cis-cyclooctene and norbornene usually possess degree of strain larger than 5 kcal/mol.<sup>26</sup> Some low ring-strain olefins like cyclohexene have very little driving force, which is why they are not suitable for ROMP.

## 2.6 ROMP monomers

The most popular monomers used in ROMP are norbornene and its derivatives. Norbornene has a high ring strain of about 27.2 kcal/mol,<sup>27</sup> which promotes efficient polymerization and high molecular weight. A wide range of substituted norbornenes have been commercially available and they are usually prepared by multiple-step syntheses. In many of these cases, esterification, etherification, or amidation reactions of norbornene carboxylic acid or norbornenol derivatives are used to attach the functional unit to the polymerizable group. The group connecting the functional unit to the norbornene moiety is called the anchor group. The configuration of substituted norbornenes could affect the polymerization rate of ROMP. For instance, when polymerizing a mixture of endo- and exo-2-norbornene derivatives, the exo isomers react faster than endo isomers due to steric and electronic effects.<sup>28</sup> Further research revealed that both propagation rate and initiation rate constant were affected by the anchor group, which consequently altered molecular weight and molecular weight distribution.<sup>29</sup> Less-strained monomers, like cyclooctene and cyclooctadiene, can also be polymerized via ROMP. Yet significant chain transfer might occur due to the unhindered polymer chains formed from low-strain monomers.<sup>30</sup>

## 2.7 Applications of ROMP

Norbornene-derived polymers with various functionalized groups were widely investigated in past decades. Adekunle *et al.* reported the synthesis and crossover reaction of TEMPO containing block copolymer via ROMP in which a norbornene derivative with TEMPO moieties as side chains was used as monomer.<sup>31</sup> Griesser *et al.* reported a photosensitive polymer bearing aryl esters or amides in the side chains that undergo Photo-Fries rearrangement upon irradiation with UV light.<sup>32</sup> Most of these polymers were prepared with Grubbs catalysts that have high tolerance towards functional groups. Pawar *et al.* used ROMP-derived, polymer-bound Cu-catalysts for click-chemistry and hydrosilylation reactions under micellar conditions. The polymer-bound Cu-catalyst was found to be an efficient catalysts for all reactions they investigated.<sup>33</sup>

The application of ROMP has been beyond the scope of homopolymers. For example, the new donor-acceptor materials were prepared by the random copolymerization of phthalocyanine (Pc) and fullerene (C-60) bearing monomers. The obtained random copolymer exhibited a favorable photo-induced electron transfer.<sup>34</sup> Relevant work was also performed by preparing block ROMP copolymers from zinc-porphyrin and C-60 bearing norbornenes.<sup>35</sup> Thus ROMP offers a simple and straightforward approach to build either random or block copolymers with well-defined properties.

## **2.8 Polymerization in dispersed systems**

The significance of polymerization in dispersed media arises from several aspects. First, using water largely reduces the environmental impact and health concerns of organic solvents. Second, the dispersed phase improves heat transfer, decreases viscosity, and minimizes the cost of post-reaction separation. Finally, the obtained products, known as polymer latexes, can be readily applied in many areas like coating, adhesives, biomedical materials, and pharmaceutical products.<sup>36</sup> Dispersed-phase polymerization can further be divided into (conventional) emulsion polymerization, miniemulsion polymerization, and microemulsion polymerization, as listed in Table 2.2.<sup>37</sup>

**Table 2.2 Comparison among emulsion, miniemulsion, and microemulsion polymerization.<sup>37</sup>**

Emulsion Type	Emulsion	Miniemulsion	Microemulsion
<b>Droplet size range</b>	> 1 $\mu\text{m}$	50 to 500 nm	10 to 100 nm
<b>Duration of stability</b>	seconds to hours	hours to months	indefinitely
<b>Diffusional stabilization</b>	kinetic	kinetic	thermodynamic
<b>Nucleation mechanism</b>	micellar, homogeneous	droplet	droplet
<b>Emulsifier concentration</b>	moderate	moderate	high
<b>Costabilizer type</b>	none	hexadecane, cetyl alcohol	hexanol, pentanol
<b>Homogenization method</b>	none	mechanical or ultrasonic	none
<b>Particle size range</b>	50 to 500 nm	50 to 500 nm	10 to 100 nm
<b><math>N_p</math> range (per L H<sub>2</sub>O)</b>	$10^{16}$ to $10^{19}$	$10^{16}$ to $10^{19}$	$10^{18}$ to $10^{21}$

## 2.9 Emulsion polymerization

Emulsion polymerization is the most widely reported used method to produce polymer nanoparticles/latexes in industry.<sup>37</sup> For a typical oil-in-water emulsion polymerization, the reaction starts with an emulsion incorporating water, monomer, and surfactant (emulsifier). The initiators used in emulsion polymerization are normally water-soluble. The word “emulsion polymerization” does not mean that the polymerization occurs inside the droplets of a monomer emulsion. Instead, according to the theory developed by Smith and Ewart,<sup>38</sup> and Harkins,<sup>39</sup> the polymer particles are formed in the aqueous phase via micellar or homogeneous nucleation during interval I (0-10% conversion). The mechanism of emulsion polymerization is explained in more detail below.

### 2.9.1 Three intervals in emulsion polymerization

In a typical emulsion polymerization, a surfactant is added above its critical micelle concentration (CMC) to disperse monomer in water; and a water-soluble initiator is introduced to initiate polymerization in micelles or the aqueous phase. As a result, short chains (or oligomers) are generated and they eventually

nucleate particles when reaching to a critical chain length (~2-5 monomer units).<sup>40</sup> This particle nucleation period is referred to as Interval I (Figure 2.1).

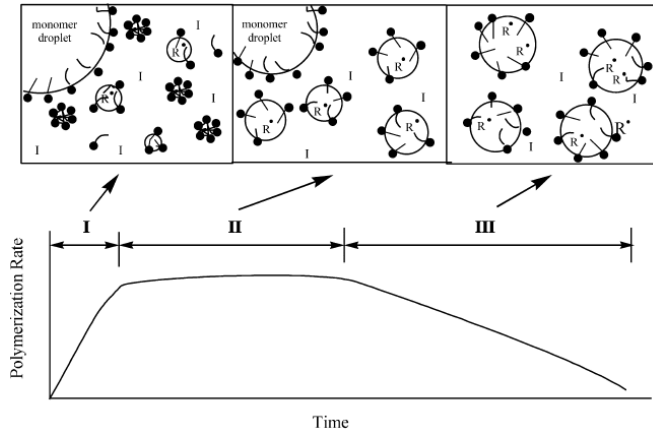


**Figure 2.1 Intervals in emulsion polymerization.**<sup>41</sup>

To maintain a constant concentration in growing particles, monomer from large droplets diffuses into particles and participates in the chain growth. This period is known as Interval II. Eventually, all monomer droplets disappear and all remaining monomer is located in the particles. The final stage, indicated by a decreasing rate of polymerization, is marked as Interval III. The product is obtained as a polymer latex in water.

Extensive research has been focused on the mechanistic study of emulsion polymerization to better understand the three intervals. The first kinetic model, known as S-E model, was proposed by Smith and Ewart<sup>38</sup> in which the average number of growing chains per particle,  $\bar{n}$ , was introduced to describe the overall rate of polymerization:

$$R = k_p \frac{N_p \bar{n}}{N_A} [M] \quad \text{Equation 2.2}$$

Where  $N_p$  is the number of particles per unit volume,  $\bar{n}$  is the average number of growing chains per particle, and  $N_A$  is Avogadro's number. The term  $\frac{N_p \bar{n}}{N_A}$  is considered the apparent concentration of growing chains in emulsion. In general, the S-E model is useful to illustrate the difference between emulsion polymerization and homogeneous polymerization kinetics. Compared to a typical homogeneous polymerization in an organic solution, the segregation of the propagating radicals inside the particles leads to a radical compartmentalization. In this case, the radicals in different particles have no chance to terminate with each other and the overall radical concentration is larger with long radical lifetimes.<sup>42</sup> Also, the S-E model was developed based on several assumptions. For instance, it assumes that coagulation of particles does not occur and the number of particles remains constant during polymerization, which is reasonable when an emulsion polymerization process is well-behaved. Since this model was developed from the experimental understanding of free-radical polymerization, it is thus also assumed that bimolecular termination of the radicals inside the particle occurs instantaneously.

Based on these assumptions, it is reasonable that any particles with propagating chains contain either one or zero free radical. An average value of 0.5 can be achieved in this case. Interestingly, the concentration of monomer inside the monomer-swollen particles does not vary with the progress of polymerization in Interval II, which is why a steady polymerization rate can be achieved during Interval II in emulsion polymerization. Furthermore, it should be noted that both micellar nucleation and homogeneous nucleation can occur in emulsion, especially when the surfactant concentration is below the CMC. In either way, primary particles can be formed when the oligomers become insoluble in water and are then surrounded by surfactant molecules.

### **2.9.2 Particle nucleation**



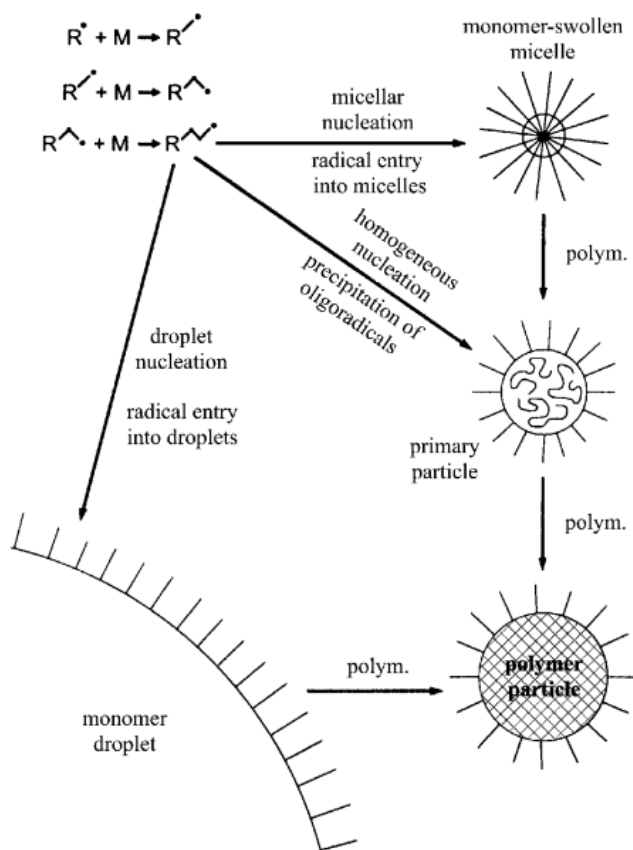


**Figure 2.2 Micellar, homogeneous and droplet nucleation in free radical emulsion polymerization.**<sup>37</sup>

The complex chemistry that occurs during emulsion polymerization cannot be fully predicted by the Smith-Ewart theory since it describes only the average number of particles and overall rate of polymerization. In Interval I, radicals generated by the initiator can react with monomer dissolved in the water phase to form oligomers. As shown in Figure 2.2, the oligomers can either aggregate in water to form primary particles by homogeneous nucleation, enter monomer-swollen micelles to form primary particles by micellar nucleation, or enter monomer droplets directly to cause droplet nucleation. When the monomer is somewhat water-soluble, like methyl methacrylate or vinyl acetate, homogeneous nucleation may occur.<sup>43</sup> Meanwhile, the frequency of droplet nucleation is low because there are few droplets present and the entry of oligomer into a micelle is favored over entry into a droplet as the micelles have a very high total interfacial area for radical capture compared to the interfacial area of the droplets.<sup>36</sup> Thus

droplet nucleation can be neglected in emulsion polymerization, although this is not the case for miniemulsion polymerization.

## **2.10 Miniemulsion polymerization**

A miniemulsion refers to a stable dispersion prepared by intensive homogenization to break large droplets into submicron oil droplets. Similar to emulsion polymerization, a miniemulsion polymerization also includes a combination of water, surfactant, monomer and initiator (water- or oil- soluble). Both ionic and nonionic surfactants can be applied in the preparation of miniemulsions. A high-shear device is required as an input of external energy to obtain submicron oil droplets. In addition, a hydrophobic “co-stabilizer” is usually introduced to result in thermodynamically unstable but kinetically stable monomer droplets. The particle size of these monomer droplets ranges roughly from 60 to 200 nm. A key feature of miniemulsion polymerization is that the polymerization occurs inside the monomer droplets directly and ideally each monomer droplet can be converted to a polymer particle.

Although a variety of high-shear devices for homogenization have been reported such as rotor-stator systems, sonicators, and high-pressure homogenizers<sup>44</sup>, sonication remains as a very simple and popular solution for laboratory use to generate miniemulsions efficiently (Figure 2.3). The sonication process is marked by the decrease of droplet diameters and the increase of total interfacial area (droplet formation). A miniemulsion may be kinetically stable because droplet degradation cannot be avoided for a long period of time. In general, droplet formation, droplet degradation and droplet nucleation in miniemulsion polymerization are the key features that distinguish miniemulsion polymerization from conventional emulsion polymerization.

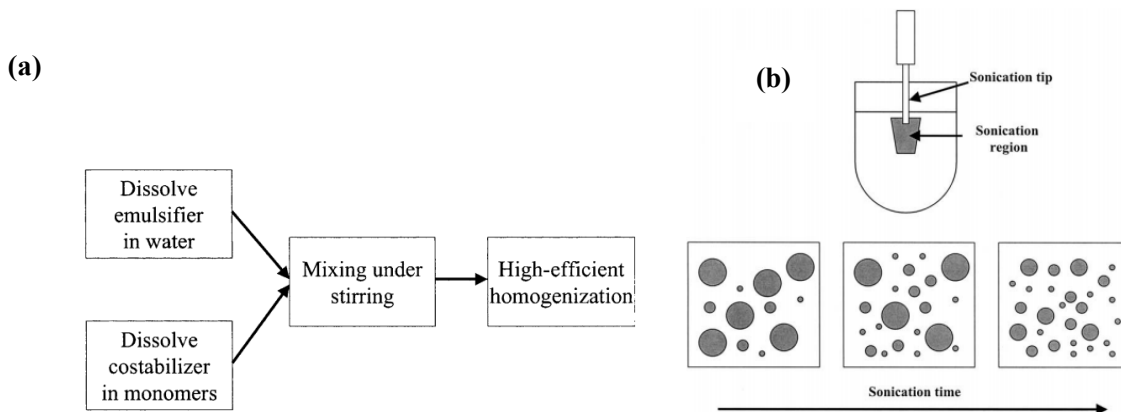


**Figure 2.3 Preparation of monomer miniemulsion: (a) a general procedure, (b) homogenization by sonication.**<sup>36</sup>

### 1.3.1 Droplet formation and degradation

Figure 2.3 describes a general procedure to prepare monomer miniemulsions and highlights the decrease of droplet size during sonication. In this process, two things will occur concurrently:

- (i) Large droplets are broken into smaller ones and more interfacial area is created;
- (ii) Newly formed droplets need more surfactants from the continuous phase to remain stable, thus reducing and eventually fully consuming the number of micelles.

As a result, the monomer droplet size is significantly reduced ( $< 500$  nm) and a miniemulsion is obtained.

However, it is important to note that the obtained miniemulsion cannot be perfectly stable because it is generally believed that monomer droplets in miniemulsions can undergo degradation in two pathways:

- (i) Droplet coalescence. Two or more droplets contact each other and merge into a larger droplet (caused by Brownian motion, settling or creaming);
- (ii) Droplet diffusion degradation (or Ostwald ripening). Two or more droplets of different sizes will exchange monomer (net diffusion from small droplets to large) without making direct contact through monomer diffusion across the aqueous phase.<sup>45</sup>

The first pathway (droplet coalescence) can be stopped by adding sufficient surfactant, so that the surfactant can be readily adsorbed onto the surface of droplets. The droplets are able to repel each other by either electrostatic forces (ionic surfactants) or steric repulsion forces (nonionic surfactants). The second pathway (Ostwald ripening) can be effectively minimized by using a costabilizer to retard monomer diffusion from the smaller droplets to the larger ones. To meet this goal, a costabilizer should be highly insoluble in aqueous phase (so that the diffusion of costabilizer itself will not occur), and highly soluble in monomer droplets (so that the diffusion of monomer will be retarded).

The stability of monomer miniemulsion has been a key factor of determining the property of final polymer latexes. The partial molar Gibbs free energy of monomer in a monomer droplet containing a water-insoluble costabilizer is giving by:

$$\frac{\Delta G_m}{RT} = \ln(\phi_m) + (1 - m_{mh})\phi_h + \chi_{mh}(\phi_h)^2 + \frac{2V_m\sigma}{rRT} \quad \text{Equation 2.3}$$

where  $\phi_m$  and  $\phi_h$  are the volume fractions of monomer and costabilizer in the monomer droplets,  $m_{mh}$  the ratio of the molar volume of monomer ( $V_m$ ) to that of costabilizer ( $V_h$ ),  $\chi$  the interaction parameter,  $\sigma$  the droplet-water interfacial tension, and  $r$  the volume of the droplet. The equation shows that monomer diffusion is a kinetic process that cannot be perfectly avoided when preparing a monomer miniemulsion. The addition of costabilizer can reduce the monomer diffusion rate, which provides a long period of stability for monomer miniemulsion systems.

Hexadecane is one of the most often used costabilizers in publications.<sup>46</sup> Other examples include cetyl alcohol and dodecane. These compounds are insoluble in water and may stay inside the particles, which means the addition of costabilizer may have an impact on the physical properties of the polymer latexes. Alduncin *et al.* suggested minimizing these negative effects of costabilizer by incorporating the costabilizer molecules into the obtained polymer backbones.<sup>47</sup> In this case, a series of oil-soluble initiators like lauroyl peroxide, benzoyl peroxide and azobis(iso-butyronitrile) were used as both initiators and

costabilizers. The side effect of costabilizer was minimized in this case but a drawback is that the concentration of initiator affects not just miniemulsion stability, but also the polymerization rate as well as the molecular weight of the final products.<sup>47</sup>

### 1.3.2 Particle nucleation in miniemulsion polymerization

In a miniemulsion, ideally all of the micelles have been sacrificed during homogenization so that micellar nucleation is eliminated. Also, the monomers used are usually hydrophobic and homogeneous nucleation may not be obvious in this case. Instead, the droplet nucleation dominates in miniemulsion polymerization. The nucleation takes place directly in droplets and no monomer diffusion is involved. To maintain the simplicity of the nucleation mechanism in the ROMP experiments, I adapted miniemulsion polymerization (and not emulsion polymerization) as the primary strategy.

## 2.11 Polymer latexes and nanoparticles

### 2.11.1 Particle Size and Particle Size Distribution

The particle size and particle size distributions (PSDs) are important indicators of the quality of polymer latexes obtained from polymerizations in a dispersed phase. Ideally, the particle size and particle size distribution should be controlled within a range in order to meet its applications that require certain properties.

Note that most of the final products from emulsion or miniemulsion polymerization do not have uniform particle size. Instead, a narrow or broad distribution is usually observed. Therefore, the particle size for typical polymer latex refers to the diameters in terms of averages. Depending on the way used to calculate the average, several types of particle diameter can be defined as follows:

Number-average diameter ( $D_n$ ):

$$D_n = \frac{\sum n_i d_i}{\sum n_i}$$

Equation 2.4

Volume-average diameter ( $D_v$ ):

$$D_v = \left( \frac{\sum n_i d_i^3}{\sum n_i} \right)^{\frac{1}{3}} \quad \text{Equation 2.5}$$

Weight-average diameter ( $D_w$ ):

$$D_w = \frac{\sum n_i d_i^4}{\sum n_i d_i^3} \quad \text{Equation 2.6}$$

where  $n_i$  is the number of particles with diameter  $d_i$ . The number of particles per liter of water ( $N_p$ ) is then calculated from the volume-average diameter as below:

$$N_p = \frac{6m}{\pi \rho D_v^3} \quad \text{Equation 2.7}$$

where  $m$  is the polymer mass divided by the water mass and  $\rho$  is the density of polymer material.

In practice, the most straightforward way to measure particle size is via microscopy including optical microscopy, electron microscopy, and dark field microscopy. The second method is through light scattering techniques like dynamic light scattering (DLS). Some other techniques like hydrodynamic chromatography (HDC) can also be employed based on the movement of particles. In practice, small particle sizes (~100 nm) are measured using DLS or electron microscopy. Large particle sizes (> 1000 nm) are usually measured by static light scattering, optical microscopy or electrozone sensing, or by sieving.

### 2.11.2 Electrical Double Layer, Zeta-potential and Particle Stability

An electrical double layer (EDL) exists on the surface of a charged object when it is exposed to a fluid. Helmholtz<sup>48</sup> first realized that charged electrodes in electrolytic solutions repel the co-ions of the charge while attracting counterions to their surfaces. He also showed that an electrical double layer (EDL) is essentially a molecular dielectric, and the charge was stored electrostatically. In this model, the differential capacitance depends on the dielectric constant of the electrolyte solvent and the thickness of the double-layer. However, it does not include several key factors like diffusion of ions, the adsorption onto the surface and the interaction between solvent dipole moments and electrode. Later on, the “Gouy-

Chapman model”<sup>49</sup> made improvements by including diffusion in the model. In this model, the electric potential decreases exponentially away from the surface of the fluid bulk. However, the model could not fit the actual case for highly charged double layers. The Helmholtz model and Gouy-Chapman model were combined by Stern in 1924.<sup>50</sup> In the new model, a portion of ions adhere to the electrode and form a Stern layer, and some ions form a Gouy-Chapman diffuse layer.

Zeta potential is defined as the potential difference between the dispersion medium and stationary layer of fluid attached to the dispersed particle. Other terms like Stern potential or electric surface potential are also mentioned in interfacial and colloidal science. Zeta potential is a key indicator of the stability of polymer latexes. The magnitude of zeta potential usually reflects the degree of electrostatic repulsion among charged particles. Therefore, a polymer latex with higher zeta potential (absolute value) is more stable compared to colloids with low zeta potentials.

## **2.12 Conclusion**

This chapter gives a brief review of the basic concepts involved in my PhD work. The fundamentals of olefin metathesis and ROMP were reviewed including the latest developments in metathesis catalysts. ROMP has some of the same advantages as other living polymerization techniques such as RAFT, ATRP, etc. (although ROMP is more sensitive to oxygen) but the unique mechanism also offers more novel synthetic routes for the synthesis of thermoplastics or thermosets from a variety of resources. In the second half of this chapter, it was shown that the use of proper surfactants and initiation system would promote well-defined polymer latexes, although the nucleation mechanism may vary from case to case depending on which dispersed system is used.

## 2.13 References

- (1) Grubbs, R. H. Olefin Metathesis. *Tetrahedron* **2004**, *60* (34), 7117–7140.
- (2) Tebbe, F. N.; Parshall, G. W.; Ovenall, D. W. Titanium-Catalyzed Olefin Metathesis. *J. Am. Chem. Soc.* **1979**, *101* (17), 5074–5075.
- (3) Scholl, M.; Ding, S.; Lee, C. W.; Grubbs, R. H. Synthesis and Activity of a New Generation of Ruthenium-Based Olefin Metathesis Catalysts Coordinated with 1,3-Dimesityl-4,5-Dihydroimidazol-2-Ylidene Ligands. *Org. Lett.* **1999**, *1* (6), 953–956.
- (4) Love, J. A.; Morgan, J. P.; Trnka, T. M.; Grubbs, R. H. A Practical and Highly Active Ruthenium-Based Catalyst That Effects the Cross Metathesis of Acrylonitrile. *Angew. Chem. Int. Ed. Engl.* **2002**, *41* (21), 4035–4037.
- (5) Truett, W. L.; Johnson, D. R.; Robinson, I. M.; Montague, B. A. Polynorbornene by Coördination Polymerization I. *J. Am. Chem. Soc.* **1960**, *82* (9), 2337–2340.
- (6) Grubbs, R. H.; Miyashita, A.; Liu, M.-I. M.; Burk, P. L. The Preparation and Reactions of Nickelocyclopentanes. *J. Am. Chem. Soc.* **1977**, *99* (11), 3863–3864.
- (7) Katz, T. J.; McGinnis, J. Metathesis of Cyclic and Acyclic Olefins. *J. Am. Chem. Soc.* **1977**, *99* (6), 1903–1912.
- (8) Jean-Louis Hérisson, P.; Chauvin, Y. Catalyse de Transformation Des Oléfines Par Les Complexes Du Tungstène. II. Télomérisation Des Oléfines Cycliques En Présence D'oléfines Acycliques. *Die Makromol. Chemie* **1971**, *141* (1), 161–176.
- (9) Tebbe, F. N.; Parshall, G. W.; Reddy, G. S. Olefin Homologation with Titanium Methylene Compounds. *J. Am. Chem. Soc.* **1978**, *100* (1961), 3611–3613.
- (10) Slugovc, C. The Ring Opening Metathesis Polymerisation Toolbox. *Macromol. Rapid Commun.* **2004**, *25* (14), 1283–1297.
- (11) Schwab, P.; Grubbs, R. H.; Ziller, J. W. Synthesis and Applications of  $\text{RuCl}_2(\text{CHR}^i)(\text{PR}_3)_2$ : The Influence of the Alkylidene Moiety on Metathesis Activity. *J. Am. Chem. Soc.* **1996**, *118* (1), 100–110.



- (12) Scholl, M.; Ding, S.; Lee, C. W.; Grubbs, R. H. Synthesis and Activity of a New Generation of Ruthenium-Based Olefin Metathesis Catalysts Coordinated with 1,3-Dimesityl-4,5-Dihydroimidazol-2-ylidene Ligands. *Org. Lett.* **1999**, *1* (6), 953–956.
- (13) Rinehart, R. E.; Smith, H. P. The Emulsion Polymerization of the Norbornene Ring System Catalyzed by Noble Metal Compounds. *J. Polym. Sci. Part B Polym. Lett.* **1965**, *3* (12), 1049–1052.
- (14) Claverie, J. P.; Viala, S.; Maurel, V.; Novat, C. Ring-Opening Metathesis Polymerization in Emulsion. *Macromolecules* **2001**, *34* (3), 382–388.
- (15) Cornils, B.; Herrmann, W. A. *Aqueous-Phase Organometallic Catalysis: Concepts and Applications*; John Wiley & Sons, 2004.
- (16) Mohr, B.; Lynn, D. M.; Grubbs, R. H. Synthesis of Water-Soluble, Aliphatic Phosphines and Their Application to Well-Defined Ruthenium Olefin Metathesis Catalysts. *Organometallics* **1996**, *15* (20), 4317–4325.
- (17) Gallivan, J. P.; Jordan, J. P.; Grubbs, R. H. A Neutral, Water-Soluble Olefin Metathesis Catalyst Based on an N-Heterocyclic Carbene Ligand. *Tetrahedron Lett.* **2005**, *46* (15), 2577–2580.
- (18) Hong, S. H.; Grubbs, R. H. Highly Active Water-Soluble Olefin Metathesis Catalyst. *J. Am. Chem. Soc.* **2006**, *128* (11), 3508–3509.
- (19) Breitenkamp, K.; Emrick, T. Amphiphilic Ruthenium Benzylidene Metathesis Catalyst with PEG-Substituted Pyridine Ligands. *J. Polym. Sci. Part A Polym. Chem.* **2005**, *43* (22), 5715–5721.
- (20) Quémener, D.; Héroguez, V.; Gnanou, Y. Design of PEO-Based Ruthenium Carbene for Aqueous Metathesis Polymerization. Synthesis by the “macromonomer Method” and Application in the Miniemulsion Metathesis Polymerization of Norbornene. *J. Polym. Sci. Part A Polym. Chem.* **2006**, *44* (9), 2784–2793.
- (21) Samanta, D.; Kratz, K.; Zhang, X.; Emrick, T. A Synthesis of PEG- and Phosphorylcholine-Substituted Pyridines to Afford Water-Soluble Ruthenium Benzylidene Metathesis Catalysts. *Macromolecules* **2008**, *41* (3), 530–532.

- (22) Burtscher, D.; Grela, K. Aqueous Olefin Metathesis. *Angew. Chem. Int. Ed. Engl.* **2009**, *48* (3), 442–454.
- (23) Roberts, A. N.; Cochran, A. C.; Rankin, D. A.; Lowe, A. B.; Schanz, H.-J. Benzylidene-Functionalized Ruthenium-Based Olefin Metathesis Catalysts for Ring-Opening Metathesis Polymerization in Organic and Aqueous Media. *Organometallics* **2007**, *26* (26), 6515–6518.
- (24) Sanford, M. S.; Love, J. A.; Grubbs, R. H. Mechanism and Activity of Ruthenium Olefin Metathesis Catalysts. *J. Am. Chem. Soc.* **2001**, *123* (27), 6543–6554.
- (25) Gordon, A. J.; Ford, R. A. The Chemist's Companion, John Wiley and Sons. *New York* **1972**, 537.
- (26) Benson, S. W.; Cruickshank, F. R.; Golden, D. M.; Haugen, G. R.; O'Neal, H. E.; Rodgers, A. S.; Shaw, R.; Walsh, R. Additivity Rules for the Estimation of Thermochemical Properties. *Chem. Rev.* **1969**, *69* (3), 279–324.
- (27) Schleyer, P. R.; Williams, J. E.; Blanchard, K. R. The Evaluation of Strain in Hydrocarbons. *J. Am. Chem. Soc.* **1970**, *92*, 2377–2386.
- (28) Huang, L.; Hu, J.; Lang, L.; Wang, X.; Zhang, P.; Jing, X.; Wang, X.; Chen, X.; Lelkes, P. I.; Macdiarmid, A. G.; Wei, Y. Synthesis and Characterization of Electroactive and Biodegradable ABA Block Copolymer of Polylactide and Aniline Pentamer. *Biomaterials* **2007**, *28* (10), 1741–1751.
- (29) Slugovc, C.; Demel, S.; Riegler, S.; Hobisch, J.; Stelzer, F. The Resting State Makes the Difference: The Influence of the Anchor Group in the ROMP of Norbornene Derivatives. *Macromol. Rapid Commun.* **2004**, *25* (3), 475–480.
- (30) Chen, Z.-R.; Claverie, J. P.; Grubbs, R. H.; Kornfield, J. a. Modeling Ring-Chain Equilibria in Ring-Opening Polymerization of Cycloolefins. *Macromolecules* **1995**, *28*, 2147–2154.
- (31) Adekunle, O.; Tanner, S.; Binder, W. H. Synthesis and Crossover Reaction of TEMPO Containing Block Copolymer via ROMP. *Beilstein J. Org. Chem.* **2010**, *6* (1), 59.
- (32) Griesser, T.; Kuhlmann, J.-C.; Wieser, M.; Kern, W.; Trimmel, G. UV-Induced Modulation of the Refractive Index and the Surface Properties of Photoreactive Polymers Bearing N -Phenylamide

- Groups. *Macromolecules* **2009**, *42* (3), 725–731.
- (33) Pawar, G. M.; Bantu, B.; Weckesser, J.; Blechert, S.; Wurst, K.; Buchmeiser, M. R. Ring-Opening Metathesis Polymerization-Derived, Polymer-Bound Cu-Catalysts for Click-Chemistry and Hydrosilylation Reactions under Micellar Conditions. *Dalton Trans.* **2009**, No. 41, 9043–9051.
- (34) De La Escosura, A.; Martínez-Díaz, M. V.; Torres, T.; Grubbs, R. H.; Guldi, D. M.; Neugebauer, H.; Winder, C.; Drees, M.; Sariciftci, N. S. New Donor-Acceptor Materials Based on Random Polynorbornenes Bearing Pendant Phthalocyanine and Fullerene Units. *Chem. - An Asian J.* **2006**, *1* (1-2), 148–154.
- (35) Charvet, R.; Acharya, S.; Hill, J. P.; Akada, M.; Liao, M.; Seki, S.; Honsho, Y.; Saeki, A.; Ariga, K. Block-Copolymer-Nanowires with Nanosized Domain Segregation and High Charge Mobilities as Stacked P/n Heterojunction Arrays for Repeatable Photocurrent Switching. *J. Am. Chem. Soc.* **2009**, *131* (50), 18030–18031.
- (36) Schork, F. J.; Luo, Y.; Smulders, W.; Russum, J. P.; Butté, A.; Fontenot, K. Miniemulsion Polymerization. *Adv. Polym. Sci.* **2005**, *175*, 129–255.
- (37) Anderson, C. D.; Daniels, E. S. Emulsion Polymerisation and Latex Applications. *Rapra Rev. Reports* **2003**, *14* (4), 1–145.
- (38) Smith, W. V.; Ewart, R. H. Kinetics of Emulsion Polymerization. *J. Chem. Phys.* **1948**, *16* (1948), 592.
- (39) Harkins, W. D. A General Theory of the Mechanism of Emulsion Polymerization 1. *J. Am. Chem. Soc.* **1947**, *69* (6), 1428–1444.
- (40) Gilbert, R. G. *Emulsion Polymerization, a Mechanistic Approach*; Academic Press, London, 1995.
- (41) Qiu, J.; Charleux, B.; Matyjaszewski, K. Controlled/living Radical Polymerization in Aqueous Media: Homogeneous and Heterogeneous Systems. *Prog. Polym. Sci.* **2001**, *26* (10), 2083–2134.
- (42) la Cal, J. C.; Leiza, J. R.; Asua, J. M.; Butte, A.; Storti, G.; Morbidelli, M. Handbook of Polymer Reaction Engineering, Ed. T. Meyer and J. Keurentjes. Wiley-VCH, Weinheim 2005.
- (43) Fitch, R. M. The Homogeneous Nucleation of Polymer Colloids. *Br. Polym. J.* **1973**, *5* (6), 467–

483.

- (44) Samer, C. J.; Schork, F. J. The Role of High Shear in Continuous Miniemulsion Polymerization. *Ind. Eng. Chem. Res.* **1999**, *38* (5), 1801–1807.
- (45) Voorhees, P. W. The Theory of Ostwald Ripening. *J. Stat. Phys.* **1985**, *38*, 231–252.
- (46) Tang, P. L.; Sudol, E. D.; Adams, M.; El-Aasser, M. S.; Asua, J. M. Seeded Emulsion Polymerization of N-Butyl Acrylate Utilizing Miniemulsions. *J. Appl. Polym. Sci.* **1991**, *42* (7), 2019–2028.
- (47) Alduncin, J. A.; Forcada, J.; Asua, J. M. Miniemulsion Polymerization Using Oil-Soluble Initiators. *Macromolecules* **1994**, *27* (8), 2256–2261.
- (48) Helmholtz, H. Ueber Einige Gesetze Der Vertheilung Elektrischer Ströme in Körperlichen Leitern Mit Anwendung Auf Die Thierisch-Elektrischen Versuche. *Ann. der Phys. und Chemie* **1853**, *165* (6), 211–233.
- (49) Stigter, D. Micelle Formation by Ionic Surfactants . I. I. Two Phase Model, Gouy-Chapman Model, Hydrophobic Interactions. *J. Colloid Interface Sci.* **1974**, *47* (2).
- (50) Oldham, K. B. A Gouy-Chapman-Stern Model of the Double Layer at a (Metal)/(ionic Liquid) Interface. *J. Electroanal. Chem.* **2008**, *613* (2), 131–138.
- (51) Jiang, J.; Oberdörster, G.; Biswas, P. Characterization of Size, Surface Charge, and Agglomeration State of Nanoparticle Dispersions for Toxicological Studies. *J. Nanoparticle Res.* **2009**, *11* (1), 77–89.

## Chapter 3

### Ring opening metathesis polymerization in homogeneous systems

ROMP can produce highly living and well controlled polymer chains in appropriate organic solvents.  $\text{CH}_2\text{Cl}_2$  is reported as a good solvent for metathesis because it can promote the ligand dissociation of metathesis catalysts but will not coordinate with transition metals.<sup>1</sup> However, performing ROMP in aqueous dispersed systems such as emulsion or miniemulsion is much more challenging for several reasons. First, when a metathesis catalyst is activated in the presence of water and surfactants to polymerize cyclic olefins, the propagating behavior might be altered and a deviation of monomer conversion or molecular weight from expected values can be observed. Second, the particle nucleation is a key process for any heterogeneous system, but it has not been fully investigated in the context of ROMP rather than free radical chemistry. To eliminate any complexity caused by water, surfactants, or particle nucleation, this chapter covers the initial study of ROMP with a focus on the polymerization kinetics of ROMP in homogeneous systems. The recipes and reaction conditions to perform a well-behaved homogeneous ROMP are described in detail, and a kinetic study was performed to exam the livingness and control of the ROMP experiments.

Assuming the organic solvents used in ROMP can be recycled properly, homogeneous ROMP would be a suitable approach to produce specialized polymers with minimal environmental foot print. Previously, homogeneous polymerizations were conducted in unconventional solvents like super critical  $\text{CO}_2$ ,<sup>2</sup> and ionic liquids<sup>3</sup> in order to simplify the post-reaction separation or purification. Interestingly, the switchable solvents<sup>4</sup> worked in a similar way to typical organic solvents like DCM or toluene when running a polymerization; yet the solvent can be recycled and reused efficiently without any distillation or condensation processes. I took significant steps in understanding the polymerization kinetics of ROMP in DCHMA, a  $\text{CO}_2$ -triggered switchable solvent, and a proposed strategy of removing and recycling the solvent is discussed in detail.

### 3.1 Ring opening metathesis polymerization in DCM

Considering the high reactivity of the Grubbs' catalyst used in this study, the best strategy of running ROMP in solution is preparing monomer solution and catalyst solution separately and then mixing them to trigger the reaction. A solution polymerization was carried out in a 25 mL reaction tube fitted with an N<sub>2</sub> inlet, a magnetic stir set at 900 rpm and a sampling valve. In a representative experiment using 1,5-cyclooctadiene (COD) as the monomer, degassed COD (0.5 g, 4.63 mmol) and PEGylated Grubbs' catalyst (9.8 mg, 0.0093 mmol) were charged separately in two flame-dried reaction tubes under inert atmosphere. 4 mL degassed DCM was then added to the monomer tube while 1 mL of degassed DCM was added to the catalyst tube. Both monomer and catalyst solutions were further degassed by additional freeze-pump-thaw cycles. The ROMP was triggered by mixing catalyst solution and monomer solution via cannula transfer. The reaction temperature was set at 0°C to slow down the reaction and facilitate the sampling. Each sample (0.5 mL) was quenched by a small amount of ethyl vinyl ether (0.05 mL).

### 3.2 Kinetic study of ring opening metathesis polymerization in solution

An effective method to examine the reactivity of a metathesis catalyst is through monitoring the ROMP of a low-strain cyclic olefin like 1,5-cyclooctadiene (COD) (strain energy = 55.6 kJ/mol). Each sample was quenched with ethyl vinyl ether (EVE); and the conversion was then estimated using <sup>1</sup>H NMR by comparing the intensities of vinyl peaks between the monomer (1,5-cyclooctadiene) and polymer (polybutadiene). Figure 3.1 indicates a 97% conversion within 12 hours to yield polybutadiene (PB), indicating the catalyst displayed high reactivity even at a low temperature (0 °C). The synthesized catalyst contains a saturated *N*-heterocyclic carbene (NHC) ligand and maintains the similar reactivity and functional group compatibility as Grubbs second and third generation catalysts since they are supposed to generate identical propagating species.

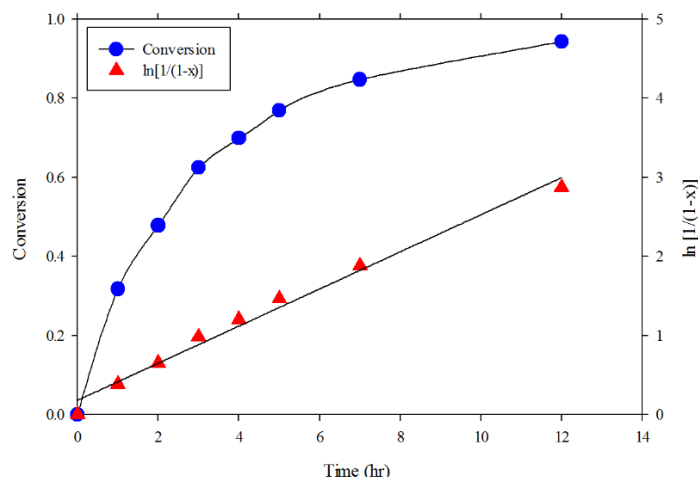


**Figure 3.1 Conversion (x) and  $\ln[1/(1-x)]$  plots for ROMP of 1,5-cyclooctadiene (COD) using PEGylated Grubbs Catalyst as catalyst. 0 °C, [monomer]/[catalyst] = 500:1, [Catalyst] = 1 mM,  $\text{CD}_2\text{Cl}_2$  as solvent. COD/Catalyst/ $\text{CD}_2\text{Cl}_2$  = 54 mg/1 mg/1.36 g (0.5 mmol/ $1 \times 10^{-3}$  mmol/15.6 mmol).**

### 3.2.1 Controlled character

According to Figure 3.1, a pseudo first-order kinetic profile was observed. Considering the high reactivity of Ru-based metathesis catalyst, here we assume a much faster initiation rate than propagation rate and a constant concentration of propagating chains ( $[Ru]$ ). Recall **Equation 3.1**:

$$R_p = -\frac{d[M]}{dt} = k_p[M][Ru] \quad \text{Equation 3.1}$$

By integration we get:

$$\ln\left(\frac{[M]_0}{[M]_t}\right) = \ln\left(\frac{1}{1-x}\right) = k_p[Ru]t \quad \text{Equation 3.2}$$

Where  $R_p$  is the rate of propagation,  $[Ru]$  is the concentration of living chains assuming every single catalyst will initiate one living chain,  $[M]_0$  and  $[M]_t$  are the concentrations of the monomer at time zero and t respectively, and x is conversion. The experimental value of  $k_p$  can be readily calculated as below:

$$k_p = \frac{\text{Slope}}{[Ru]} = \frac{0.2347 \text{ hr}^{-1}}{3600 \frac{\text{s}}{\text{hr}} \times 1 \times 10^{-3} \frac{\text{mol}}{\text{L}}} = 0.0652 \text{ L s}^{-1} \text{ mol}^{-1}$$

### 3.2.2 Number average molecular weight ( $M_n$ ) and molecular weight distribution (MWD)

According to the GPC data in Figure 3.2, the number average molecular weight ( $M_n$ ) of polymer product increased from 17,000 g/mol at 3% conversion to 36,000 g/mol at 97% conversion. At the early stages of reaction, the experimental data fit the calculated value and the catalyst efficiencies at conversions of 3% and 5% were calculated as 94.8% and 97.4% respectively, indicating almost all Ru complex has participated in the initiation process. At 50% conversion, however, an obvious deviation between the experimental  $M_n$  and theoretical  $M_n$  was identified. At the end of the reaction, the actual  $M_n$  was found only 2/3 of the calculated theoretical value, which suggested that a large number of new polymer chains were generated. Since almost all Ru complex had dissociated at the early stage, the new polymer chains were presumably generated by another mechanism other than initiation. Considering 1,4-polybutadiene, the product of this polymerization, is a linear polymer with low glass transition temperature ( $T_g$ ) and low steric hindrance, a secondary metathesis (or chain transfer) was suspected to occur synchronously during the polymerization<sup>5</sup> to generate more polymer chains than expected.

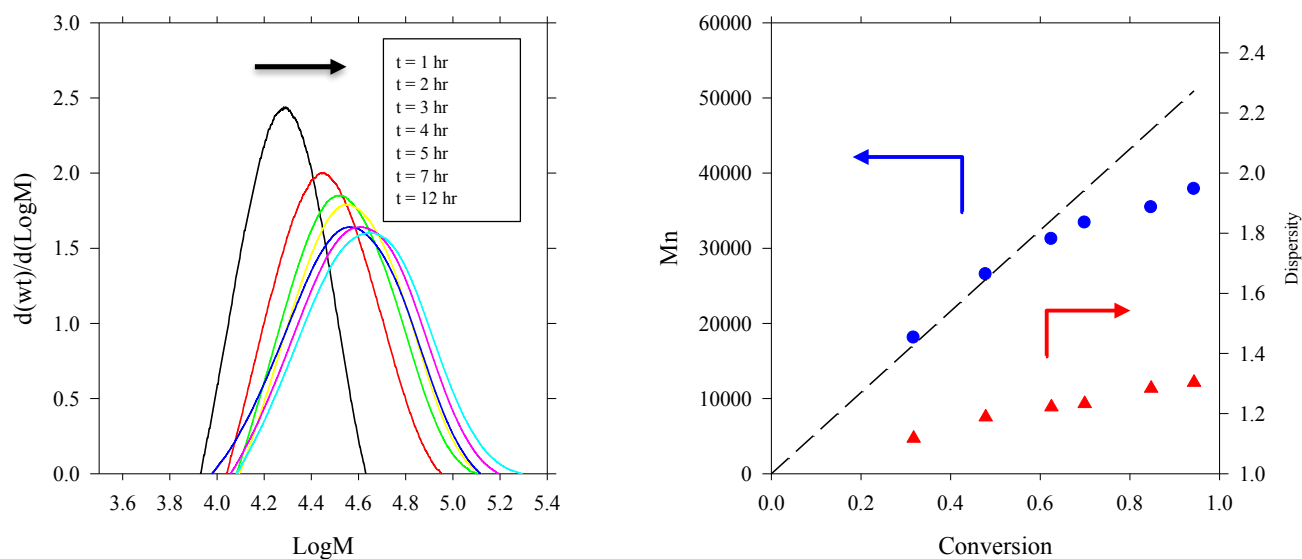


**Figure 3.2 Molecular weight distribution (MWD), molecular weight ( $M_n$ ) and dispersity ( $\mathbb{D}$ ) profiles for ROMP of COD. The experimental conditions were the same as in Figure 3.1.  $M_n$  and  $\mathbb{D}$  were measured by THF SEC relative to PS standards and corrected with Mark-Houwink parameters.**



### 3.3 ROMP in unconventional solvents

Ring-opening metathesis polymerization (ROMP) is a powerful tool to deliver precise and functional macromolecular architectures. Several categories of transition metal alkylidenes like Grubbs' catalysts<sup>6-8</sup> and Schrock catalysts<sup>9,10</sup> have been introduced to facilitate control over chain propagation. Although sophisticated synthetic strategies by ROMP have been available to allow many applications such as biomaterials<sup>11</sup>, liquid crystalline polymers<sup>12</sup>, self-healing materials<sup>13</sup>, and nanocomposites<sup>14</sup>, most examples were run in dichloromethane, toluene, and some other volatile organic compounds (VOCs) as non-coordinating solvents.<sup>1</sup> For industrial applications, the separation of ROMP products involves evaporation or distillation of VOCs, which may cause issues like increased risk of flammability, smog formation, and inhalation risks.

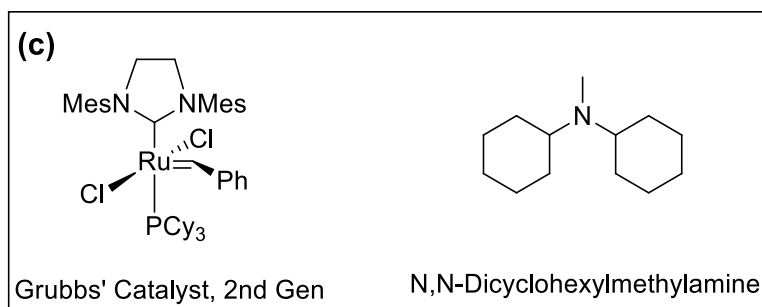
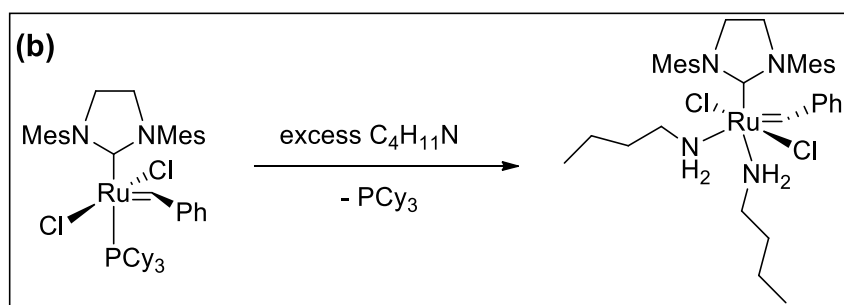
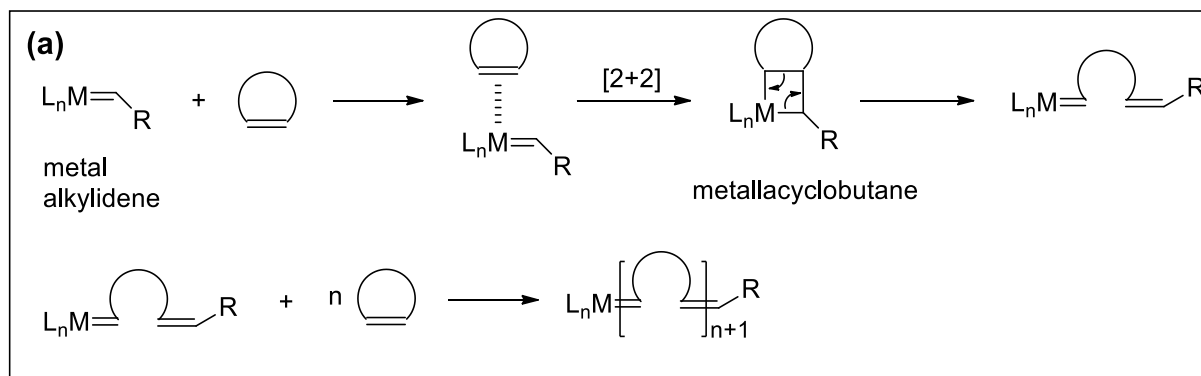
Several approaches using unconventional solvents as reaction media have been reported to overcome the limitation of VOCs. Vygodskii *et al.* conducted ROMP in neat ionic liquids (ILs) for synthesizing polymers with high molecular weights.<sup>15</sup> This approach did not lead to well-controlled polymerizations, and methanol was added to precipitate the polymer products due to the difficulty to evaporating ILs. Fürstner *et al.* introduced supercritical CO<sub>2</sub> (scCO<sub>2</sub>) as a clean reaction medium for ROMP.<sup>16</sup> The polymers could be readily isolated but this method required compressed CO<sub>2</sub> under high pressure. Some ruthenium catalysts could not be readily dissolved in scCO<sub>2</sub>, which might cause uncontrolled polymerization kinetics and broad distributions of molecular weight.<sup>16</sup>

We considered a switchable hydrophilicity solvent as an alternative medium to produce ROMP polymers with reduced environmental impact. A switchable hydrophilicity solvent (SHS) is a liquid that can switch between a hydrophilic form and hydrophobic form by adding or removing CO<sub>2</sub> {solvent (hydrophobic form) + H<sub>2</sub>O + CO<sub>2</sub> = [solvent·H<sup>+</sup>][HCO<sub>3</sub><sup>-</sup>] (hydrophilic form)}.<sup>17</sup> It has been well studied for the extraction of organic products from biomass.<sup>18</sup> To our knowledge, no one has pursued ROMP in a SHS,

assumedly due to the potential interaction between amine-containing compounds and transition metal-based species. The scope of our contribution is to eliminate multiple separation steps and recycle the solvents by selecting the SHS with minimal side effects, so that ROMP can be performed directly in a CO<sub>2</sub>-switchable system without out any VOC involved.

### **3.4 ROMP of 1,5-cyclooctadine (COD) in *N,N*-Dicyclohexylmethylamine (DCHMA)**

Since amines can reportedly coordinate to the metal center of metathesis catalysts and interfere with catalytic activity (Scheme 3.1 (b))<sup>19</sup>, several considerations were taken to minimize this side effect. First, the stability of the well-known second generation Grubbs' catalyst (G2) with N-heterocyclic carbene (NHC) is higher than the first generation catalyst (G1) because the NHC group cannot be easily displaced by amines. Secondly, when using amine-containing substrates, the majority of successful metathesis reactions were performed with hindered tertiary amines because the steric hindrance prevents the amine from coordinating to the transition metal center.<sup>20</sup> Thirdly, a bulky group on a neighboring atom can be introduced to further increase steric hindrance and minimize the coordination. Therefore, we chose second generation Grubbs' catalyst (G2) as the catalyst and DCHMA as the solvent in our study (Scheme 3.1 (c)).



**Scheme 3.1 (a) Mechanism of ROMP; (b) The formation of a ruthenium-amine complex;<sup>19</sup> (c) The catalyst (2<sup>nd</sup> generation Grubbs' catalyst) and SHS (*N,N*-dicyclohexylmethylamine) employed in this study.**

### 3.5 Experimental Procedures for ROMP in SHS

All reagents were purchased from Sigma-Aldrich and used without further purification unless otherwise specified. Grubbs' second generation catalyst (G2) was received from Materia Inc.. All the solvents used in this study were degassed through freeze-pump-thaw cycles. Prior to polymerization, the monomer was purified by passing through basic alumina. <sup>1</sup>H NMR was recorded on a 400 MHz Bruker Avance-400 spectrometer. The conversion was determined by integration of multiplet signals at  $\delta = 5.51$  ppm (m,

monomer) and 5.46 ppm (m, polymer).<sup>21</sup> Molecular weight and molecular weight distribution were determined by size exclusion chromatography (SEC) relative to polystyrene standards on a Waters 2695 separations module combined with Waters 410 differential refractometer.

A typical polymerization was carried out at room temperature in a 25 mL reaction tube fitted with an argon inlet, a magnetic stir and a sampling valve. In a representative experiment, G2 (9.8 mg, 0.0093 mmol) was charged in the flame-dried reaction tubes under inert atmosphere. The degassed SHS (5 mL) was then added to the tube to fully dissolve the catalyst. The catalyst solution was further degassed by additional freeze-pump-thaw cycles. The ROMP was triggered by injecting degassed COD (0.5 g, 4.63 mmol) into catalyst solution. Each sample was quenched by ethyl vinyl ether.

After the polymerization, the polymer solution was collected and a 10 eq volume of water was added. The biphasic mixture was subjected to CO<sub>2</sub> bubbling until the amine and water layers combined, leaving the polymer layer floating at the surface or stuck to the glass wall of the tube. The polymer layer was then carefully collected, washed with water, dried under open air and dissolved in CDCl<sub>3</sub> for NMR analysis. The hydrophilic protonated SHS/water mixture was separated into its respective amine and aqueous layers by bubbling argon and sitting over night until the two layers were resolved.

### **3.6 Catalyst reactivity and reaction kinetics**

Two experiments were run with different monomer concentrations. The amount of SHS in entry 2 was five times larger than entry 1 (Table 3.1). The molar ratio of monomer versus catalyst was 463:1 for both cases so that the theoretical molecular weights were the same (50,000 g/mol). Other factors like temperature (25 °C) and stirring rate were also kept the same. Both catalyst (G2) and monomer (COD) were completely soluble in DCHMA so that the polymerizations were performed in a homogeneous system. Each sample was quenched with ethyl vinyl ether (EVE) and the conversion was estimated by

comparing the intensities of vinyl peaks between the monomer and polymer. Detailed NMR spectra and assignments are found in supporting information.

**Table 3.1 Experimental conditions of ROMP of COD in DCHMA at 25 °C initiated by 2<sup>nd</sup> generation Grubbs' catalyst.**

Entry	SHS (mL)	Monomer (g)	[M]/[C]	Theoretical $M_n$	Catalyst (mg)
1	1	0.216	463	50,000	3.7
2	5	0.216	463	50,000	3.7

Figure 3.3 shows both reactions were able to achieve full conversion to yield polybutadiene (PB), indicating that the catalyst with a *N*-heterocyclic carbene (NHC) ligand maintained the reactivity and functional group compatibility instead of being deactivated. By comparing entry 1 and entry 2, the polymerization rate decreased when using a diluted catalyst concentration. By comparing our study with the results in commonly used solvents like DCM,<sup>22</sup> the polymerization rate of COD was slower in DCHMA, suggesting the amine groups present in the system may alter the phosphane dissociation so that the chain propagation was affected.

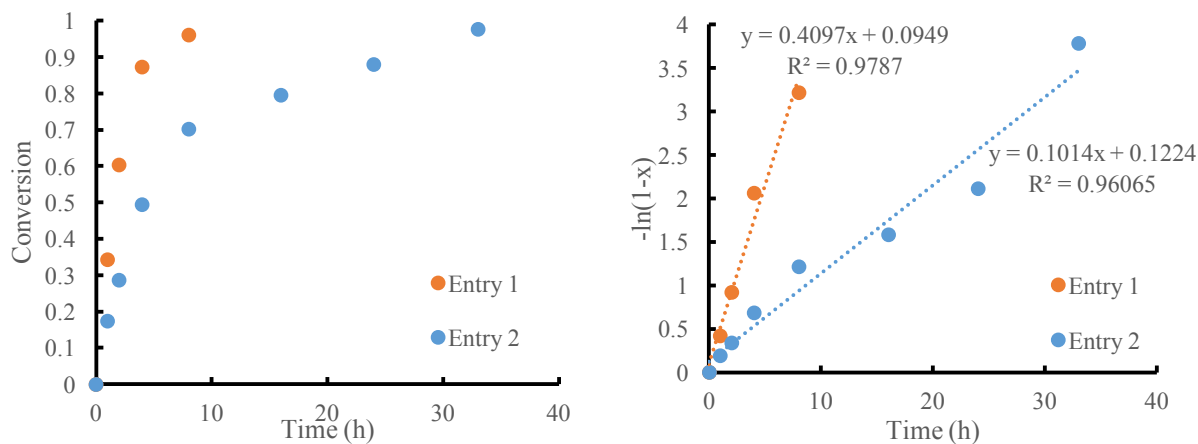


**Figure 3.3 Conversion (x) and  $-\ln(1-x)$  plots for ROMP of 1,5-cyclooctadiene (COD) in DCHMA.**

Previous literature in ILs, and scCO<sub>2</sub> did not lead to a well-controlled polymerization and little has been done to study reaction kinetics, although this topic is extremely important in understanding the behavior of the catalyst. In this study, pseudo first-order kinetics was observed for both experiments (Figure 3.3). According to Equation 3.1 and 3.2, the experimental value of  $k_p$  can be readily calculated as 0.026 mol·L<sup>-1</sup>·min<sup>-1</sup> for entry 1 and 0.032 mol·L<sup>-1</sup>·min<sup>-1</sup>. Note that  $k_p$  is temperature-dependent and ideally not affected by monomer concentrations. Thus the disparity of two values indicates the unreliability of some assumptions. For instance, the value of  $[Ru]$  may not be exactly the same as initial concentration of catalyst and may vary from case to case.

### 3.7 Molecular weight and molecular weight distribution

Figure 3.4 shows the evolution of number average molecular weight ( $M_n$ ) with conversion. Interestingly, entry 1 and entry 2 demonstrated different behavior although they were designed with the same theoretical  $M_n$ . For entry 1, the  $M_n$  increased from 29,300 g/mol at 35% conversion to 41,100 g/mol at 96% conversion; whereas for entry 2 the  $M_n$  increased from 10,100 g/mol at 29% conversion to 16,000 g/mol at 80% conversion. For the final products of both entry 1 and entry 2, the experimental values of  $M_n$  were smaller than targeted value, indicating more chains were generated. Since almost all Ru complex had dissociated at the early stage, the new polymer chains were presumably generated by a secondary metathesis (or chain transfer).<sup>5</sup> Using more solvent in entry 2 generally slowed down the chain propagation and provided a longer polymerization time, which facilitated intra-molecular chain transfer. In addition, for both entries the dispersity values were maintained at around 1.5-1.6, a consequence of multiple factors mentioned above like solvent effects and chain transfer.

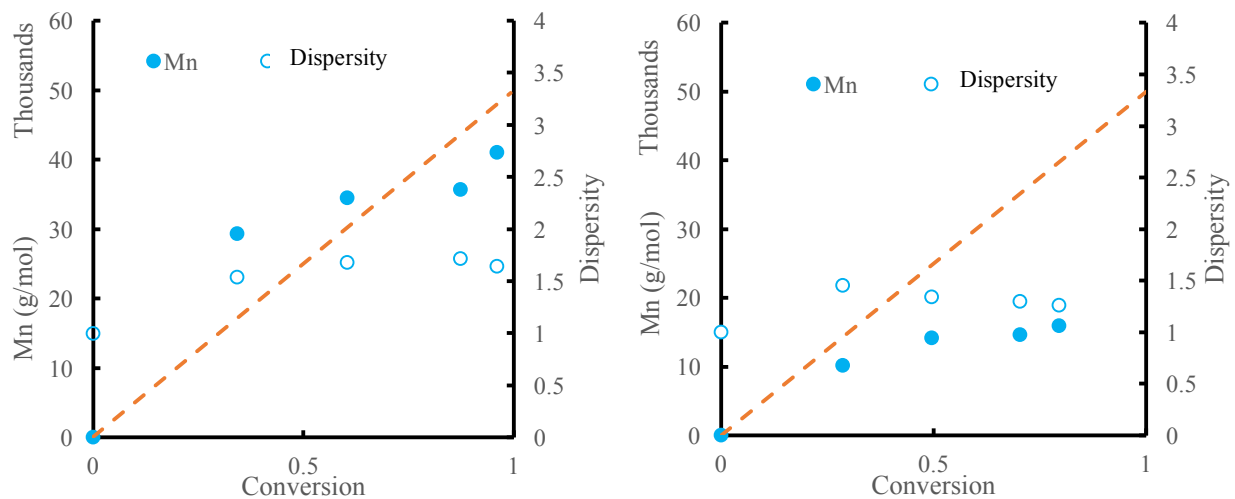


**Figure 3.4**  $M_n$  vs conversion profile for entry 1 (left) and entry 2 (right). The dot lines indicate the theoretical values of molecular weights.

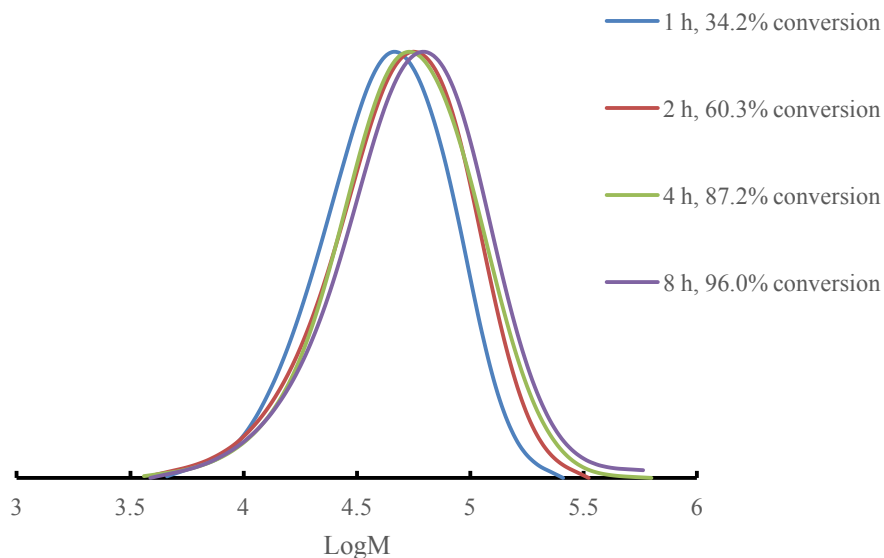


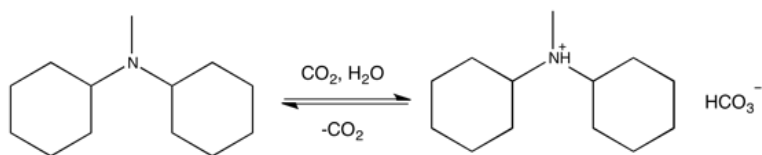
**Figure 3.5** Evolution of normalized SEC traces for entry 1.

The SEC traces in Figure 3.5 shows a reasonable livingness and control of molecular weight during polymerization, suggesting the chain propagation was not totally deactivated by the existence of amine-containing groups.

### 3.8 Removal and recycling of SHS

In a typical solution polymerization in DCHMA, a homogeneous polymer solution is obtained at the end of the polymerization. Water was then added to form a biphasic mixture. The solvent, DCHMA, was protonated by bubbling  $\text{CO}_2$  (Scheme 3.2) so that a pure polymer product (Figure 3.6 (a)) was obtained.

Two conditions were chosen to increase extraction of the SHS into the water phase: (a) a large amount of water was added (Water: SHS = 10:1, v/v), (b) the bubbling time for  $\text{CO}_2$  was extended to as long as 45 min. The NMR spectra indicated pure polymer products can be obtained under these conditions considering the error ( $\sim 1\%$ ) for NMR measurement.



**Scheme 3.2 Protonation and deprotonation of N,N-dicyclohexylmethylamine (DCHMA).**

After collecting the polymer products, a solution of protonated SHS (Figure 3.6 (b)) in water was left. The SHS was then switched back to hydrophobic form by simply bubbling argon for another 45 min. The deprotonated form of SHS (Figure 3.6 (c)) could be recovered except a tiny amount of protonated SHS in water (Figure 3.6 (d)).



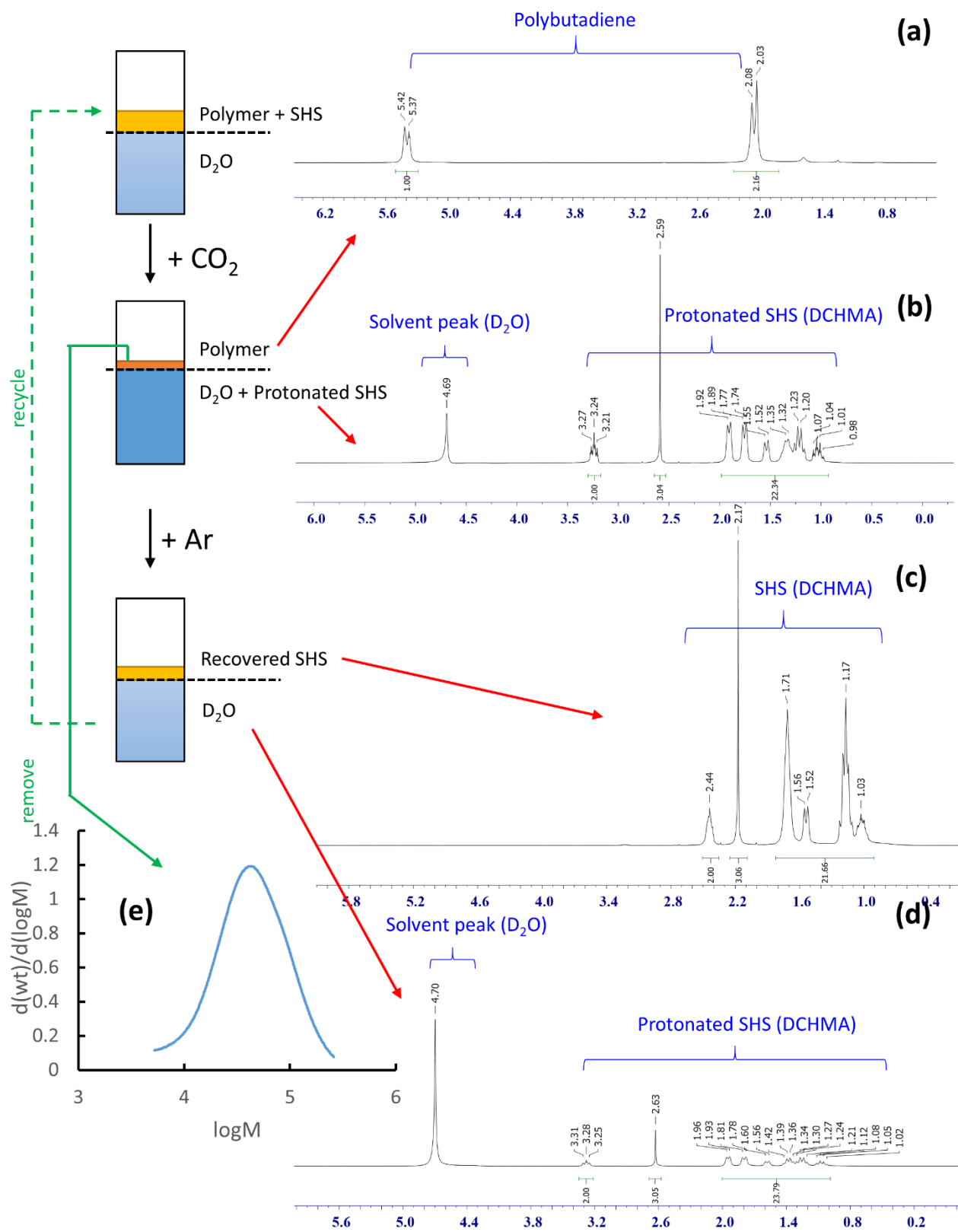


**Figure 3.6 Removal and recycling of SHS by biphasic extraction. (a)  $^1\text{H}$  NMR of pure polybutadiene ( $\text{CDCl}_3$  as NMR solvent) after bubbling  $\text{CO}_2$ ; (b)  $^1\text{H}$  NMR of extracted SHS in  $\text{D}_2\text{O}$ . SHS was fully extracted into water and protonated; (c)  $^1\text{H}$  NMR of recovered SHS, the SHS was deprotonated ( $\text{CDCl}_3$  as NMR solvent); (d)  $^1\text{H}$  NMR of recovered  $\text{D}_2\text{O}$  with a small amount of residual protonated SHS inside. (e) THF SEC trace of final polymer product.**

It is difficult to fully switch off DCHMA unless enough time is given to bubble argon. In most cases, a tiny amount of solvent may always stay protonated in the water phase (Figure 3.6 (d)). However, considering that the function of water is to extract the SHS, it is not necessary to achieve a full recovery of SHS and the water containing trace amounts of protonated SHS can be reused multiple times. In conclusion, ROMP can be used to make polymer in a homogeneous system using DCHMA as solvent and after collecting the final products, the SHS can be readily recycled via a water/oil biphasic system.

### **3.9 Conclusion**

This chapter demonstrates the concept of homogeneous ROMP by Grubbs catalysts with NHC ligands in a conventional solvent and a switchable hydrophilicity solvent. DCHMA was selected as a SHS with minimal interaction with the transition metal center on the metathesis catalyst. Although the polymerization rate varies with different catalyst concentration, the livingness of ROMP in the SHS was demonstrated. This is the first example reported to run ROMP in a SHS.

### 3.10 References

- (1) Sanford, M. S.; Love, J. A.; Grubbs, R. H. Mechanism and Activity of Ruthenium Olefin Metathesis Catalysts. *J. Am. Chem. Soc.* **2001**, *123* (27), 6543–6554.
- (2) Kendall, J. L.; Canelas, D. a.; Young, J. L.; DeSimone, J. M. Polymerizations in Supercritical Carbon Dioxide. *Chem. Rev.* **1999**, *99* (2), 543–564.
- (3) Kubisa, P. Application of Ionic Liquids as Solvents for Polymerization Processes. *Prog. Polym. Sci.* **2004**, *29* (1), 3–12.
- (4) Jessop, P. G.; Mercer, S. M.; Heldebrant, D. J. CO<sub>2</sub>-Triggered Switchable Solvents, Surfactants, and Other Materials. *Energy Environ. Sci.* **2012**, *5* (6), 7240.
- (5) Chen, Z.-R.; Claverie, J. P.; Grubbs, R. H.; Kornfield, J. a. Modeling Ring-Chain Equilibria in Ring-Opening Polymerization of Cycloolefins. *Macromolecules* **1995**, *28*, 2147–2154.
- (6) Schwab, P.; Grubbs, R. H.; Ziller, J. W. Synthesis and Applications of RuCl<sub>2</sub>(CHR')(PR<sub>3</sub>)<sub>2</sub>: The Influence of the Alkylidene Moiety on Metathesis Activity. *J. Am. Chem. Soc.* **1996**, *118* (1), 100–110.
- (7) Scholl, M.; Ding, S.; Lee, C. W.; Grubbs, R. H. Synthesis and Activity of a New Generation of Ruthenium-Based Olefin Metathesis Catalysts Coordinated with 1,3-Dimesityl-4,5-Dihydroimidazol-2-ylidene Ligands. *Org. Lett.* **1999**, *1* (6), 953–956.
- (8) Love, J. A.; Morgan, J. P.; Trnka, T. M.; Grubbs, R. H. A Practical and Highly Active Ruthenium-Based Catalyst That Effects the Cross Metathesis of Acrylonitrile. *Angew. Chem. Int. Ed. Engl.* **2002**, *41* (21), 4035–4037.
- (9) Schrock, R. R. High-Oxidation-State Molybdenum and Tungsten Alkylidyne Complexes. *Acc. Chem. Res.* **1986**, *19* (11), 342–348.
- (10) Schrock, R. R. High Oxidation State Alkylidene and Alkylidyne Complexes. *Chem. Commun.*

(Camb). **2005**, No. 22, 2773–2777.

- (11) Wathier, M.; Lakin, B. A.; Bansal, P. N.; Stoddart, S. S.; Snyder, B. D.; Grinstaff, M. W. A Large-Molecular-Weight Polyanion, Synthesized via Ring-Opening Metathesis Polymerization, as a Lubricant for Human Articular Cartilage. *J. Am. Chem. Soc.* **2013**, *135* (13), 4930–4933.
- (12) Haque, H. A.; Kakehi, S.; Hara, M.; Nagano, S.; Seki, T. High-Density Liquid-Crystalline Azobenzene Polymer Brush Attained by Surface-Initiated Ring-Opening Metathesis Polymerization. *Langmuir* **2013**, *29* (25), 7571–7575.
- (13) White, S. R.; Sottos, N. R.; Geubelle, P. H.; Moore, J. S.; Kessler, M. R.; Sriram, S. R.; Brown, E. N.; Viswanathan, S. Correction: Autonomic Healing of Polymer Composites. *Nature* **2002**, *415* (6873), 817–817.
- (14) Kalluru, S. H.; Cochran, E. W. Synthesis of Polyolefin/layered Silicate Nanocomposites via Surface-Initiated Ring-Opening Metathesis Polymerization. *Macromolecules* **2013**, *46*, 9324–9332.
- (15) Vygodskii, Y. S.; Shaplov, A. S.; Lozinskaya, E. I.; Filippov, O. A.; Shubina, E. S.; Bandari, R.; Buchmeiser, M. R. Ring-Opening Metathesis Polymerization (ROMP) in Ionic Liquids: Scope and Limitations. *Macromolecules* **2006**, *39* (23), 7821–7830.
- (16) Fürstner, A.; Ackermann, L.; Beck, K.; Hori, H.; Koch, D.; Langemann, K.; Liebl, M.; Six, C.; Leitner, W. Olefin Metathesis in Supercritical Carbon Dioxide. *J. Am. Chem. Soc.* **2001**, *123* (37), 9000–9006.
- (17) Durelle, J.; Vanderveen, J. R.; Quan, Y.; Chalifoux, C. B.; Kostin, J. E.; Jessop, P. G. Extending the Range of Switchable-Hydrophilicity Solvents. *Phys. Chem. Chem. Phys.* **2015**, *17* (7), 5308–5313.
- (18) Boyd, A. R.; Champagne, P.; McGinn, P. J.; MacDougall, K. M.; Melanson, J. E.; Jessop, P. G. Switchable Hydrophilicity Solvents for Lipid Extraction from Microalgae for Biofuel Production.

*Bioresour. Technol.* **2012**, *118*, 628–632.

- (19) Wilson, G. O.; Porter, K. a.; Weissman, H.; White, S. R.; Sottos, N. R.; Moore, J. S. Stability of Second Generation Grubbs' Alkylidenes to Primary Amines: Formation of Novel Ruthenium-Amine Complexes. *Adv. Synth. Catal.* **2009**, *351* (11-12), 1817–1825.
- (20) Compain, P. Olefin Metathesis of Amine-Containing Systems: Beyond the Current Consensus. *Adv. Synth. Catal.* **2007**, *349* (11-12), 1829–1846.
- (21) P'Pool, S. J.; Schanz, H. J. Reversible Inhibition/activation of Olefin Metathesis: A Kinetic Investigation of ROMP and RCM Reactions with Grubbs' Catalyst. *J. Am. Chem. Soc.* **2007**, *129* (46), 14200–14212.
- (22) Ligands, N. C.; Bielawski, C. W.; Grubbs, R. H. Highly Efficient Ring-Opening Metathesis Polymerization ( ROMP ) Using New Ruthenium Catalysts Containing. **2000**, 2903–2906.

### 3.11 Supporting Information

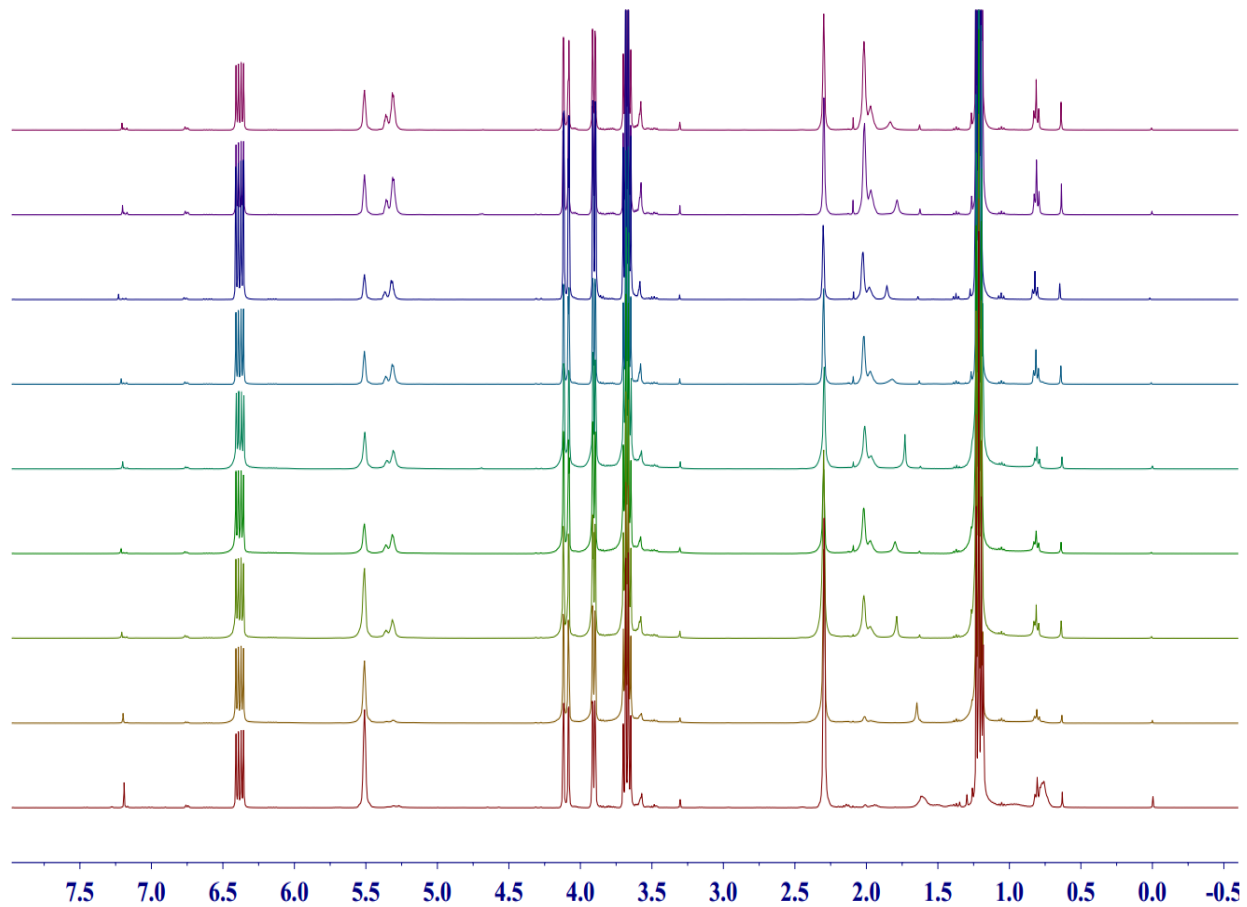


**Figure S1** <sup>1</sup>H NMR spectra for solution ROMP of 1,5-cyclooctadiene (COD) using PEGylated Grubbs' catalyst as catalyst. 0 °C, [monomer]/[catalyst] = 500:1 (molar ratio), [Catalyst] = 1 mM, CD<sub>2</sub>Cl<sub>2</sub> as solvent. COD/Catalyst/CD<sub>2</sub>Cl<sub>2</sub> = 54 mg/1 mg/1.36 g (0.5 mmol/1×10<sup>-3</sup> mmol/15.6 mmol).

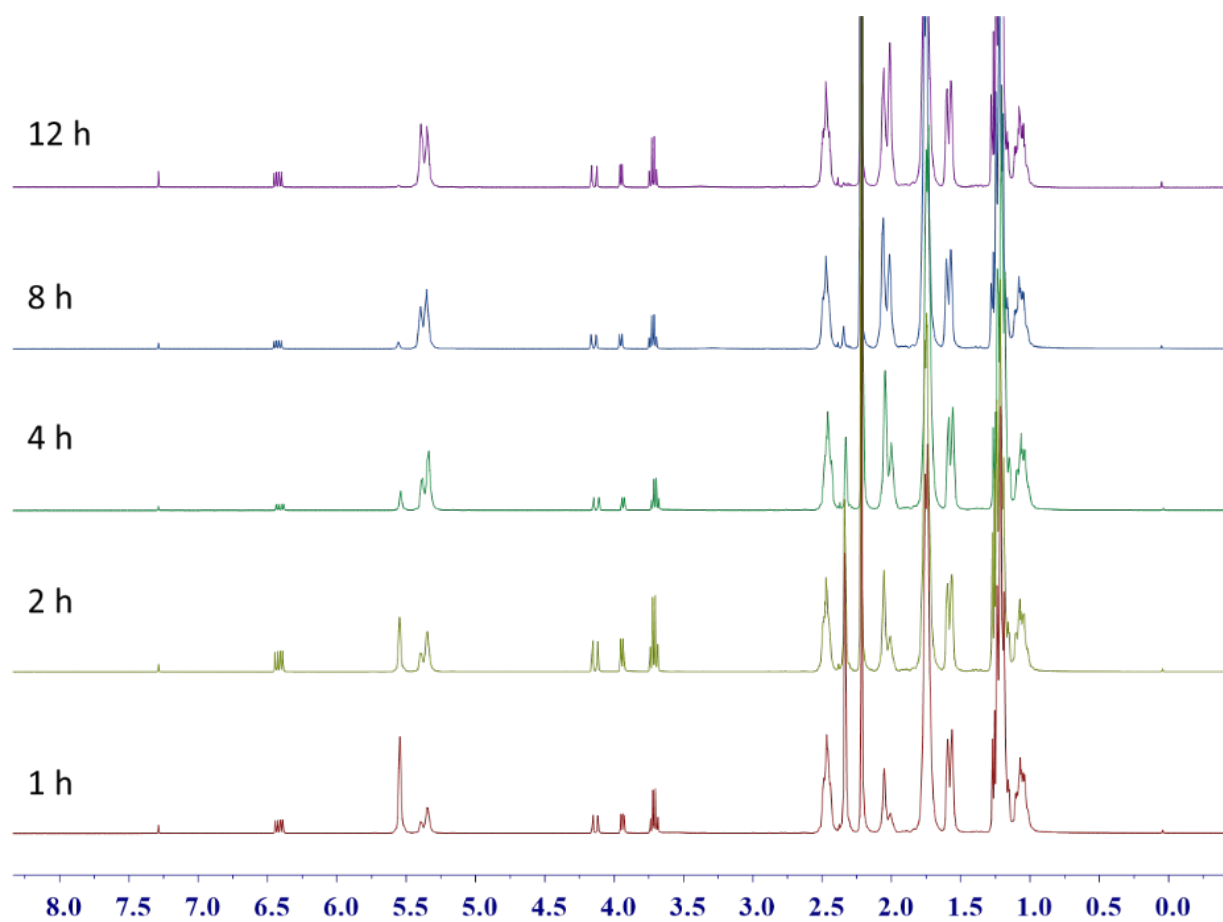


**Figure S2 <sup>1</sup>H NMR for ROMP in a CO<sub>2</sub>-triggered switchable solvent (Entry 1).**

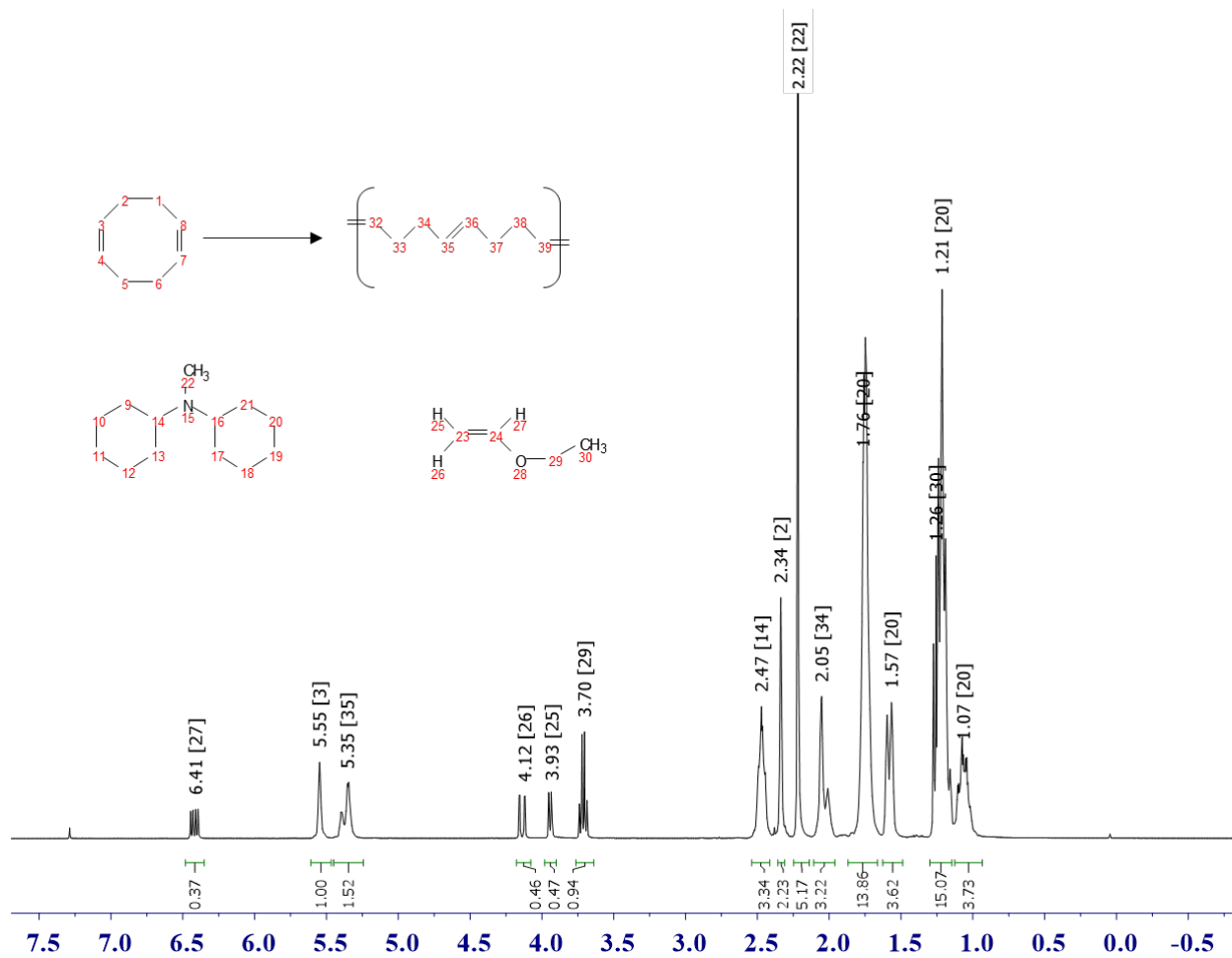


Figure S3  $^1\text{H}$  NMR assignment for peaks in Figure S1.



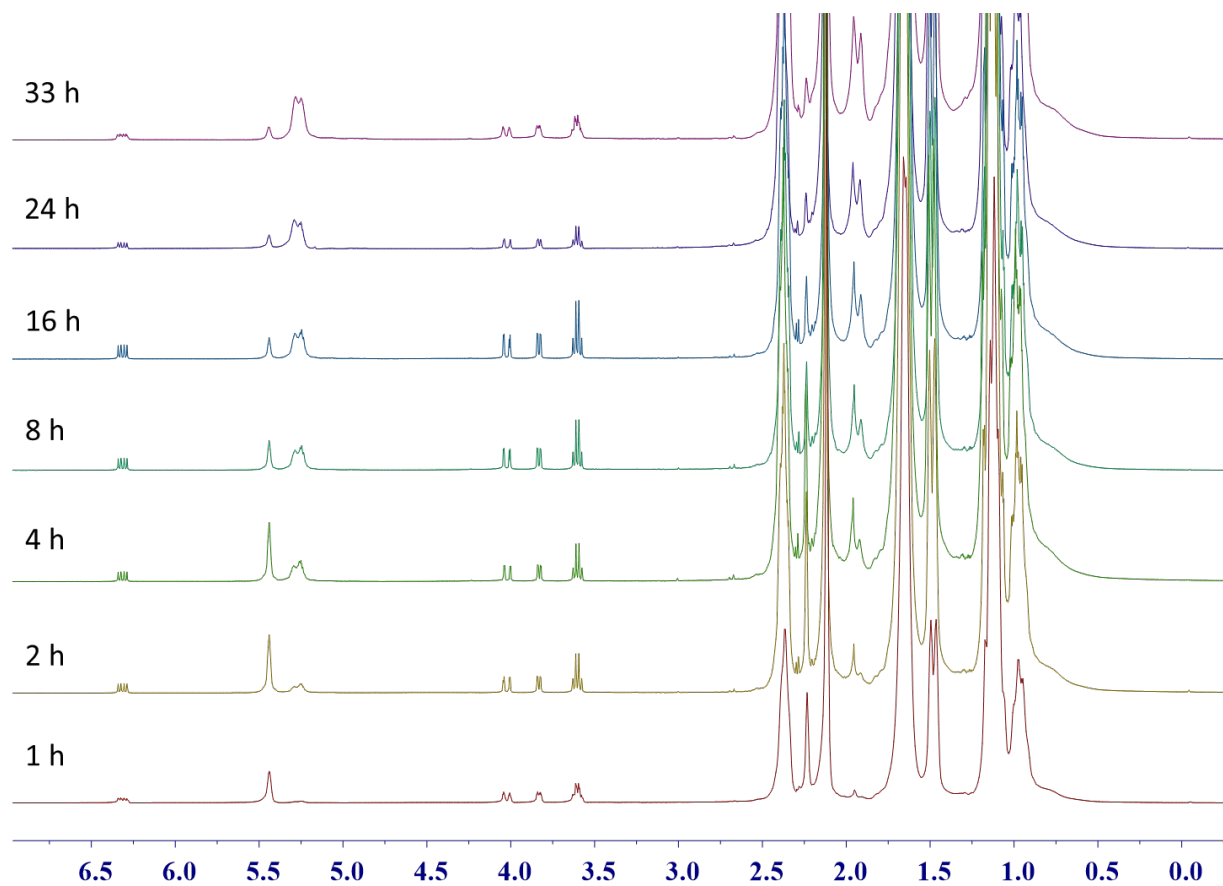


Figure S4  $^1\text{H}$  NMR for ROMP in a switchable solvent (Entry 2).

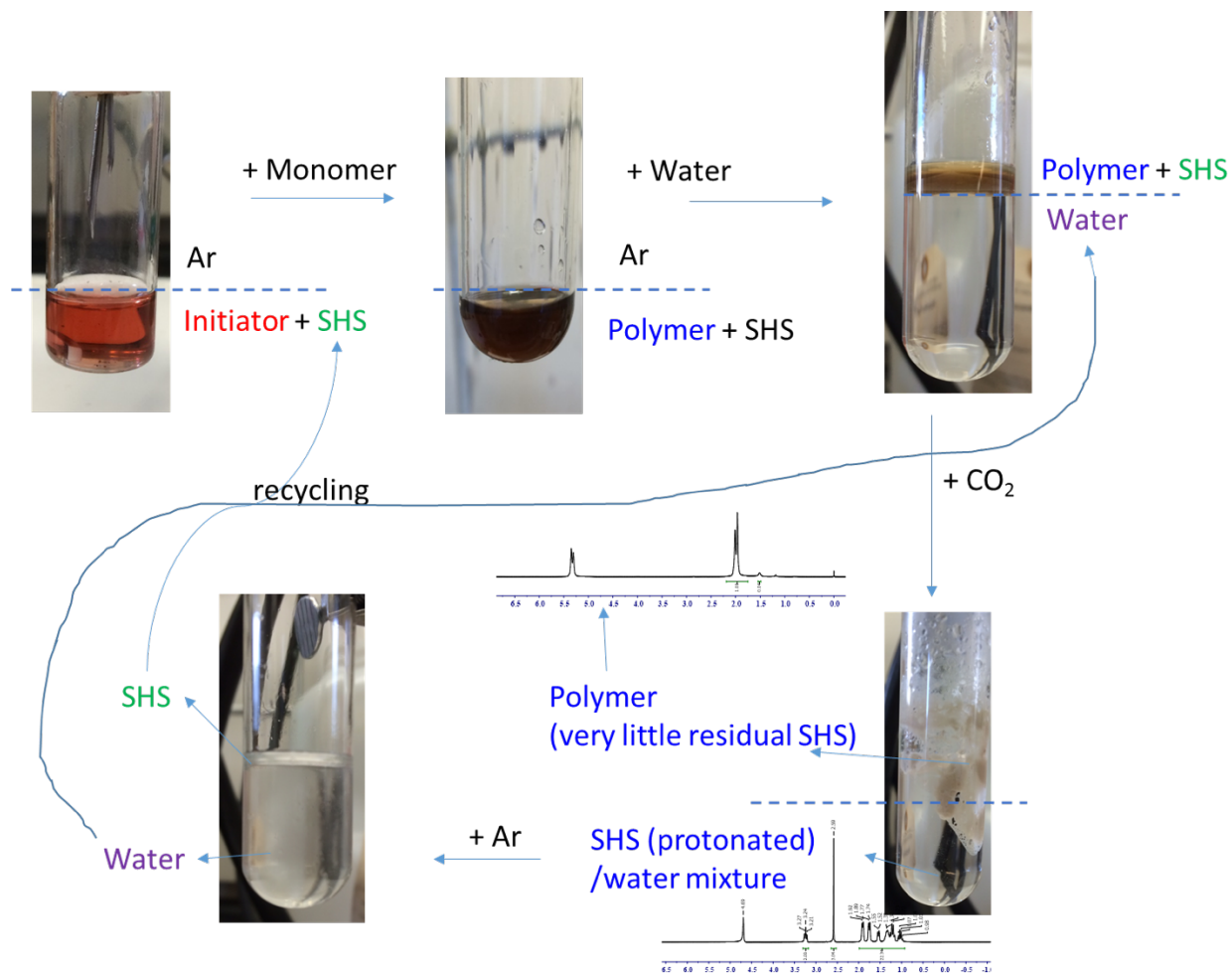


Figure S5 Extraction of ROMP polymers from SHS and the recycling of SHS and water.

# Chapter 4 Ring opening metathesis polymerization in miniemulsion using PEGylated ruthenium-based metathesis catalyst

## 4.1 Preface

As the main focus of my PhD research, this study aims to conduct ROMP in miniemulsion using a PEGylated ruthenium-based metathesis catalyst to eliminate the use of organic solvents in a ROMP process. Previously the Crudden laboratory had synthesized and purified a PEGylated metathesis catalyst. In 2013, I started working with this catalyst, showing for the first time that it could be used in a miniemulsion system. As the first successful example in this area, this chapter was completed by showing that stable and well-defined latex particles could be obtained with nearly full conversion by running miniemulsion ROMP at room temperature. The experimental results including  $^1\text{H}$  NMR spectra and GPC traces are found in Supporting Information.

## 4.2 Abstract

Ring opening metathesis polymerization (ROMP) of 1,5-cyclooctadiene (COD) in miniemulsion was conducted utilizing a water-soluble PEGylated ruthenium alkylidene as the catalyst. The highly efficient catalyst yielded colloiddally stable polymer latexes with ~ 100% conversion in 1 hour. Kinetic studies revealed first-order kinetics with excellent livingness as confirmed by the shift of gel permeation chromatography (GPC) traces. Depending on the surfactants used, the particle sizes ranged from 100 to 300 nm with monomodal distributions. More strained cyclic olefins norbornene (NB) could also be efficiently polymerized in miniemulsion with full conversion and without coagulum formation.

## 4.3 Introduction

Since the origin of olefin metathesis in the mid-1950s, ring opening metathesis polymerization (ROMP) has been recognized as an efficient technique to prepare highly unsaturated polymeric materials with narrow molecular weight distributions.<sup>1</sup> Ruthenium-based metathesis catalysts are employed extensively in ROMP due to their tolerance to air, moisture, and various functional groups.<sup>2</sup> These features allow

potential applications of ROMP in many fields such as biomaterials,<sup>3</sup> liquid crystalline polymers,<sup>4</sup> self-healing materials,<sup>5</sup> degradable plastics,<sup>6</sup> and nanocomposites.<sup>7</sup> To date, most reports of ROMP are conducted in dichloromethane, toluene, and other non-coordinating organic solvents.<sup>8</sup> However, little attention has been given so far to extend ROMP in aqueous dispersed systems from the viewpoint of eco-friendly chemical processes.

Polymerization in an aqueous dispersed system offers numerous advantages. Introducing water as the continuous phase largely reduces the environmental impact and health concerns associated with using organic solvents. A dispersed system also improves heat transfer, decreases viscosity, and minimizes the cost of post-reaction separations.<sup>9</sup> Common subtypes of dispersed-phase polymerization, such as emulsion polymerization<sup>10</sup> and miniemulsion polymerization<sup>11</sup>, have been highly successful in free radical polymerization (FRP)<sup>12,13</sup> and some types of controlled/living radical polymerization (CLRP).<sup>14,15</sup> However, reports related to ROMP in dispersed systems are less common. In the limited publications on this topic, the polymerization was typically characterized by low yields and poor control,<sup>16,17</sup> poor colloidal stability,<sup>18,19</sup> and in some cases a large amount of coagulum.<sup>20,21</sup>

Early attempts showed that hydrates of Ru chlorides could polymerize norbornene (NB) in emulsion with low yields,<sup>16</sup> likely due to the ineffective generation of catalytically active species. With the rise in popularity of Grubbs' catalysts, Claverie *et al.* introduced a hydrophilic Ru alkylidene in emulsion ROMP by modifying the phosphorous-based labile ligands of Grubbs' first-generation catalyst (G1).<sup>18</sup> Polynorbornene (PNB) nanoparticles (50 ~ 100 nm) were obtained by emulsion polymerization with high yield, but the resulting latex was prone to flocculation. Alternatively, by modifying the benzylidene moiety of G1, Quemener *et al.* synthesized PNB and polybutadiene (PB) nanoparticles in alcoholic or aqueous media via dispersion and suspension ROMP.<sup>20</sup> However, a large amount of coagulum was observed, and the polymer properties were irreversibly modified by the incorporation of functional groups into the resulting polymer. The inadequate polymerization rates and low level of control of the

polymerization are largely because most of the work to date was carried out based on the 1990 generation catalysts, however significant improvements in catalyst activity have taken place in the last 20 years.

Fully realizing the benefits of well-defined metathesis catalysts in aqueous dispersed systems requires solubilizing the catalysts in water with appropriate hydrophilic ligands. Due to the difficulty of dissociating a non-polar phosphorous-based ligand from the coordination sphere of Ru in water,<sup>22,23</sup> the promising examples of polar metathesis catalysts are complexes in which these phosphorous-based ligands are absent.<sup>24</sup> With the goal of developing a tuned catalyst that is able to initiate in water, but then diffuse to and react in the growing (hydrophobic) polymer droplets, we approached the water solubilization of ruthenium NHC catalysts from the standpoint of the labile pyridine ligands associated with Grubbs' third-generation catalyst (G3). This approach has also been explored by Emrick *et al.*, although their multistep synthetic strategy gave a low yield of unpurified mixture with excess ligands.<sup>25,26</sup>

We synthesized and purified a PEGylated ruthenium-based catalyst by a simple and efficient strategy. The obtained PEGylated catalyst was readily dissolved in the aqueous phase of a miniemulsion system and became hydrophobic upon the dissociation of PEG-tagged pyridines. The activated catalyst subsequently diffused to the submicron monomer droplets, where the remainder of the polymerization occurred. Due to a good tolerance and high efficiency of the catalyst in a polar environment, latex particles ranging from 100 to 300 nm were produced with ~100% conversion. This is the first report of latex formation by using water-soluble ruthenium catalyst in miniemulsion via ROMP. The reaction kinetics, evolution of molecular weight and the colloidal characteristics of the miniemulsion polymerization were investigated in detail. The effects of surfactants, catalyst loading, and monomer content are also discussed.

## **4.4 Experimental section**

### **4.4.1 Materials**

All reagents were purchased from Sigma-Aldrich and used without further purification unless otherwise specified. Grubbs second-generation catalyst (G2) was received from Materia Inc. All solvents and monomers used in this study were degassed through freeze-pump-thaw cycles and stored in a glovebox filled with argon prior to use. All manipulations were performed under argon using Schlenk techniques.

#### 4.4.2 Characterization

$^1\text{H}$  NMR and  $^{13}\text{C}$  NMR were recorded on a 400 MHz Bruker Avance-400 spectrometer. Monomer conversion was determined by  $^1\text{H}$  NMR. Molecular weight and molecular weight distribution were determined by Gel Permeation Chromatography (GPC) relative to polystyrene standards on a Waters 2695 separations module combined with Waters 410 differential refractometer. THF was used as eluent and molecular weights were corrected according to Mark–Houwink parameters.<sup>27</sup> Mark–Houwink parameters were used for polybutadiene ( $a = 0.74$  and  $K = 0.000256$  dl/g)<sup>28</sup> and polynorbornene ( $a = 0.68$  and  $K = 0.000099$  dl/g).<sup>29</sup> Particle size distributions were determined by Dynamic Light Scattering (DLS) on a Zetasizer Nano ZS from Malvern Instruments at 25 °C with a 173° scattering angle.

#### 4.4.3 Synthesis of PEGylated Ru-based metathesis catalyst

2,5,8-tetraoxatridecan-10-yl 4-methylbenzenesulfonate (complex 1)

Triethylene glycol mono-methyl ether (12.80 mL, 80 mmol) and *p*-toluenesulfonyl chloride (16.0 g, 84 mmol) were dissolved in DCM, followed by the addition of powdered KOH (18.0 g, 320 mmol) slowly at 0 °C. After stirring for 5 hours (below 5 °C), the reaction mixture was quenched with water. The product was extracted into DCM, washed with brine, dried over  $\text{MgSO}_4$ , and used without further purification.

Yield: 25.2g, 99%.  $^1\text{H}$  NMR (400 MHz,  $\text{CDCl}_3$ , ppm): 7.80 - 7.82 (dd, 2H), 7.34 - 7.37 (dd, 2H), 4.16 - 4.19 (tr, 2H), 3.69 - 3.71 (tr, 2H), 3.60 - 3.63(m, 6H), 3.53 - 3.55 (tr, 2H), 3.38 (s, 3H) 2.56 (s, 3H);  $^{13}\text{C}$  NMR (400MHz,  $\text{CDCl}_3$ , ppm):  $\delta$  144.77, 133.09, 129.81, 127.97, 71.91, 70.75, 70.56, 70.55 69.22, 68.67, 59.01. 21.62. HRMS (ESI)  $m/z$ : calc., 318.1137; found, 318.1129.

4-(2,5,8-trioxatridecan-10-yl-oxy) pyridine (complex 2)

2,5,8-Trioxatridecan-10-yl 4-methylbenzenesulfonate (9.5 g, 30 mmol), CsCO<sub>3</sub> (19.5 g, 60 mmol) and 4-hydroxypyridine (6.0 g, 60 mmol) were dissolved in dry DMF. The reaction mixture was refluxed for 48 hours under argon, and DMF was removed under vacuum. Water and DCM were then added to the crude reaction mixture. The product was extracted into DCM, washed with brine, dried over MgSO<sub>4</sub>, and further purified by silica gel column chromatography using 9% MeOH in DCM as eluent.

Yield: 3.1g, 43%. <sup>1</sup>H NMR (400 MHz, CDCl<sub>3</sub>, ppm): δ 8.41 (dd 2H), 6.81 (dd 2H), 4.15 (tr, 2H), 3.86 (tr, 2H), 3.63–3.73 (m, 6H), 3.52-3.55 (tr, 2H), 3.36 (s, 3H); <sup>13</sup>C NMR (400 MHz, CDCl<sub>3</sub>) δ 164.78, 151.07, 110.31, 71.91, 70.88, 70.64, 70.57, 69.31, 67.19, 58.99. HRMS (ESI) *m/z*: calc., 242.13868; found 242.13812

PEGylated ruthenium-based catalyst (complex 3)

Grubbs second-generation catalyst (G2) (40 mg, 0.05 mmol) was weighed into a 20 mL vial in an argon-filled glove box. Dry DCM (1 mL) was added to the vial and the mixture was vigorously shaken to dissolve the catalyst. Complex 2 (180 mg, 0.75 mmol) was then added to the vial. A color change from brown to green was observed instantaneously. Pentane was added to the vial and a green precipitate was observed. The vial was kept refrigerated in the glove box for 12 hours at -26 °C; and the pentane was then decanted. The product was washed with pentane, dried under vacuum to give a green viscous oil, and further purified by silica gel column chromatography using 9% MeOH in DCM as eluent.

Yield: 23 mg, 45%. Due to the slow rotation around the ruthenium/N-heterocyclic carbene bond (2-3), it is not possible to identify the peaks by <sup>1</sup>H NMR spectroscopy. Only peak locations and multiplicity are reported for the <sup>1</sup>H NMR spectrum. <sup>1</sup>H NMR (CD<sub>2</sub>Cl<sub>2</sub>, 25 ° C, ppm): δ 19.16-19.11 (s), 8.45 (d), 7.72 (broad), 7.65 (d), 7.51 (tr), 7.09 (tr), 6.99 (broad), 6.85 (d), 6.53 (broad), 4.20 (broad), 4.06 (broad), 3.87 (broad), 3.77 (broad), 3.53-3.71 (m), 3.34-3.37 (s with broad shoulder), 2.59 (broad), 2.24-2.38 (broad). FTMS + p ESI Full ms; *m/z* calc for C<sub>52</sub>H<sub>70</sub>O<sub>8</sub>N<sub>4</sub>ClRu: 1051.3661, found 1051.3687.

#### 4.4.4 The influence of air and moisture on catalytic performance of complex 3

The influence of air and moisture on catalytic performance was monitored by monomer conversion with  $^1\text{H}$  NMR. An NMR tube with a screw cap was charged with 0.5 mg PEGylated catalyst (complex **3**) and 0.5 mL anhydrous degassed  $\text{CD}_2\text{Cl}_2$  in a glovebox to form a catalyst solution ( $9.5 \times 10^{-4}$  mol/L). 0.06 mL of COD was added into the catalyst solution under argon to trigger the polymerization. The monomer conversion was monitored by comparing the vinyl peaks of COD (7.50 ppm) and 1,4-polybutadiene (7.34 ppm). The polymerization was terminated by adding ethyl vinyl ether after 3 hours. A series of parallel experiments with alternative solvents such as degassed wet  $\text{CD}_2\text{Cl}_2$ , and a mixture of degassed  $\text{CD}_2\text{Cl}_2$  and water were also performed by following the similar procedure.

#### **4.4.5 ROMP of 1,5-cyclooctadiene (COD) and norbornene (NB) in miniemulsion**

An oil-in-water miniemulsion consists of two phases. The organic phase was obtained by mixing degassed COD (1.25 g, 11.5 mmol) and degassed dodecane (0.12 g, 0.73 mmol, 10 wt% of monomer). The water phase was obtained by mixing degassed deionized water (25 g) and cetyltrimethylammonium chloride (0.125 g, 0.5 wt% of water). The organic phase and water phase were mixed sufficiently, followed by ultrasonication in ice bath for 15 min at 15 watts. The ultrasonication was conducted under argon to maintain an inert atmosphere.

The miniemulsion polymerization was carried out in a 25 mL schlenk tube fitted with an argon inlet and a magnetic stir set at 900 rpm. To initiate the polymerization, the catalyst was added as an aqueous solution into the miniemulsion and the reaction tube was magnetically stirred at room temperature. The ROMP of norbornene (NB) in miniemulsion followed a similar procedure, except that DCM was introduced to dissolve NB (monomer concentration: 50 wt%) properly.

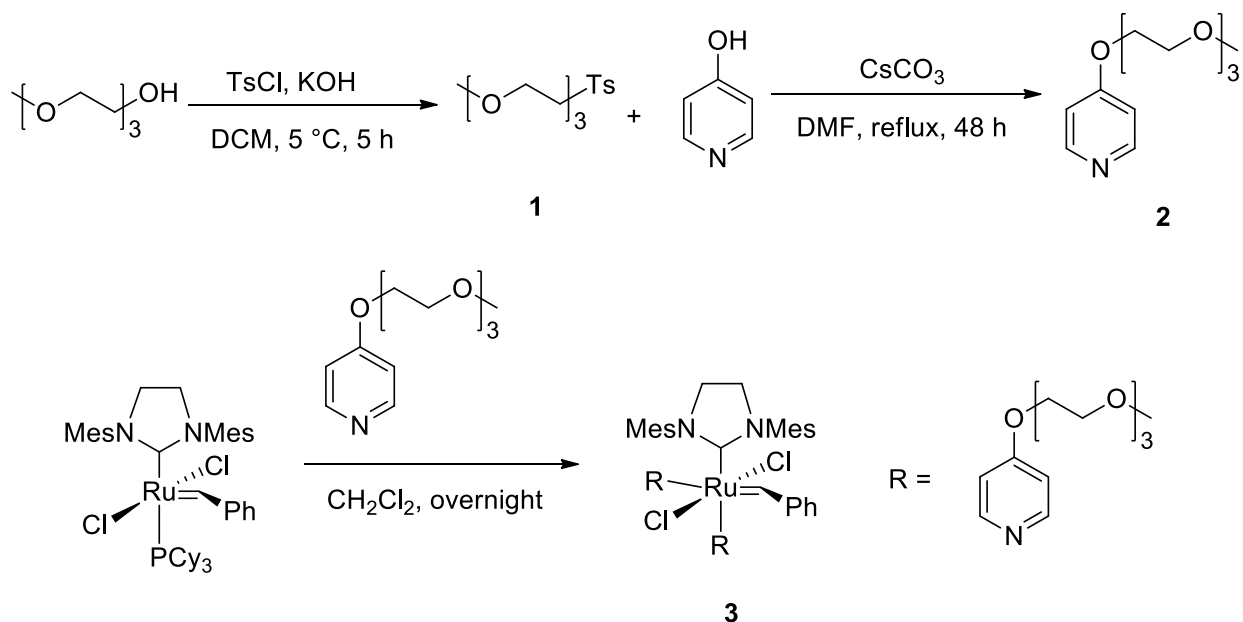
## **4.5 Results and discussion**

### **4.5.1 Catalyst design**

PEGylated metathesis catalysts have garnered considerable interest.<sup>19,22,23,25</sup> In our study, the readily available triethylene-glycol mono-methyl ether was used to prepare catalyst **3** in three simple steps



(Scheme 4.1). PEG methyl ether tosylate **1** was obtained after tosylation (99% yield Figure S1 and Figure S2), and was used without further purification to form PEG-attached pyridine **2** (43% yield) by interacting with 4-hydroxypyridine ( $S_N2$  reaction) (Figure S3 and Figure S4). Then PEG-attached pyridine **2** was introduced directly to replace the tricyclohexylphosphine ligands of G2 and produced PEGylated ruthenium-based catalyst (complex **3**). Complex **3** was further purified by chromatography with 45% yield (Figure S5).



#### Scheme 4.1 Synthesis of PEGylated Ru-based metathesis catalyst.

To investigate the influence of air and moisture on the catalytic activity of complex **3** in polar media, ROMP of COD was carried out individually in: (a) degassed dry  $\text{CD}_2\text{Cl}_2$ , (b) degassed wet  $\text{CD}_2\text{Cl}_2$ , and (c) a mixture of 1:1 (v/v)  $\text{CD}_2\text{Cl}_2$  and degassed heavy water ( $\text{D}_2\text{O}$ ). When 0.1 mol% catalyst was used (Figure 4.1), the polymerization proceeded to 100% conversion within 20 min. The ROMP of COD in degassed wet  $\text{CD}_2\text{Cl}_2$  was slower and proceeded to 83% conversion after 40 min, and 71% conversion was observed in the mixture of  $\text{CD}_2\text{Cl}_2$  and degassed  $\text{D}_2\text{O}$  after 1 hour. The decreasing polymerization rate in wet solvents when using a lower catalyst loading (0.1 mol% of monomer) may be attributed to the

formation of inactive species when water attacks the hydrophobic ruthenium center.<sup>23,31,32</sup> In contrast, when a higher catalyst loading (0.2 mol% of monomer) was used (Figure 4.2), the difference among three experiments was not so obvious and a full conversion was observed within 15 min under all conditions. Additionally, when the same reaction was conducted in the open air (squares in Figure 4.2), the conversion dropped dramatically to 15% from full conversion. Overall, these results indicated that complex **3** remained active in the presence of water, but was extremely air sensitive. It also suggested 0.2 mol% of catalyst ([Monomer]/[Catalyst] ratio = 500:1) be used to maintain a high rate of polymerization, as implemented in the following miniemulsion polymerization.

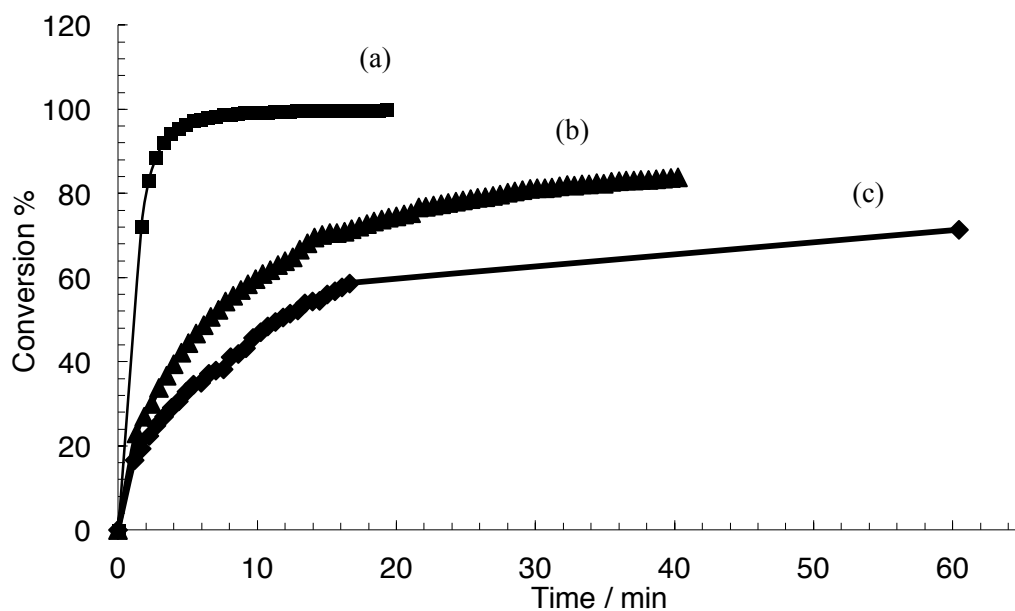


**Figure 4.1 Conversion vs time plots for ROMP in different solvents with 0.1 wt% PEGylated catalyst (complex 3): (a) degassed dry  $\text{CD}_2\text{Cl}_2$  (squares); (b) degassed wet  $\text{CD}_2\text{Cl}_2$  (triangles); and (c) a mixture of wet degassed  $\text{CD}_2\text{Cl}_2$  and degassed  $\text{D}_2\text{O}$  (rhombi).**

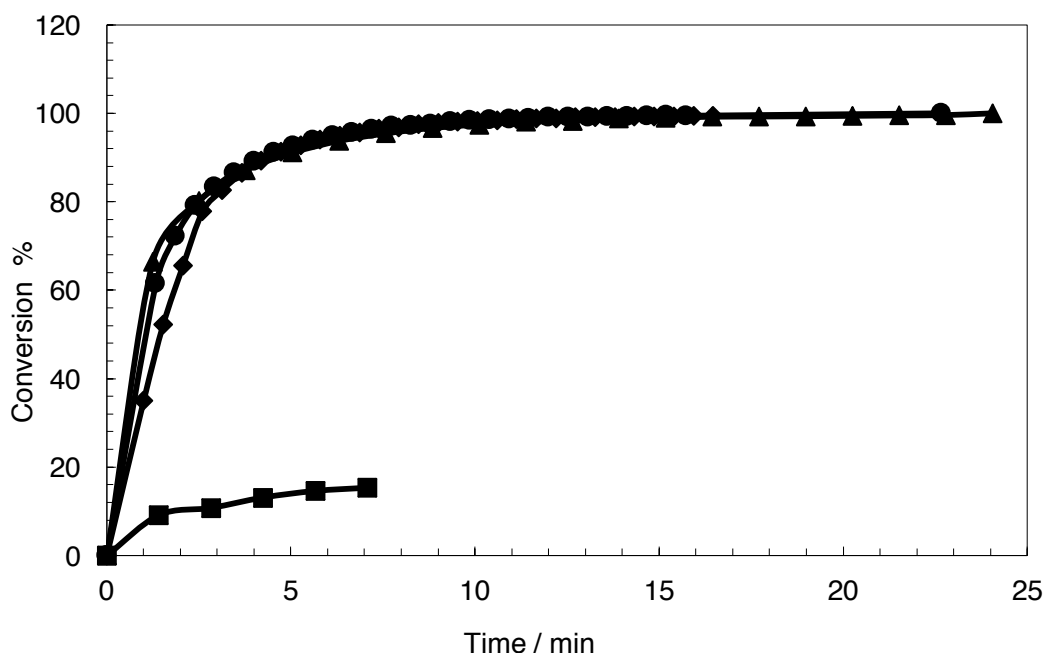


**Figure 4.2 Conversion vs time curves for COD ROMP in different solvents with 0.2 wt% PEGylated catalyst: (a) degassed dry CD<sub>2</sub>Cl<sub>2</sub> (rhombi); (b) degassed wet CD<sub>2</sub>Cl<sub>2</sub> (triangles); (c) a mixture of wet degassed CD<sub>2</sub>Cl<sub>2</sub> and degassed D<sub>2</sub>O (circles); and (d) wet CD<sub>2</sub>Cl<sub>2</sub> in air (squares).**

#### 4.5.2 Monomer miniemulsion

After obtaining complex **3**, we first attempted to carry out a conventional emulsion polymerization as described in a previous report.<sup>18</sup> A large amount of coagulum was identified and no quantitative result of particle size was obtained, which indicated a poor reproducibility during the nucleation period. Then we turned to a miniemulsion technique that produced monomodal and stable latex particles via a droplet nucleation mechanism. In this approach, a monomer miniemulsion is prepared by intensive homogenization during which large droplets are broken into smaller ones, thus creating more interfacial area. The droplets degradation by coalescence (droplets merge into larger droplets) can be effectively stopped by adding enough surfactant. A costabilizer is also introduced to minimize Ostwald ripening (monomer proceeds with a net diffusion from small droplets to large ones without direct contact).<sup>33</sup> After several trials with different formulations, a stable monomer miniemulsion was obtained with 5 wt% COD

as monomer, 0.5 wt% dodecane as costabilizer, and 0.5 wt% cetyltrimethylammonium chloride (CTAC) as surfactant. The droplet size of the obtained miniemulsion was monitored by DLS over 2 hours at room temperature (Figure 4.3). The droplet radius ( $r$ ) will usually increase with time when the stability of the miniemulsion is poor. If coalescence occurs continuously in the miniemulsion,  $r^2$  would increase linearly with time, whereas  $r^3$  will increase linearly with time if the degradation is caused by Ostwald ripening.<sup>34</sup> However in Figure 4.3 no significant change of droplet radius ( $r$ ) was observed after 2 hours, which indicated the combination of surfactant and co-stabilizer were efficient in preventing the degradation of the miniemulsion. The formed COD droplets had an average diameter of  $\sim 90$  nm. The distributions were broad but PDI was stable over time.

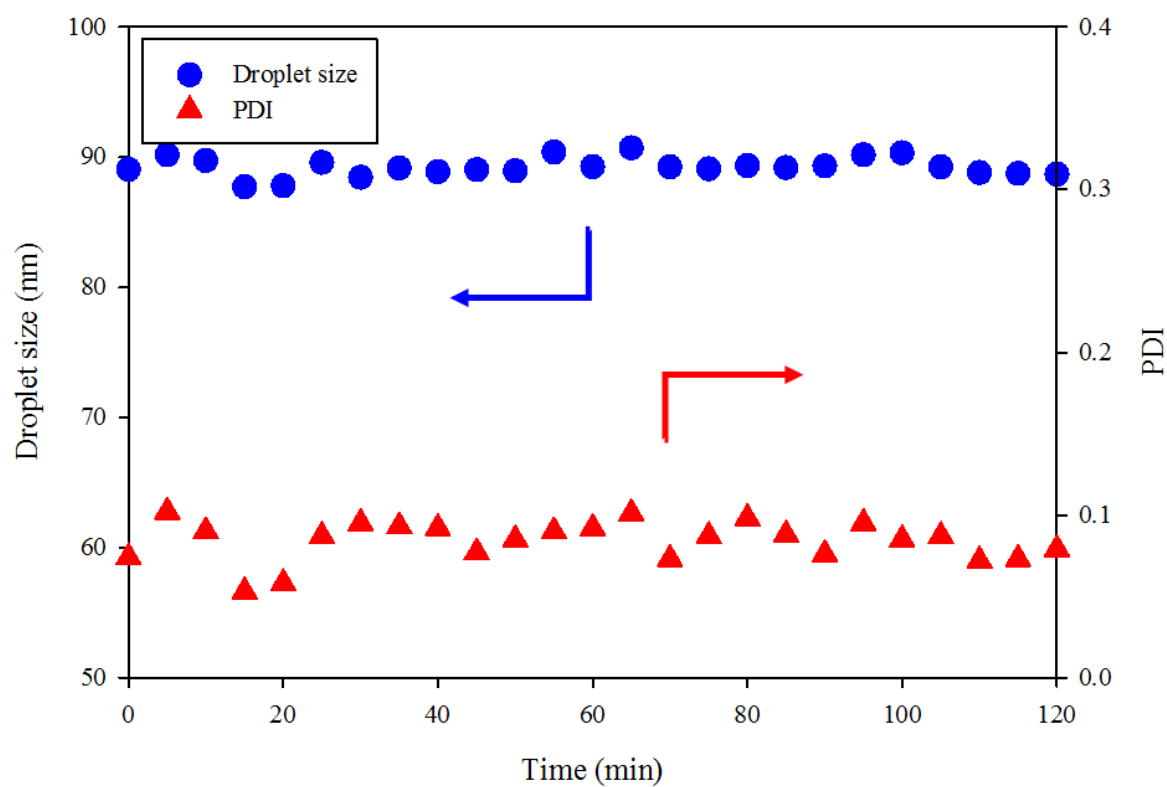
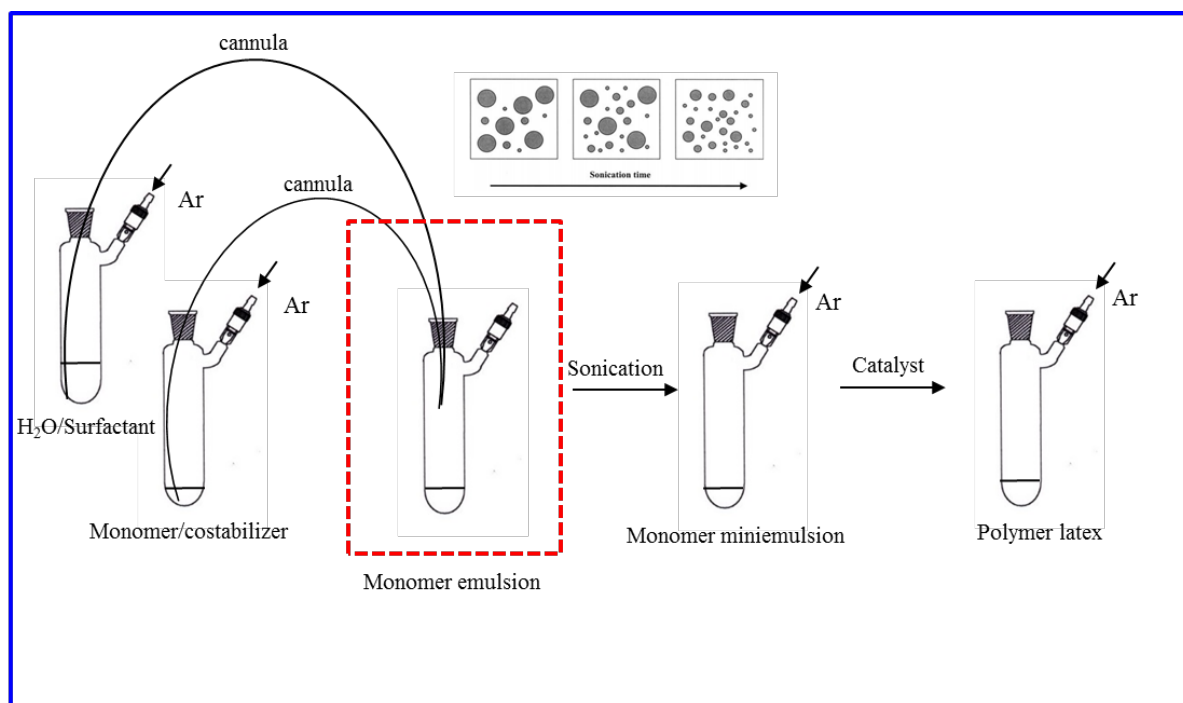


**Figure 4.3 Droplet size (●) vs time and PDI (▲) vs time for monomer miniemulsion. Recipe: dodecane/COD/CTAC/H<sub>2</sub>O = 0.125 g/1.25 g/0.125 g/25 g. Conditions: ultrasonication at 15 watt for**

15 min in an ice bath. Sample was diluted in water (0.15 mL in 1.5 mL) prior to DLS measurement at room temperature.

#### 4.5.3 Miniemulsion polymerization

Using the conditions determined above, the submicron droplets in miniemulsion were polymerized by simply adding the water-soluble catalyst (Scheme 4.2). Since the catalyst was sensitive to air, we mixed the oil phase (monomer and costabilizer) and aqueous phase (water and surfactant) in schlenk flasks via cannula transfer under argon, followed by intensive ultrasonication to form a COD miniemulsion. The catalyst was then dropped in to initiate the polymerization. It was observed that the catalyst could be dissolved in the continuous phase without visibly causing any coalescence. The color of the reaction mixture changed from green (the color of unreacted catalyst) to light grey in 10 min, indicating the activation of the catalyst. The monomer conversion reached ~100% within 1 hour. The average particle size was 101 nm (Figure 4.4) with a narrow particle size distribution (PDI = 0.083), although the initial monomer droplet size distribution was broader (PDI = 0.105).



**Scheme 4.2 Procedure for ROMP in miniemulsion with air-free conditions.**

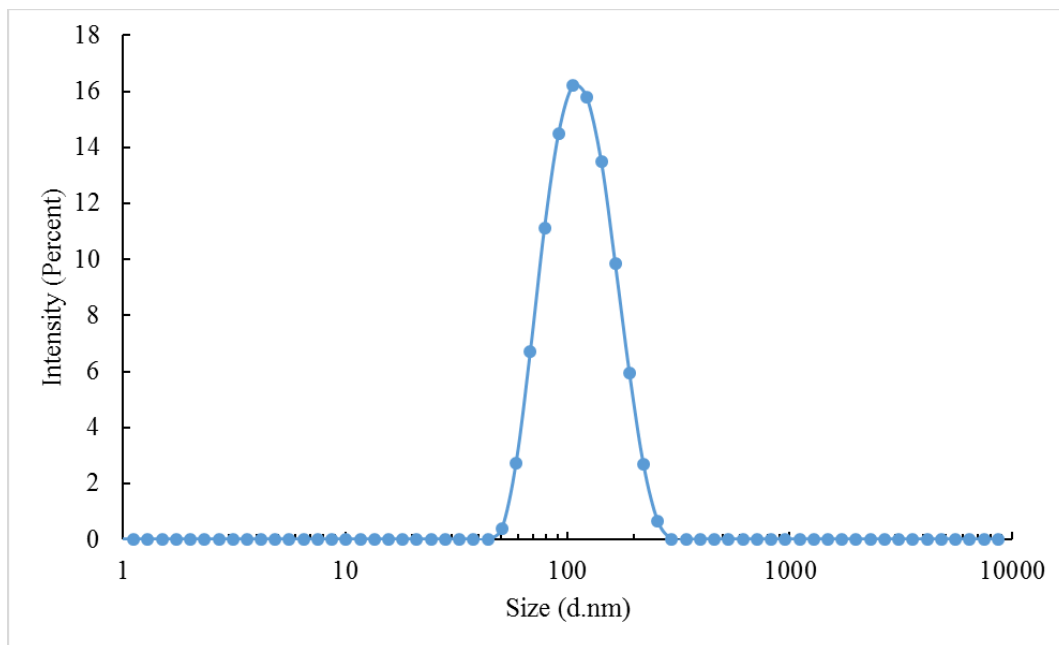


**Figure 4.4** Size distribution by intensity for polymer latex obtained from ROMP of 1,5-cyclooctadiene in miniemulsion. Z-average parameter: 101 nm, PDI: 0.083. Sample was diluted in water (0.15 mL in 1.5 mL) prior to DLS measurement at room temperature.

#### 4.5.4 Kinetic study

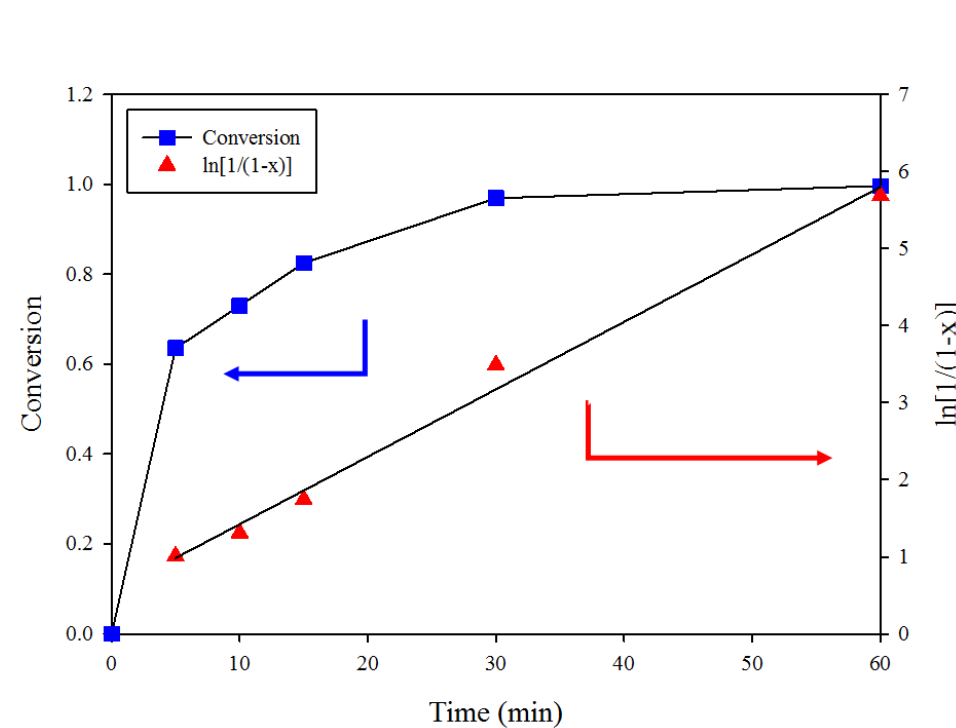


**Figure 4.5 Conversion ( $x$ ) and  $\ln[1/(1-x)]$  plots for ROMP of 1,5-cyclooctadiene (COD) in miniemulsion catalyzed by complex 3. Reaction conditions: 25 °C, [monomer]/[catalyst] = 500:1, monomer content: 5 wt% of water.**

To monitor the monomer conversion with time, we took multiple samples of the reaction mixture at given times (5 min, 10 min, 15 min, 30 min, 60 min) and quenched each sample with ethyl vinyl ether (0.025 mL) to rapidly terminate the polymerization. 60% conversion was observed in 5 min and essentially full conversion was achieved in 1 hour (Figure 4.5). As reported in Chapter 3, the rate of polymerization ( $R_p$ ) in ROMP can be estimated by Equation 3.1 and 3.2.

A pseudo first-order kinetic profile was observed in Figure 4.5, indicating a stable concentration of living species during the polymerization. Therefore, the synthesized catalyst did appear to stay reactive after being activated in an aqueous environment without significant loss of catalyst activity. Complex 3, which contains a saturated *N*-heterocyclic carbene (NHC), is expected to have similar reactivity and functional group compatibility as the Grubbs third-generation catalyst (G3) since they will generate identical propagating species.

#### 4.5.5 Molecular weight

The number average molecular weight ( $M_n$ ) is a key indicator of the chain propagation during a polymerization. Figure 4.6 shows the  $M_n$  vs conversion profile for the miniemulsion polymerization. The number average molecular weight ( $M_n$ ) increased from 12900 g/mol at 64% conversion to 41000 g/mol at 100% conversion with a final dispersity ( $\mathcal{D}$ ) at 1.7. The shift of GPC traces in Figure 4.7 indicated good livingness in the miniemulsion polymerization. In fact, the polymerization went so fast (64% conversion in 5 min) that the propagation can hardly be instantaneously terminated when quenching the first sample at 5 min, which potentially led to a molecular weight distribution curve with a shoulder.

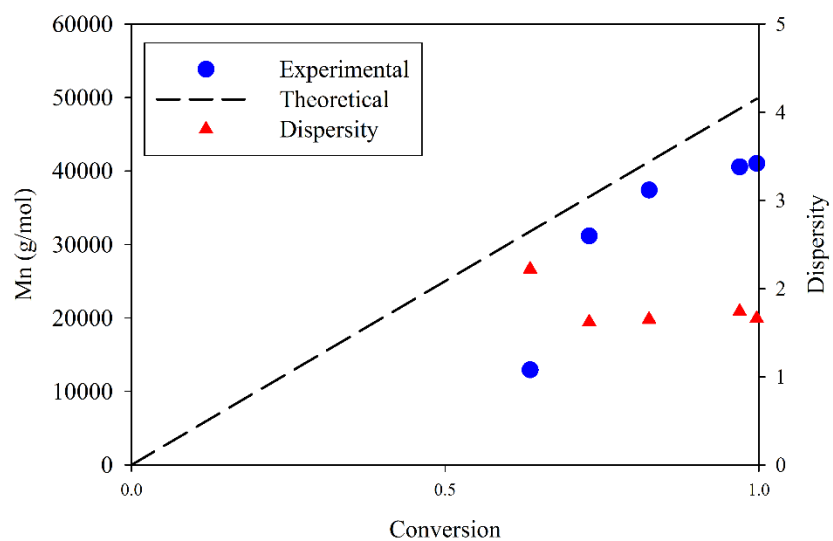


**Figure 4.6** Number average molecular weight ( $M_n$ ) and dispersity ( $\bar{D}$ ) plots for ROMP of 1,5-cyclooctadiene (COD) in miniemulsion using complex 3 as catalyst.

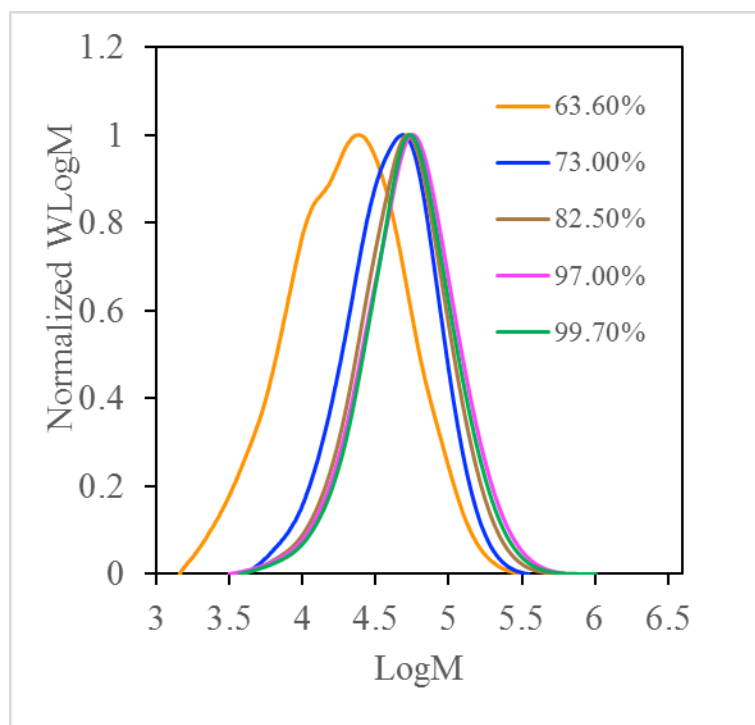


**Figure 4.7** The evolution of GPC traces (normalized height) with conversion for ROMP of 1,5-cyclooctadiene (COD) in miniemulsion using complex 3 as catalyst.



Figure 4.6 shows the experimental  $M_n$  increased with monomer conversion due to continuous chain growth. The  $M_n$  values were slightly lower than the theoretical  $M_n$ . The differences were not large, and could be attributable to errors associated with the use of the Mark-Houwink parameters or potentially due to chain transfer from secondary metathesis during the polymerization.<sup>38</sup> Chain transfer can reportedly go through two different pathways: (a) intermolecular chain transfer and (b) intramolecular chain transfer.<sup>39</sup> The intermolecular chain transfer produces polymer chains with varying molecular weight and the total number of polymer chains and active species remains unchanged. The intramolecular chain transfer produces an active polymer chain and a dead species, reducing average molecular weight and increasing dispersity.

We began the ROMP of COD in miniemulsion with a target chain length (TCL) at 500 (Exp 1 in Table 4.1). Claverie *et al.*<sup>18</sup> reported lower yields and slower kinetics when polymerizing COD compared to NB potentially due to a dramatic difference in strain energy. Here, a parallel experiment (Exp 2) with norbornene (strain energy = 90.4 kJ/mol,<sup>35</sup> COD strain energy = 55.6 kJ/mol<sup>36</sup>) as monomer was conducted and a stable polymer latex was produced with 100% conversion. It was therefore demonstrated that both high-strain and low-strain cyclic olefins could be polymerized at high conversion by using the highly efficient catalyst in our study.

**Table 4.1 Experimental conditions and results for the ROMP in miniemulsion**

Entry	Monomer	Surfactant	[M]:[C]	Monomer content	Conversion	$M_n$ (g/mol)	$M_w$ (g/mol)	$\bar{D}$	Particle size (nm)	PDI
Exp 1	COD	CTAC	500	5%	100%	41000	68400	1.67	101	0.083
Exp 2	NB	CTAC	500	5%	100%	47500	59350	1.67	140	0.167
Exp 3	COD	CTAC	1000	5%	99%	54300	94700	1.75	140	0.093
Exp 4	COD	CTAC	500	20%	100%	41300	68860	1.67	293	0.377
Exp 5	COD	CTAB	500	5%	100%	30500	50590	1.66	100	0.158
Exp 6	COD	Triton X-100	500	5%	99%	51000	88400	1.73	223	0.338

#### 4.5.6 Catalyst loading and solid content

It was revealed previously that the catalyst loading might affect the rate of polymerization due to the formation of inactive species in water. Fortunately, Exp 3 showed that when catalyst loading was reduced by 50 %, we could still produce polymer with 99% conversion. As proposed by Matsuo *et al.*, the addition of chloride salt (chloride counter-ion of CTAC in our case) could enhance the catalytic activity of olefin metathesis by contributing to the formation of active species.<sup>41</sup>

Another important concern in industry for miniemulsion polymerization is the possibility to manufacture polymer latex with high solid content (>50 wt%).<sup>42</sup> In Exp 4, the initial monomer content was raised from 5 wt% in Exp 1 up to 20 wt% relative to water. And a 100% conversion showed the potential to synthesize well-defined polymer latexes by ROMP with a high solid content. With the same surfactant concentration in Exp 1 and Exp 3, it was not surprising to find a larger particle size (223 nm) in Exp 3 because of an increase of oil phase relative to water phase.

#### **4.5.7 Surfactants**

The same experiments were also repeated with CTAB as surfactant in Exp 5 and Triton X-100 as surfactant in Exp 6. The counter ions found on the surfactants could potentially cause a loss of reactivity of the catalyst. For instance, Grubbs and coworkers noticed a possible halogen ligand exchange around the ruthenium of Grubbs first generation catalyst and they preferred to use a chloride surfactant instead of bromide surfactant.<sup>43,44</sup> In our study, both CTAC and CTAB were used as surfactants with full conversion and the halogen exchange between the surfactants and catalyst have no significant effect on the final conversion.

The ionic and nonionic surfactants exhibited different abilities to stabilize the miniemulsion system. It was observed that the particle size was smaller with ionic stabilization (100 nm for CTAC and CTAB) than with steric stabilization (220 nm for Triton X-100). The difference in the surfactant type also resulted in a broader particle size distribution (PDI) in a polymer latex stabilized by non-ionic surfactants.

#### **4.6 Conclusion**

We demonstrated the feasibility of conducting ring opening metathesis polymerizations in miniemulsion using a PEGylated Ru-based catalyst. The catalyst was found to be soluble and active in water. And the monomer miniemulsion was found to be stable with sufficient surfactant and costabilizer, which provided ideal environment for catalyst to initiate the polymerization with no coagulum. The synthesized catalyst could polymerize 1,5-cyclooctadiene and norbornene rapidly in miniemulsion with high monomer conversion. The polymerization followed first-order kinetics with an excellent livingness. The particle size ranged from 100 to 300 nm with either ionic or non-ionic surfactants used. These results encouraged us to use a lower catalyst loading (0.1 mol% to monomer) and a higher monomer content (20 wt% to water), both of which were achieved with 100% conversion. The scope of this study can be further extended to more specific applications by introducing functionalized cyclic olefins as monomers.

## 4.7 Acknowledgements

Financial support from the Ontario Research Chairs (MFC) programs, and from the Natural Sciences and Engineering Research Council of Canada is gratefully acknowledged.

## 4.8 References

- (1) Hoveyda, A. H.; Zhugralin, A. R. The Remarkable Metal-Catalysed Olefin Metathesis Reaction. *Nature* **2007**, *450* (7167), 243–251.
- (2) Nguyen, S. T.; Johnson, L. K.; Grubbs, R. H.; Ziller, J. W. Ring-Opening Metathesis Polymerization (ROMP) of Norbornene by a Group VIII Carbene Complex in Protic Media. *J. Am. Chem. Soc.* **1992**, *114* (10), 3974–3975.
- (3) Wathier, M.; Lakin, B. A.; Bansal, P. N.; Stoddart, S. S.; Snyder, B. D.; Grinstaff, M. W. A Large-Molecular-Weight Polyanion, Synthesized via Ring-Opening Metathesis Polymerization, as a Lubricant for Human Articular Cartilage. *J. Am. Chem. Soc.* **2013**, *135* (13), 4930–4933.
- (4) Haque, H. A.; Kakehi, S.; Hara, M.; Nagano, S.; Seki, T. High-Density Liquid-Crystalline Azobenzene Polymer Brush Attained by Surface-Initiated Ring-Opening Metathesis Polymerization. *Langmuir* **2013**, *29* (25), 7571–7575.
- (5) White, S. R.; Sottos, N. R.; Geubelle, P. H.; Moore, J. S.; Kessler, M. R.; Sriram, S. R.; Brown, E. N.; Viswanathan, S. Correction: Autonomic Healing of Polymer Composites. *Nature* **2002**, *415* (6873), 817–817.
- (6) Fishman, J. M.; Kiessling, L. L. Synthesis of Functionalizable and Degradable Polymers by Ring-Opening Metathesis Polymerization. *Angew. Chem. Int. Ed. Engl.* **2013**, *52*, 5061–5064.
- (7) Kalluru, S. H.; Cochran, E. W. Synthesis of Polyolefin/layered Silicate Nanocomposites via Surface-Initiated Ring-Opening Metathesis Polymerization. *Macromolecules* **2013**, *46*, 9324–

9332.

- (8) Sanford, M. S.; Love, J. A.; Grubbs, R. H. Mechanism and Activity of Ruthenium Olefin Metathesis Catalysts. *J. Am. Chem. Soc.* **2001**, *123* (27), 6543–6554.
- (9) Schork, F. J.; Luo, Y.; Smulders, W.; Russum, J. P.; Butté, A.; Fontenot, K. Miniemulsion Polymerization. *Adv. Polym. Sci.* **2005**, *175*, 129–255.
- (10) Smith, W. V.; Ewart, R. H. Kinetics of Emulsion Polymerization. *J. Chem. Phys.* **1948**, *16* (1948), 592.
- (11) Tiarks, F.; Landfester, K.; Antonietti, M. Preparation of Polymeric Nanocapsules by Miniemulsion Polymerization. *Langmuir* **2001**, *17* (3), 908–918.
- (12) Asua, J. M. Miniemulsion Polymerization. *Prog. Polym. Sci.* **2002**, *27* (7), 1283–1346.
- (13) Chern, C. S. Emulsion Polymerization Mechanisms and Kinetics. *Prog. Polym. Sci.* **2006**, *31* (5), 443–486.
- (14) Cunningham, M. F. Controlled/living Radical Polymerization in Aqueous Dispersed Systems. *Prog. Polym. Sci.* **2008**, *33* (4), 365–398.
- (15) Cunningham, M. F. Living/controlled Radical Polymerizations in Dispersed Phase Systems. *Prog. Polym. Sci.* **2002**, *27* (6), 1039–1067.
- (16) Rinehart, R. E.; Smith, H. P. The Emulsion Polymerization of the Norbornene Ring System Catalyzed by Noble Metal Compounds. *J. Polym. Sci. Part B Polym. Lett.* **1965**, *3* (12), 1049–1052.
- (17) Michelotti, F. W.; Keaveney, W. P. Coordinated Polymerization of the Bicyclo-[2.2.1]-Heptene-2 Ring System (Norbornene) in Polar Media. *J. Polym. Sci. Part A Gen. Pap.* **1965**, *3* (3), 895–905.

- (18) Claverie, J. P.; Viala, S.; Maurel, V.; Novat, C. Ring-Opening Metathesis Polymerization in Emulsion. *Macromolecules* **2001**, *34* (3), 382–388.
- (19) Quémener, D.; Héroguez, V.; Gnanou, Y. Design of PEO-Based Ruthenium Carbene for Aqueous Metathesis Polymerization. Synthesis by the “macromonomer method” and Application in the Miniemulsion Metathesis Polymerization of Norbornene. *J. Polym. Sci. Part A Polym. Chem.* **2006**, *44* (9), 2784–2793.
- (20) Quémener, D.; Chemtob, A.; Héroguez, V.; Gnanou, Y. Synthesis of Latex Particles by Ring-Opening Metathesis Polymerization. *Polymer (Guildf)*. **2005**, *46* (4), 1067–1075.
- (21) Quémener, D.; Héroguez, V.; Gnanou, Y. Latex Particles by Miniemulsion Ring-Opening Metathesis Polymerization. *Macromolecules* **2005**, *38* (19), 7977–7982.
- (22) Gallivan, J. P.; Jordan, J. P.; Grubbs, R. H. A Neutral, Water-Soluble Olefin Metathesis Catalyst Based on an N-Heterocyclic Carbene Ligand. *Tetrahedron Lett.* **2005**, *46* (15), 2577–2580.
- (23) Hong, S. H.; Grubbs, R. H. Highly Active Water-Soluble Olefin Metathesis Catalyst. *J. Am. Chem. Soc.* **2006**, *128* (11), 3508–3509.
- (24) Jordan, J. P.; Grubbs, R. H. Small-Molecule N-Heterocyclic-Carbene-Containing Olefin-Metathesis Catalysts for Use in Water. *Angew. Chem. Int. Ed. Engl.* **2007**, *46* (27), 5152–5155.
- (25) Breitenkamp, K.; Emrick, T. Amphiphilic Ruthenium Benzylidene Metathesis Catalyst with PEG-Substituted Pyridine Ligands. *J. Polym. Sci. Part A Polym. Chem.* **2005**, *43* (22), 5715–5721.
- (26) Samanta, D.; Kratz, K.; Zhang, X.; Emrick, T. A Synthesis of PEG- and Phosphorylcholine-Substituted Pyridines to Afford Water-Soluble Ruthenium Benzylidene Metathesis Catalysts. *Macromolecules* **2008**, *41* (3), 530–532.

- (27) Hamielec, A. E.; Ouano, A. C. Generalized Universal Molecular Weight Calibration Parameter in GPC. *J. Liq. Chromatogr.* **1978**, *1* (1), 111–120.
- (28) Xu, Z.; Song, M.; Hadjichristidis, N.; Fetters, L. J. Method for Gel Permeation Chromatography Calibration and the Evaluation of Mark-Houwink-Sakurada Constants. *Macromolecules* **1981**, *14*, 1591–1594.
- (29) Patil, A. O.; Zushma, S.; Stibrany, R. T.; Rucker, S. P.; Wheeler, L. M. Vinyl-Type Polymerization of Norbornene by nickel(II) Bisbenzimidazole Catalysts. *J. Polym. Sci. Part A Polym. Chem.* **2003**, *41* (13), 2095–2106.
- (30) Love, J. A.; Morgan, J. P.; Trnka, T. M.; Grubbs, R. H. A Practical and Highly Active Ruthenium-Based Catalyst That Effects the Cross Metathesis of Acrylonitrile. *Angew. Chem. Int. Ed. Engl.* **2002**, *41* (21), 4035–4037.
- (31) Vural Bütün, †; Steven P. Armes, \* and; Billingham, N. C. Selective Quaternization of 2-(Dimethylamino)ethyl Methacrylate Residues in Tertiary Amine Methacrylate Diblock Copolymers. **2001**.
- (32) Dwars, T.; Paetzold, E.; Oehme, G. Reactions in Micellar Systems. *Angew. Chemie Int. Ed.* **2005**, *44* (44), 7174–7199.
- (33) Voorhees, P. W. The Theory of Ostwald Ripening. *J. Stat. Phys.* **1985**, *38*, 231–252.
- (34) Capek, I. Degradation of Kinetically-Stable O/w Emulsions. *Adv. Colloid Interface Sci.* **2004**, *107* (2-3), 125–155.
- (35) Khoury, P. R.; Goddard, J. D.; Tam, W. Ring Strain Energies: Substituted Rings, Norbornanes, Norbornenes and Norbornadienes. *Tetrahedron* **2004**, *60* (37), 8103–8112.

- (36) Schleyer, P. R.; Williams, J. E.; Blanchard, K. R. The Evaluation of Strain in Hydrocarbons. *J. Am. Chem. Soc.* **1970**, *92*, 2377–2386.
- (37) Rule, J. D.; Moore, J. S. ROMP Reactivity of E Ndo - and E Xo -Dicyclopentadiene. *Macromolecules* **2002**, *35* (21), 7878–7882.
- (38) Chen, Z.-R.; Claverie, J. P.; Grubbs, R. H.; Kornfield, J. a. Modeling Ring-Chain Equilibria in Ring-Opening Polymerization of Cycloolefins. *Macromolecules* **1995**, *28*, 2147–2154.
- (39) Bielawski, C. W.; Grubbs, R. H. Living Ring-Opening Metathesis Polymerization. *Prog. Polym. Sci.* **2007**, *32* (1), 1–29.
- (40) Landfester, K.; Bechthold, N.; Förster, S.; Antonietti, M. Evidence for the Preservation of the Particle Identity in Miniemulsion Polymerization. *Macromol. Rapid Commun.* **1999**, *20* (2), 81–84.
- (41) Matsuo, T.; Yoshida, T.; Fujii, A.; Kawahara, K.; Hirota, S. Effect of Added Salt on Ring-Closing Metathesis Catalyzed by a Water-Soluble Hoveyda–Grubbs Type Complex To Form N-Containing Heterocycles in Aqueous Media. *Organometallics* **2013**, *32* (19), 5313–5319.
- (42) Ouzineb, K.; Graillat, C.; McKenna, T. F. High-Solid-Content Emulsions. V. Applications of Miniemulsions to High Solids and Viscosity Control. *J. Appl. Polym. Sci.* **2005**, *97* (3), 745–752.
- (43) Lynn, D. M.; Kanaoka, S.; Grubbs, R. H. Living Ring-Opening Metathesis Polymerization in Aqueous Media Catalyzed by Well-Defined Ruthenium Carbene Complexes. *J. Am. Chem. Soc.* **1996**, *118* (4), 784–790.
- (44) Lynn, D. M.; Mohr, B.; Grubbs, R. H.; Henling, L. M.; Day, M. W. Water-Soluble Ru Alkylidenes: Synthesis, Characterization, and Application to Olefin Metathesis in Protic Solvents. *J. Am. Chem. Soc.* **2000**, *122* (2), 6601–6609.



## 4.9 Supporting Information

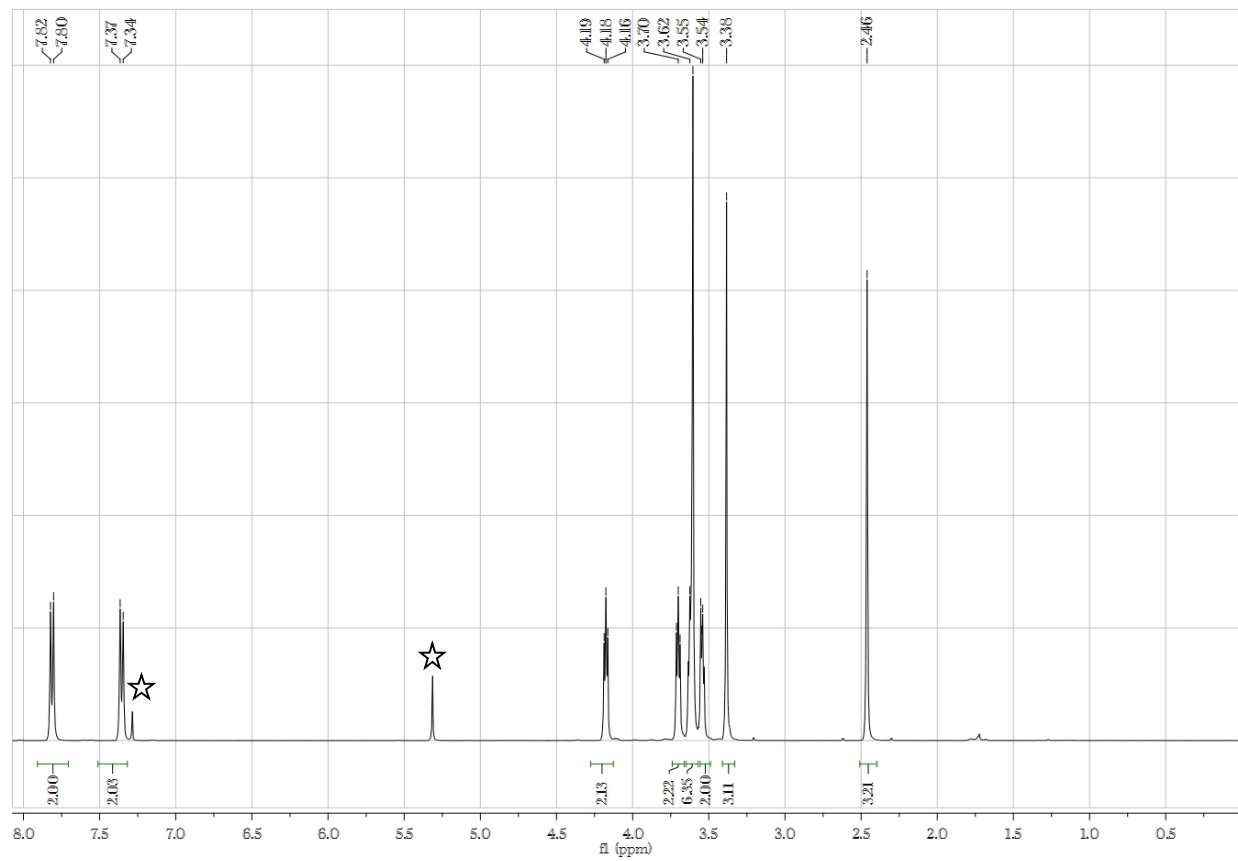


Figure S1 <sup>1</sup>H NMR of 2,5,8-tetraoxatridecan-10-yl 4-methylbenzenesulfonate.

Notes for labels:

☆: Solvent (DMSO-d<sub>6</sub>) and CH<sub>2</sub>Cl<sub>2</sub> peaks.

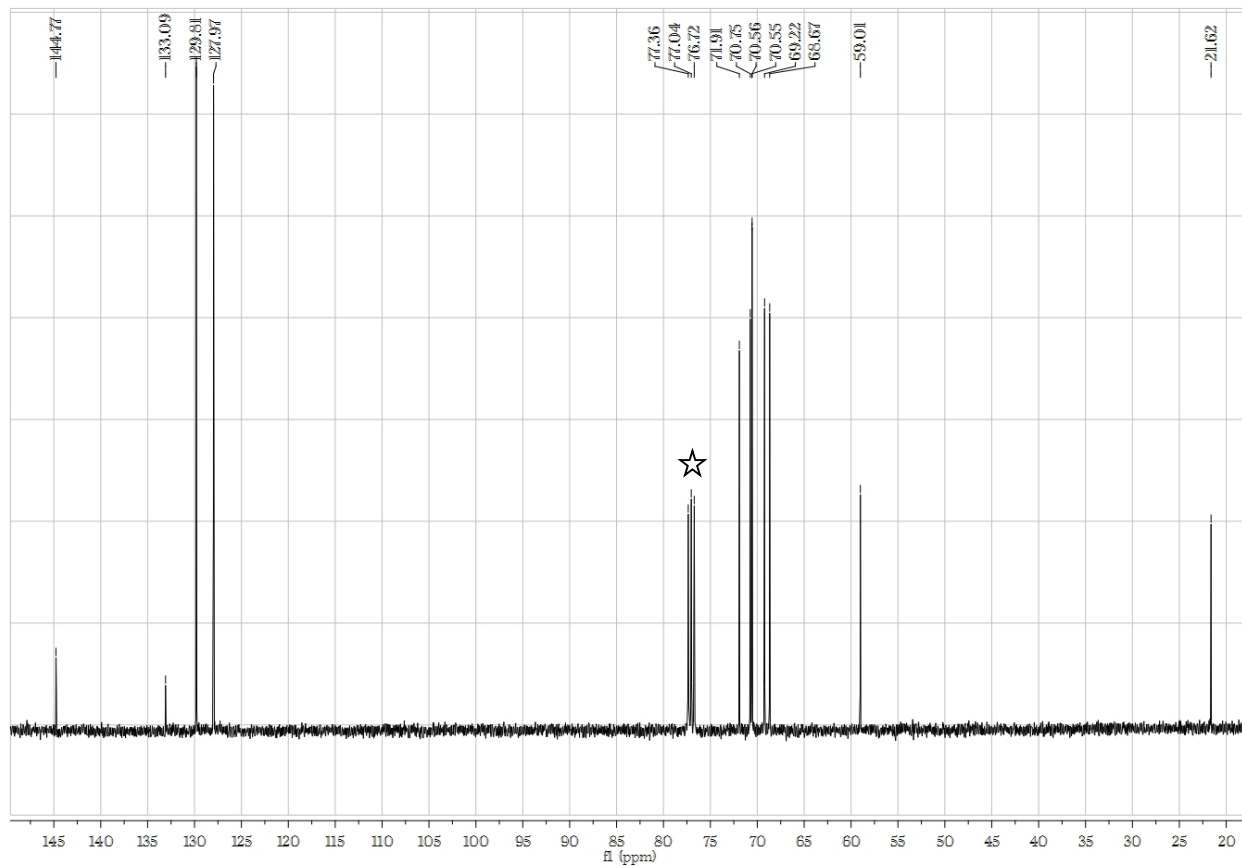
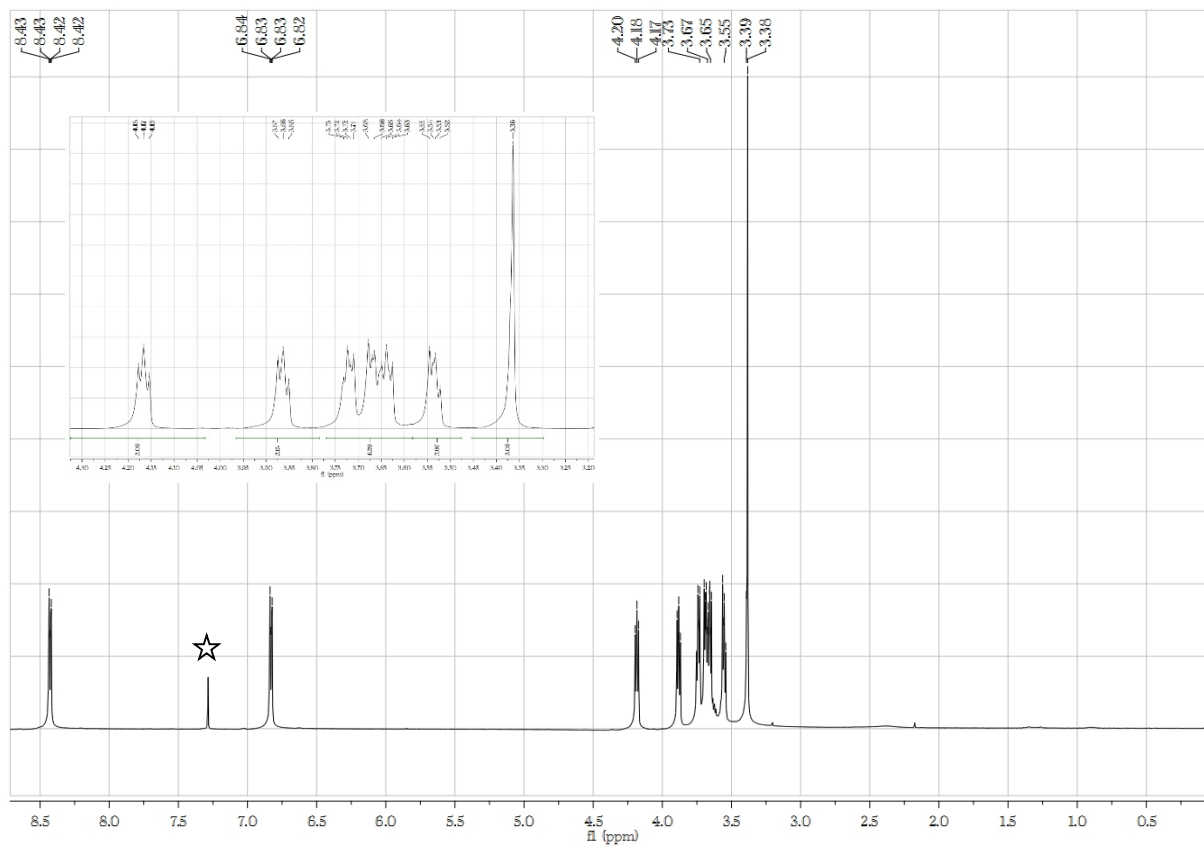


Figure S2.  $^{13}\text{C}$  NMR of 2,5,8-tetraoxatridecan-10-yl 4-methylbenzenesulfonate.

Notes for labels:

$\star$ : Solvent (DMSO- $d_6$ ) peaks.



**Figure S3.**  $^1\text{H}$  NMR of Synthesis of 4-(2,5,8-trioxatridecan-10-yl-oxy)pyridine.

Notes for labels:

☆: Solvent (DMSO- $d_6$ ) peaks

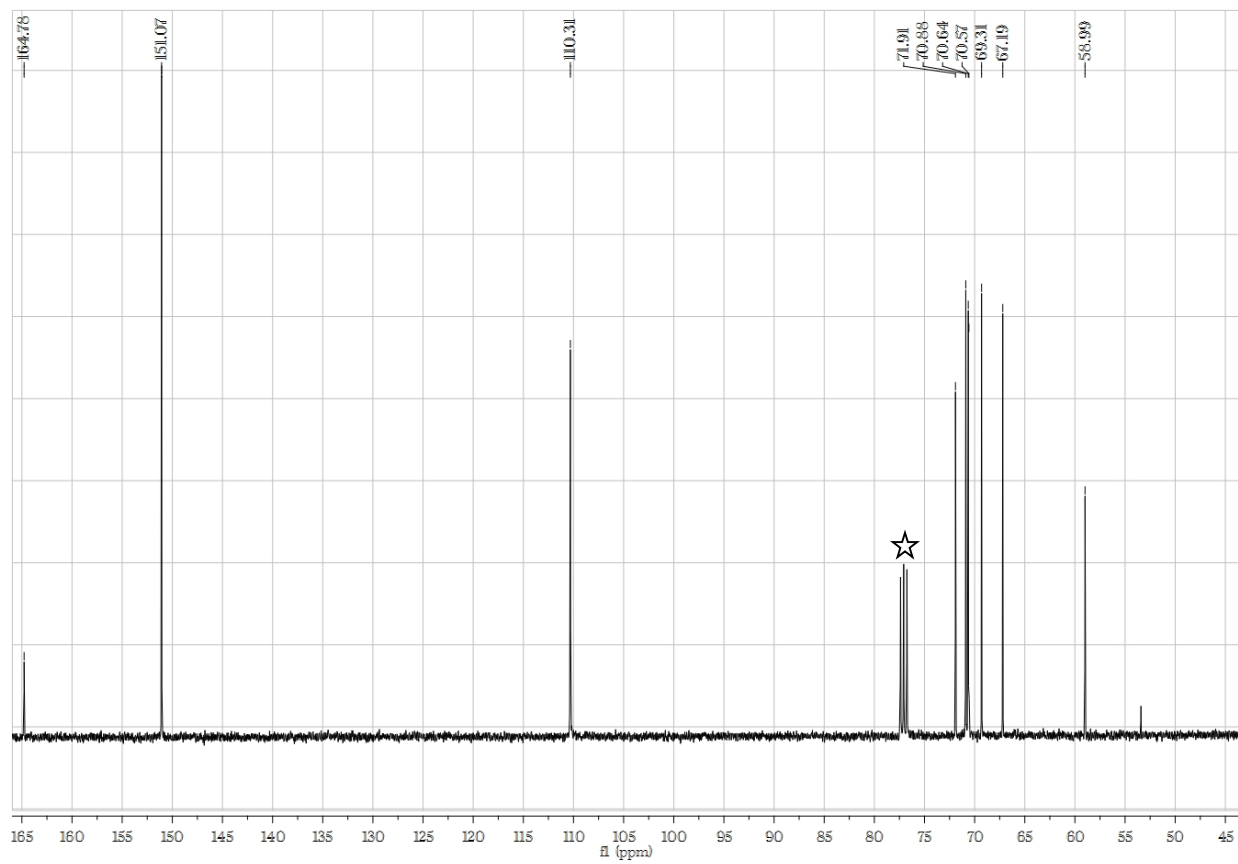


Figure S4.  $^{13}\text{C}$  NMR of Synthesis of 4-(2,5,8-trioxatridecan-10-yl-oxy)pyridine.

Notes for labels:

☆ Solvent (DMSO- $\text{d}_6$ ) peaks

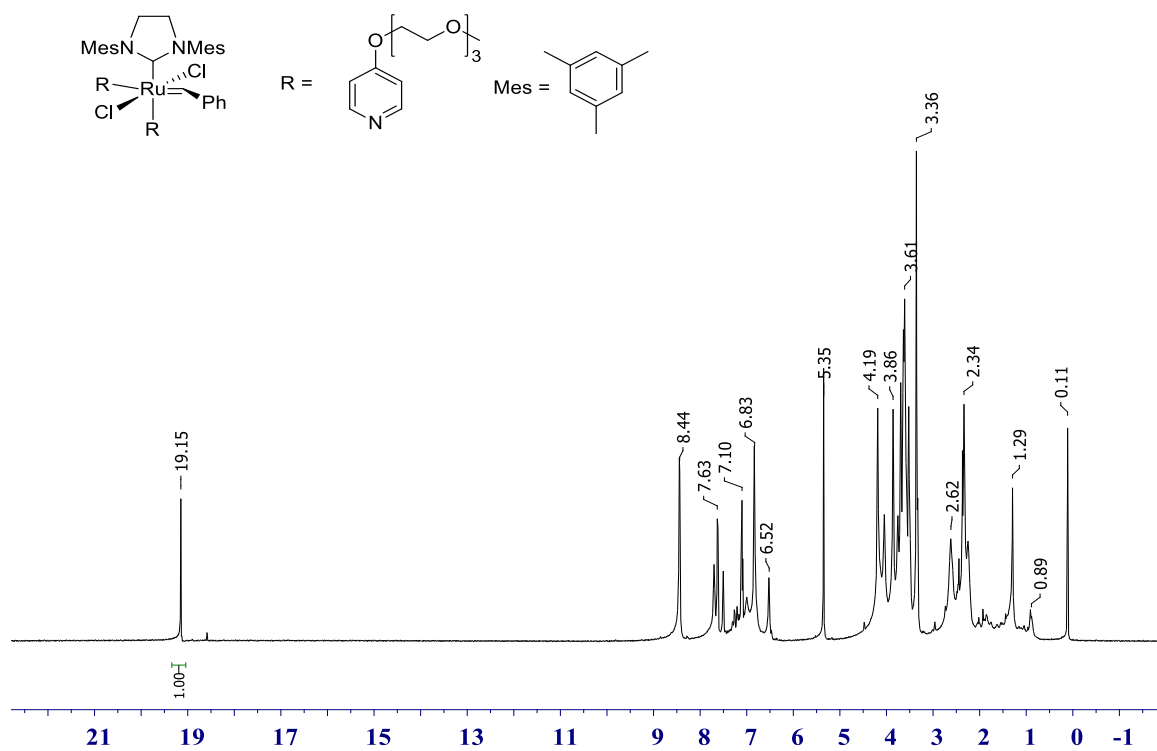
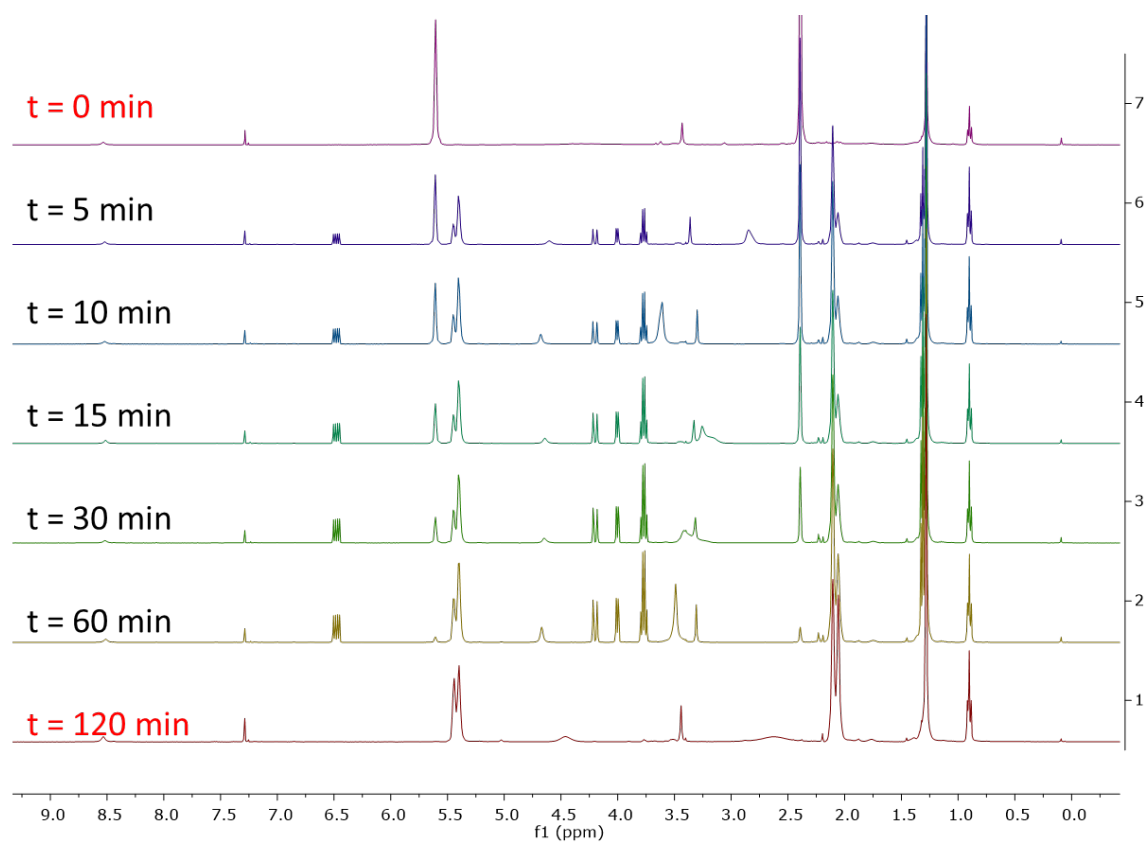
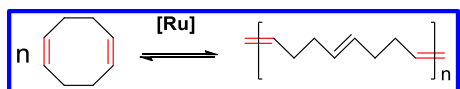
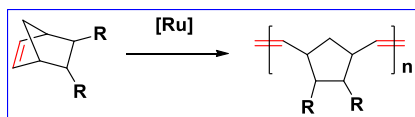


Figure S5. <sup>1</sup>H NMR of PEGylated Grubbs' catalyst in CD<sub>2</sub>Cl<sub>2</sub>.



**Figure S6.**  $^1\text{H}$  NMR for ROMP of COD in miniemulsion using CTAC as surfactant (Exp 1 in Table 1). Conditions: RT, 1,5-cyclooctadiene as monomer,  $[\text{Monomer}]/[\text{Catalyst}] = 500:1$ , DD/COD/Surfactant/ $\text{H}_2\text{O} = 0.125 \text{ g}/1.25 \text{ g}/0.125 \text{ g}/25 \text{ g}$  (0.74 mmol/11.6 mmol/0.39 mmol/1388.89 mmol). NMR samples were prepared by micro-scale extraction from 0.5 mL product into 1 mL  $\text{CDCl}_3$ .



t = 60 min



t = 0

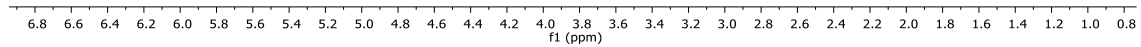


**Figure S7. <sup>1</sup>H NMR for ROMP of NB in miniemulsion using CTAC as surfactant (Exp 2 in Table 1). Conditions: RT, norbornene as monomer, [Monomer]/[Catalyst] = 500:1.**

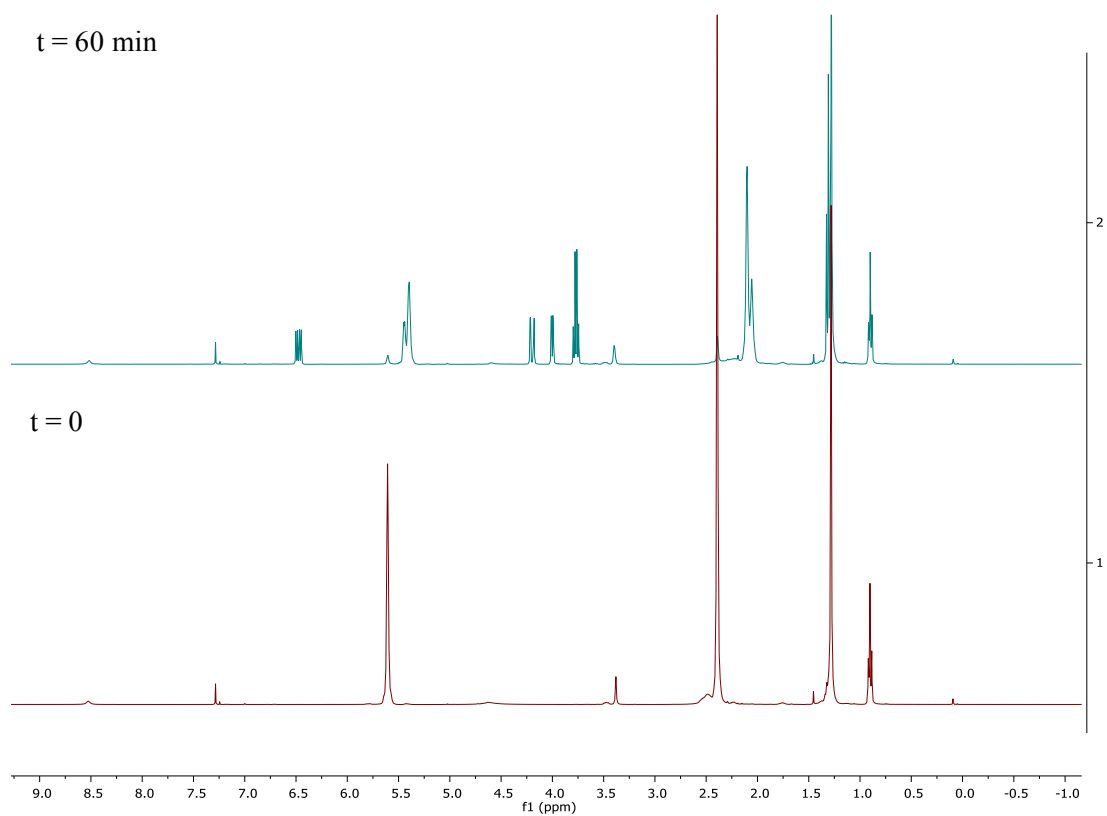
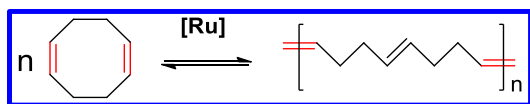


**Figure S8.  $^1\text{H}$  NMR for ROMP of COD in miniemulsion using CTAC as surfactant (Exp 3 in Table 1). Conditions: RT, norbornene as monomer,  $[\text{Monomer}]/[\text{Catalyst}] = 1000:1$ .**



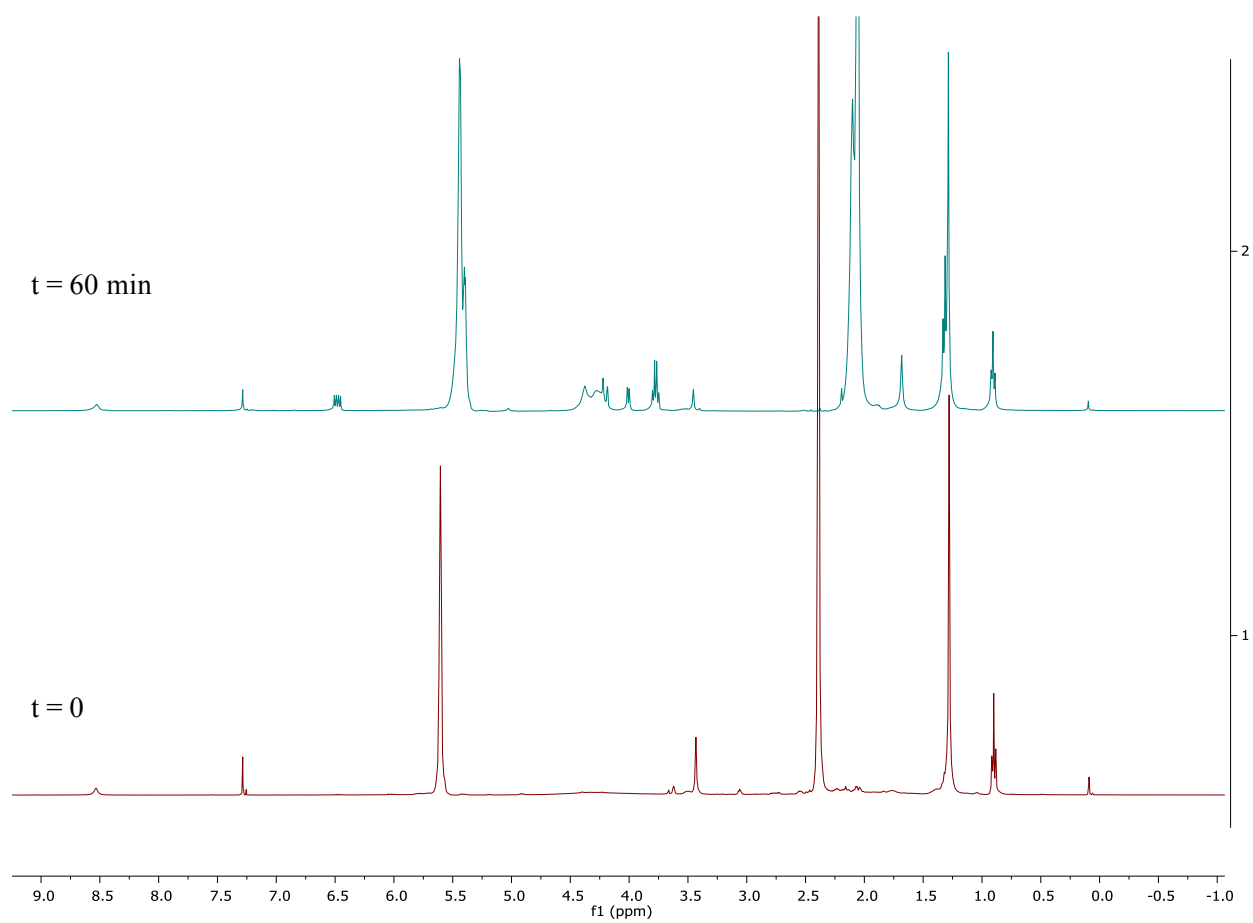
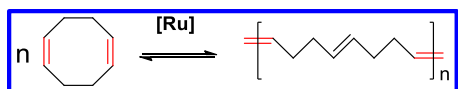


**Figure S9.  $^1\text{H}$  NMR for ROMP of COD in miniemulsion using CTAC as surfactant (Exp 4 in Table 1). Conditions: RT, norbornene as monomer,  $[\text{Monomer}]/[\text{Catalyst}] = 500:1$ . Monomer content = 20 wt% relative to water.**

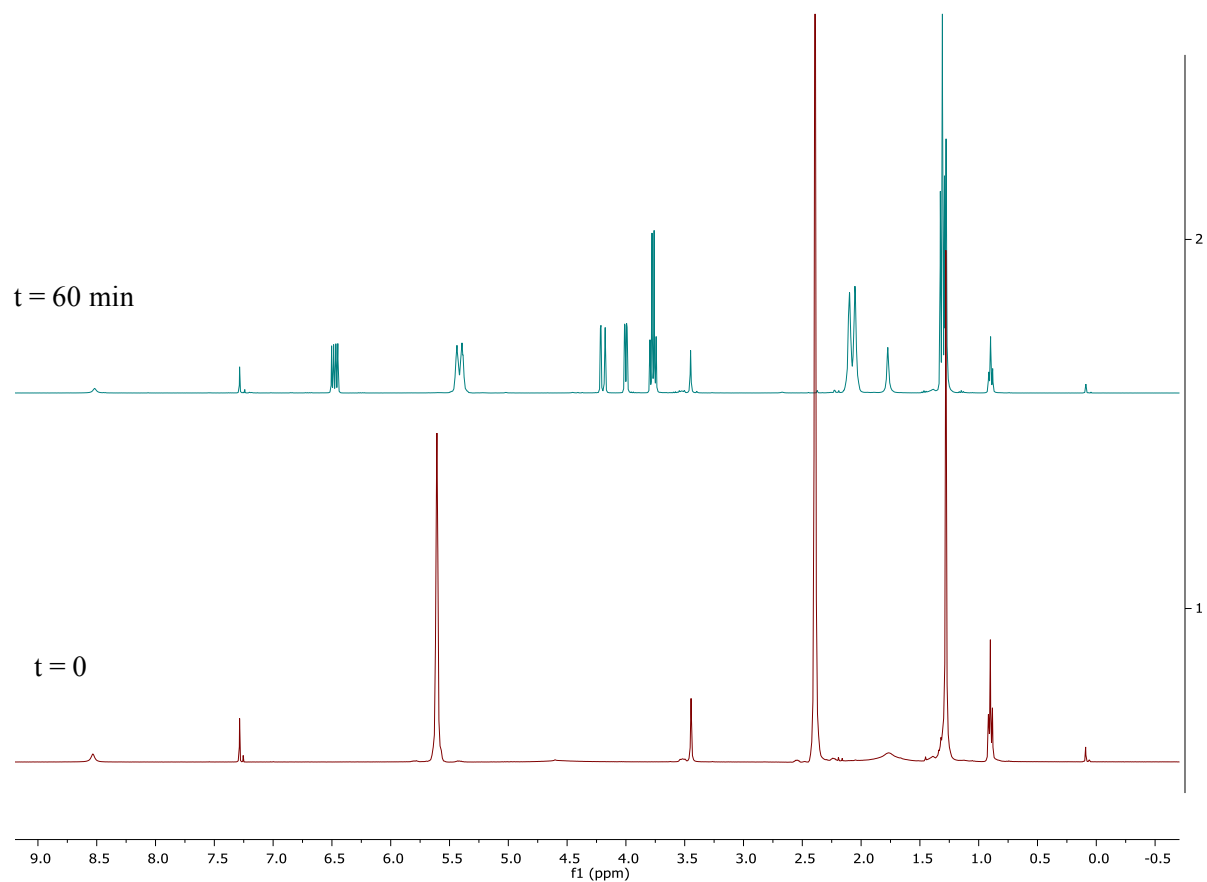
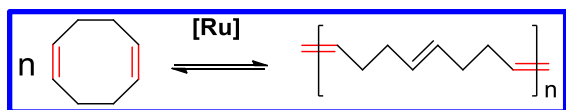


**Figure S10.  $^1\text{H}$  NMR for ROMP of COD in miniemulsion using CTAB as surfactant (Exp 5 in Table 1). Conditions: RT, norbornene as monomer,  $[\text{Monomer}]/[\text{Catalyst}] = 500:1$ .**

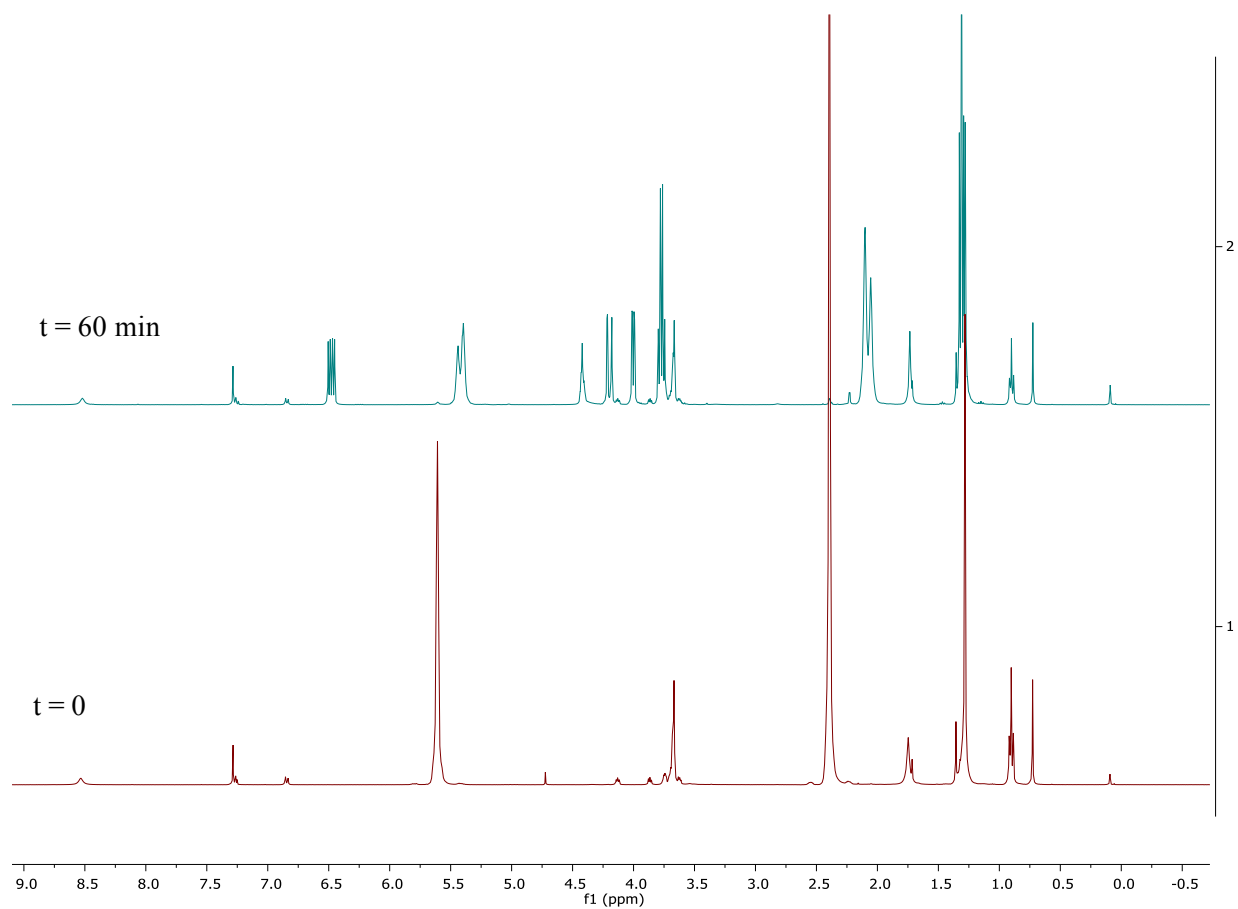
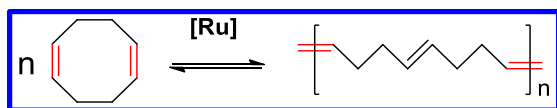


**Figure S11.  $^1\text{H}$  NMR spectra for ROMP of COD in miniemulsion using TritonX-100 as surfactant (Exp 6).**

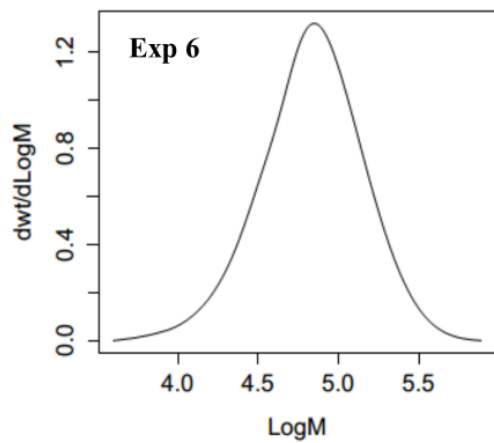
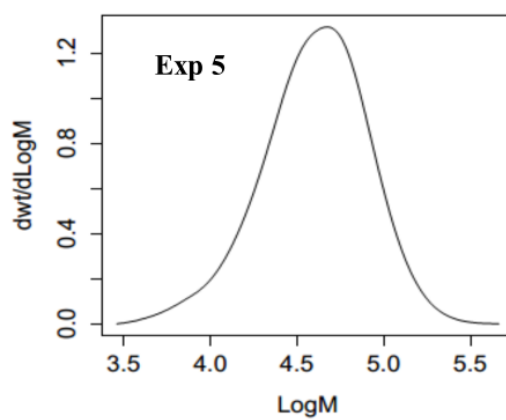
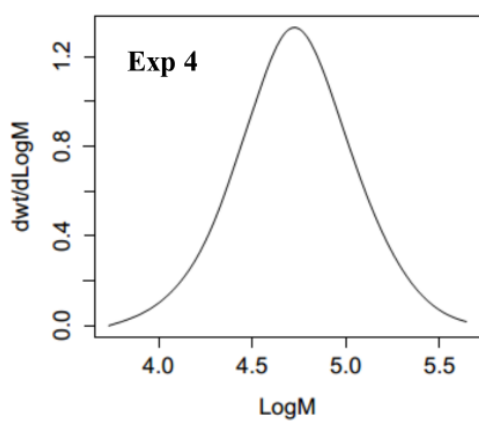
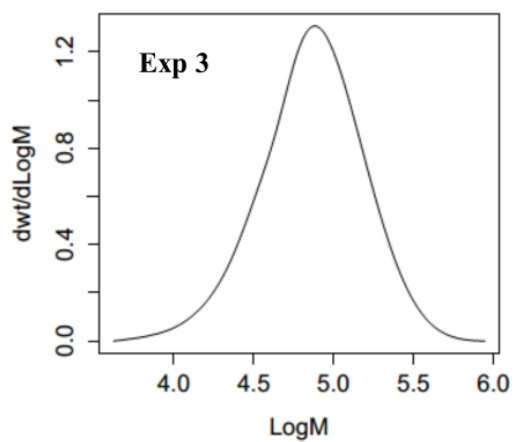
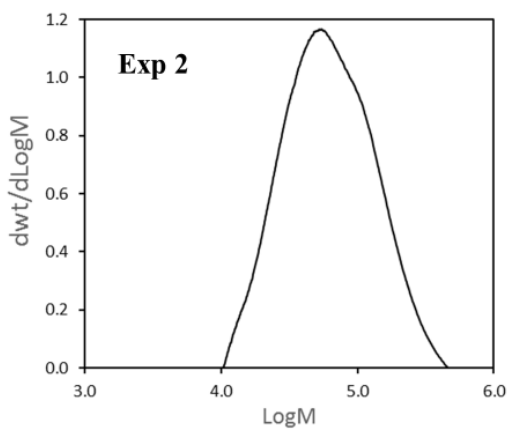
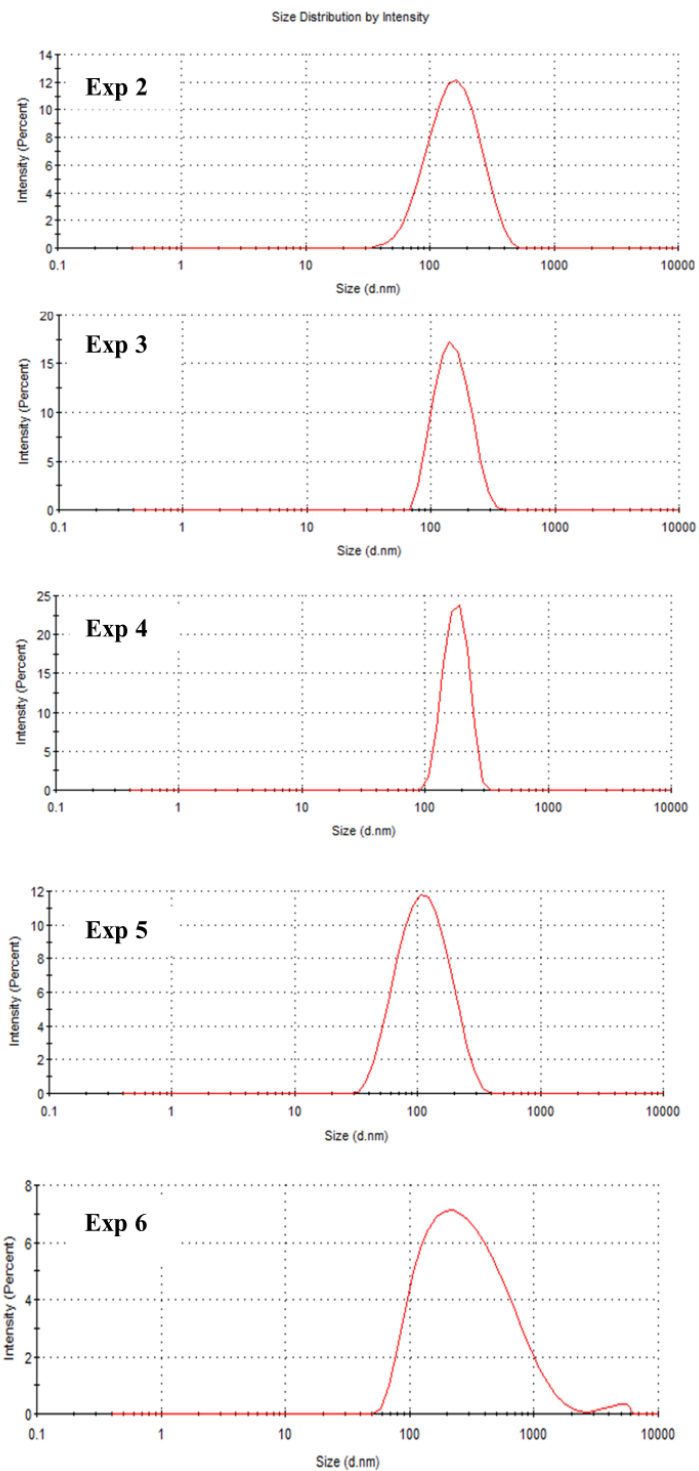


Figure S12. GPC traces of polymer products obtained from Exp 2-6.



**Figure S13. Particle size distribution (PSD) by intensity by DLS for latex particles obtained from Exp 2-6.**

## **Chapter 5 Ring opening metathesis polymerization of norbornene in miniemulsion using PEGylated ruthenium-based metathesis catalyst**

### **5.1 Preface**

Initially, I had begun my research in miniemulsion ROMP by using 1,5-cyclooctadiene (COD) as monomer due to the convenience to characterize COD and polybutadiene (PB) via NMR and GPC. The polymerization turned out to be very successful in miniemulsion. Compared to COD, the high-strained monomer norbornene (NB) may exhibit differently during the miniemulsion polymerization. This chapter presents the work using NB as monomer to prepare latexes particles with the PEGylated metathesis catalyst.

### **5.2 Abstract**

Ring opening metathesis polymerization (ROMP) of norbornene (NB) in miniemulsion was conducted using a water-soluble ruthenium alkylidene as the catalyst. At 25 °C, the highly efficient catalyst yielded colloidally stable polynorbornene (PNB) latexes with ~100% conversion in 10 min. At 0 °C, the monomer conversion could reach 93% in 90 min. Kinetic studies revealed first-order kinetics with excellent livingness as confirmed by the shift of gel permeation chromatograph (GPC) traces. Depending on the surfactants used, the particle sizes ranged from 100 to 300 nm with monomodal distributions.

### 5.3 Introduction

Ring opening metathesis polymerization (ROMP) is recognized as an efficient method to prepare functional and highly unsaturated polymeric materials with narrow molecular weight distributions.<sup>1</sup> Ruthenium-based metathesis catalysts are often employed in ROMP due to their remarkable tolerance to air, moisture, and various functional groups.<sup>2</sup> These features allow potential applications such as biomaterials,<sup>3</sup> liquid crystalline polymers,<sup>4</sup> self-healing materials,<sup>5</sup> and degradable plastics.<sup>6</sup> Particularly, norbornene (NB) and its derivatives have been extensively introduced in ROMP as monomers to prepare a wide range of polymeric structures.<sup>7,8</sup> Most of ROMP reports are conducted in dichloromethane, toluene, and other non-coordinating organic solvents.<sup>9</sup> Yet little attention has been given so far to extend ROMP in an aqueous dispersed system.

Polymerization in an aqueous dispersed system offers numerous advantages such as reducing the environmental impact and health concerns associated with using organic solvents, improving heat transfer, decreasing viscosity, and minimizing the cost of post-reaction separations.<sup>10</sup> Common subtypes of dispersed-phase polymerization such as emulsion polymerization<sup>11</sup> and miniemulsion polymerization<sup>12</sup> have been highly successful in free radical polymerization (FRP)<sup>13,14</sup> and some types of controlled/living radical polymerization (CLRP).<sup>15,16</sup> However, reports related to ROMP in dispersed systems are less common. Early attempts showed that hydrates of Ru chlorides could polymerize norbornene (NB) in emulsion with low yields,<sup>17</sup> likely due to the ineffective generation of catalytically active species. With the rise in popularity of Grubbs' catalysts, Claverie *et al.* introduced a hydrophilic Ru alkylidene in emulsion ROMP by modifying the phosphorous-based labile ligands of Grubbs' first-generation catalyst (G1).<sup>18</sup> Polynorbornene (PNB) nanoparticles (50 ~ 100 nm) were obtained by emulsion polymerization with high yield, but the resulting latex was prone to flocculation. By modifying the benzylidene moiety of G1, Quemener *et al.* synthesized PNB and polybutadiene (PB) nanoparticles in alcoholic or aqueous media via dispersion and suspension ROMP.<sup>19</sup> However, a large amount of coagulum was observed, and

the polymer properties were irreversibly modified by the incorporation of functional groups into the resulting polymer.

In our previous report, we developed a tuned catalyst that was able to initiate in water, but then reacted in the growing (hydrophobic) polymer droplets. We approached the water solubilization of ruthenium NHC catalysts from the standpoint of the labile pyridine ligands associated with Grubbs' third-generation catalyst (G3), which has also been explored by Emrick *et al.*. But their multistep synthetic strategy gave a low yield of unpurified mixture with excess ligands.<sup>20,21</sup> In contrast, we were able to synthesize and purify the PEGylated water-soluble metathesis catalyst in three simple steps. The polymerization was initiated by injecting the obtained catalyst into monomer miniemulsion, and polybutadiene (PB) latexes were successfully obtained with ~ 100% conversion by using 1,5-cyclooctadiene (COD) as monomer.

In this study, we demonstrated that the same strategy could be implemented to produce PNB latexes by polymerizing NB in a miniemulsion system with high monomer conversion and well-defined particle size. The PEGylated catalyst was expected to have a “tuned” hydrophilicity, meaning it could be readily dissolved in water and became hydrophobic upon the dissociation of PEG-tagged pyridines. The activated catalyst subsequently diffused into the submicron monomer droplets to facilitate the chain propagation in the droplets. Thanks to a good tolerance and high efficiency of the catalyst in a polar environment, latex particles ranging from 100 to 300 nm were produced with high monomer conversion. We explored the reaction kinetics and evolution of molecular weight of ROMP of norbornene. The colloidal characteristics of the miniemulsion polymerization were also investigated in detail.

## **5.4 Experimental section**

### **5.4.1 Materials**



All reagents were purchased from Sigma-Aldrich and used without further purification unless otherwise specified. Grubbs second-generation catalyst (G2) was received from Materia Inc. All solvents and monomers used in this study were degassed through freeze-pump-thaw cycles and stored in a glovebox filled with argon prior to use. All manipulations were performed under argon using Schlenk techniques. The PEGylated metathesis catalyst was synthesized according to previous procedure.

#### **5.4.2 Characterization**

$^1\text{H}$  NMR and  $^{13}\text{C}$  NMR were recorded on a 400 MHz Bruker Avance-400 spectrometer. Monomer conversion was determined by  $^1\text{H}$  NMR. Molecular weight and molecular weight distribution were determined by Gel Permeation Chromatography (GPC) relative to polystyrene standards on a Waters 2695 separations module combined with Waters 410 differential refractometer. THF was used as eluent and molecular weights were corrected according to Mark–Houwink parameters.<sup>22</sup> Mark–Houwink parameters were used for polynorbornene ( $a = 0.68$  and  $K = 0.000099$  dl/g).<sup>23</sup> Particle size distributions were determined by Dynamic Light Scattering (DLS) on a Zetasizer Nano ZS from Malvern Instruments at 25 °C with a 173° scattering angle.

#### **5.4.3 ROMP of norbornene (NB) in miniemulsion**

An oil-in-water miniemulsion consists of two phases. The organic phase was obtained by mixing degassed NB (1.25 g, 13.3 mmol) and degassed dodecane (0.12 g, 0.73 mmol, 0.5 wt% of water). Prior to the preparation of oil phase, DCM (1 mL) was introduced to dissolve the solid-state NB properly. The water phase was obtained by mixing degassed deionized water (25 g) and cetyltrimethylammonium chloride (0.125 g, 0.5 wt% of water). The organic phase and water phase were mixed sufficiently, followed by ultrasonication in an ice bath for 15 min at 15 watts. The ultrasonication was conducted under argon to maintain an inert atmosphere. The miniemulsion polymerization was carried out in a 25 mL Schlenk tube fitted with an argon inlet and a magnetic stir set at 900 rpm. To initiate the

polymerization, the water-soluble catalyst was added into the miniemulsion and the reaction tube was magnetically stirred at room temperature. To conduct a miniemulsion polymerization at 0 °C, the reaction tube was immersed in an ice bath during the polymerization.

## **5.5 Results and discussion**

### **5.5.1 Monomer miniemulsion**

A NB miniemulsion was prepared via intensive homogenization during which large droplets were broken into smaller ones, thus creating more interfacial area. Meanwhile the newly formed droplets absorb surfactant from the continuous phase (water) to remain stable, thus reducing the number of micelles. The obtained miniemulsion was not perfectly stable since the monomer droplets could undergo degradation by coalescence (droplets contact each other and merge into larger droplets) and Ostwald ripening (monomer proceeds with a net diffusion from small droplets to large ones without direct contact).<sup>24</sup> Ideally, the coalescence can be stopped by adding surfactant and the Ostwald ripening can be minimized by adding a costabilizer to retard monomer diffusion. To verify the stability of monomer miniemulsions, the droplet size of a NB miniemulsion with cetyltrimethylammonium chloride (CTAC) as surfactant and dodecane as costabilizer was monitored by DLS over 2 hours at room temperature (Figure 5.1).

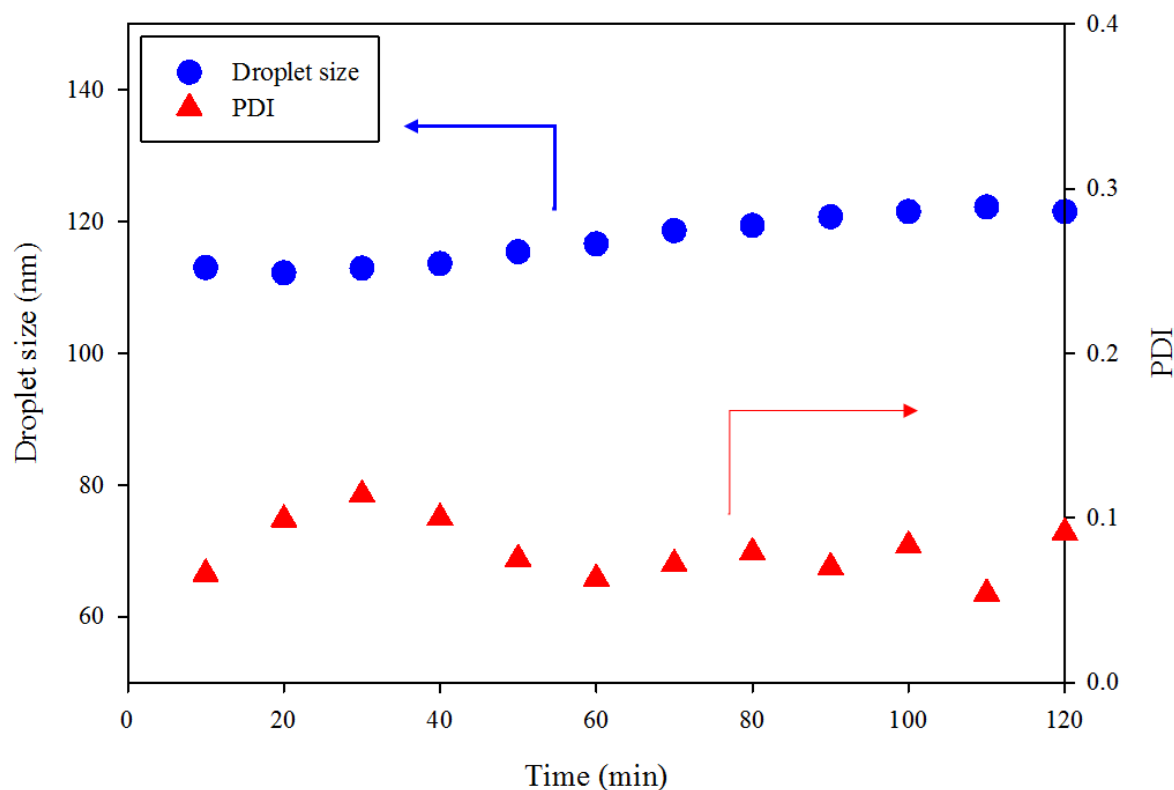


**Figure 5.1 Droplet size (●) vs time and PDI (▲) vs time for NB monomer miniemulsion. Recipe: dodecane/NB/CTAC/H<sub>2</sub>O = 0.125 g/1.25 g/0.125 g/25 g. Condition: sonication at 15 watt for 15 min in an ice bath. 1mL DCM was added in oil phase to dissolve solid-state NB. Sample was diluted in water (0.15 mL in 1.5 mL) prior to DLS measurement at room temperature.**

In general, the droplet radius ( $r$ ) will increase with time when the stability of the miniemulsion is poor. If coalescence occurs continuously in a miniemulsion,  $r^2$  would increase linearly with time, whereas  $r^3$  will increase linearly with time if the degradation is caused by Ostwald ripening.<sup>25</sup> After several trials with different formulations, a stable NB miniemulsion was obtained with 5 wt% monomer, 0.5 wt% surfactant and 0.5 wt% costabilizer (all percentages with respect to water). Figure 5.1 shows that the monomer miniemulsion displayed an intensity-average diameter that were stable over 2 hours with a range from 115 to 125 nm, indicating the combination of surfactant and costabilizer was efficient in preventing the degradation of the miniemulsion within the time scope of polymerization. A small quantity of DCM was

introduced to dissolve solid-state NB, which might lead to an increase in average droplet size through diffusion. The distributions of droplet size were broad (PDI ~ 0.09) but the PDI value was stable over time.

### 5.5.2 Miniemulsion polymerization

To investigate ROMP in miniemulsion under different conditions, multiple reactions were run as shown in Table 5.1 and Table 5.2. Overall, all experiments had excellent reproducibility with none of the latexes showing coagulation or phase separation within one week.

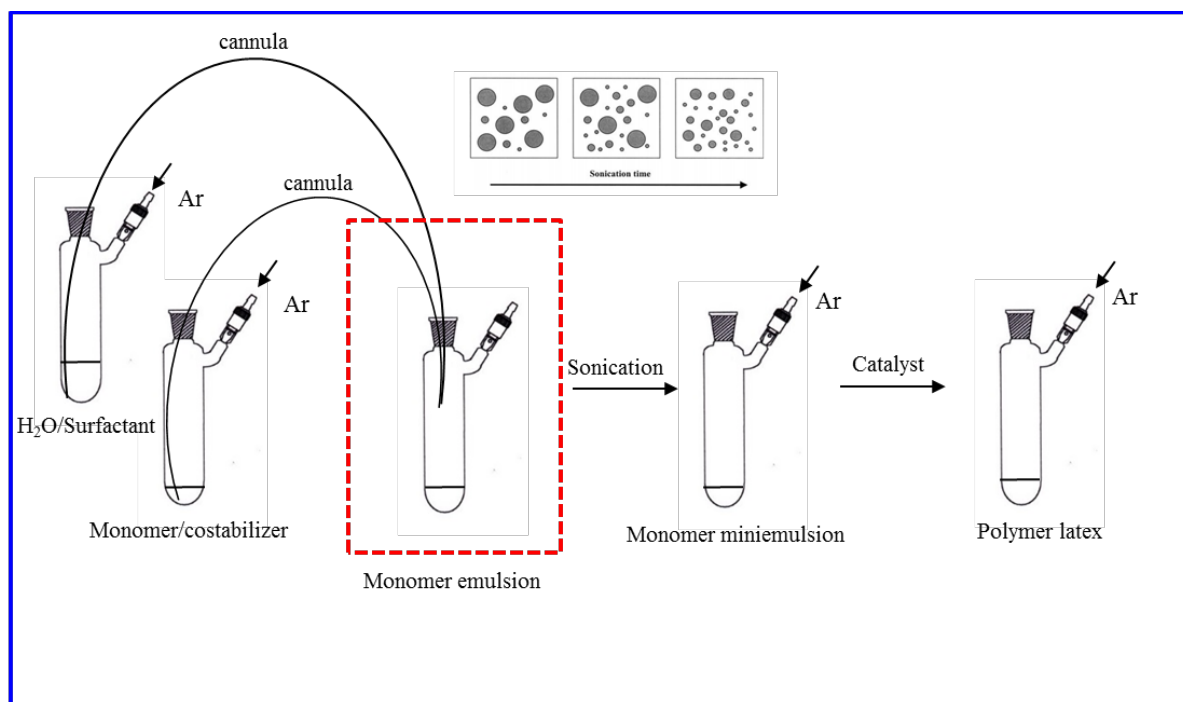
**Table 5.1 Experimental conditions and results for the ROMP of NB in miniemulsion**

Entry	Surfactant	Monomer content	Temperature (°C)	Reaction time (min)	Conversion
Exp 1	CTAC	5%	25	10	93%
				30	100%
				60	100%
				90	100%
Exp 2	CTAC	5%	0	10	58%
				30	75%
				60	87%
				90	94%
Exp 3	CTAB	5%	25	30	92%
				60	100%
Exp 4	Triton X-100	5%	25	30	87%
				60	100%

**Table 5.2 Molecular weight and particle size data for each experiment in this study.**

Entry	Surfactant	Monomer content	Temperature	Mn	Mw	Dispersity	Particle size	PDI
Exp 1	CTAC	5%	25	93000	160800	1.73	107	0.092
Exp 2	CTAC	5%	0	112500	217000	1.93	105	0.079
Exp 3	CTAB	5%	25	237000	472944	1.99	125	0.087
Exp 4	Triton X-100	5%	25	206700	437800	2.11	228	0.354

We began the ROMP of NB in miniemulsion with a target chain length (TCL) at 1000 (Exp 1). The monomer miniemulsion was prepared by intensive ultrasonication and the polymerization was initiated by adding the water-soluble metathesis catalyst into the miniemulsion under argon (Scheme 5.1). It was observed that the catalyst could be dissolved in the continuous phase without visibly causing any droplet coalescence. The color of the reaction mixture changed from green (the color of unreacted catalyst) to light grey in 5 min, indicating the fast activation of the catalyst. The monomer conversion reached ~100% and the particle size was 107 nm with a PDI = 0.09. It was demonstrated that the high-strain cyclic olefin norbornene could be polymerized at high conversion by using the water-soluble catalyst in our study.



**Scheme 5.1 Procedure for ROMP in miniemulsion with air-free conditions.**

### 5.5.3 Kinetic study

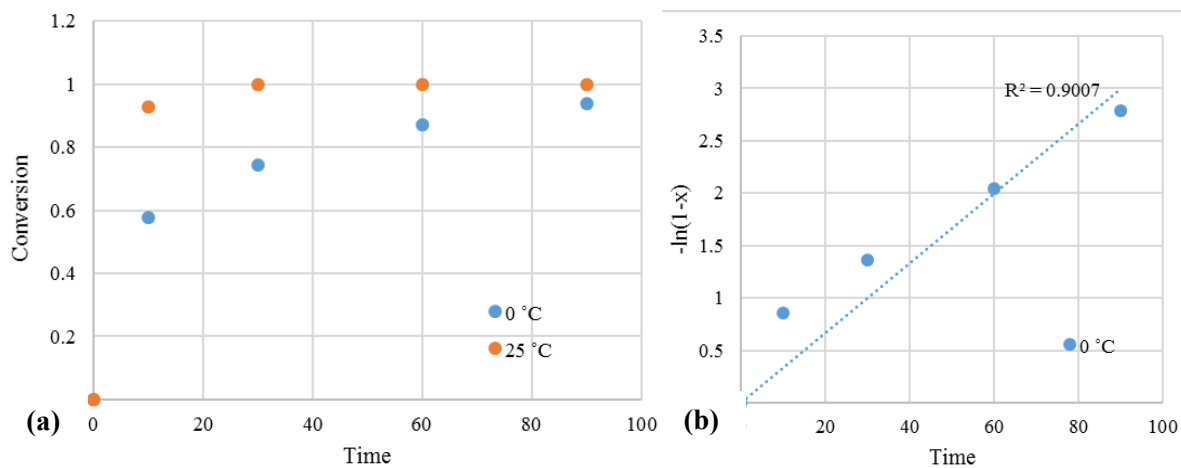


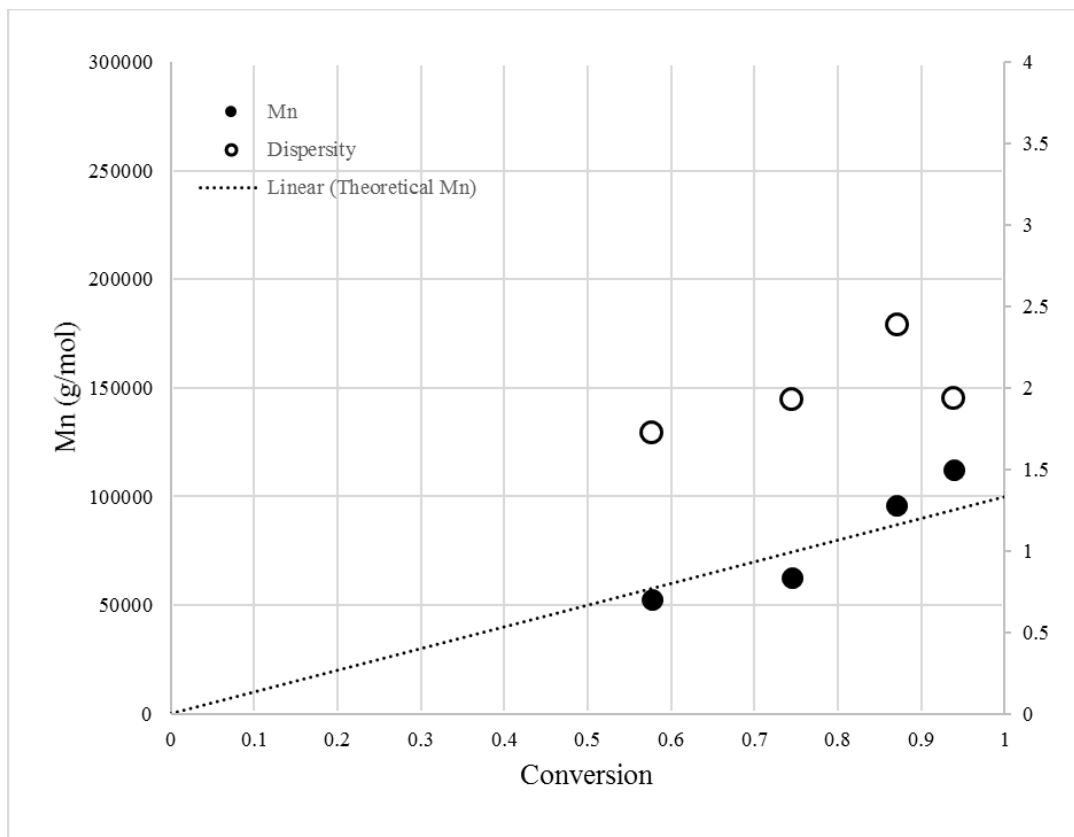
**Figure 5.2 Conversion ( $x$ ) and  $\ln[1/(1-x)]$  plots for ROMP of norbornene (NB) in miniemulsion using PEGylated metathesis catalyst.  $[\text{monomer}]/[\text{catalyst}] = 1000:1$ , monomer content: 5 wt%. Two reaction was conducted at 25 °C (Exp 1, orange dots) and 0 °C (Exp 2, blue dots).**

In Exp 1 and Exp 2, multiple samples of on-going reaction mixture were taken at given times and quenched with ethyl vinyl ether to rapidly terminate the polymerization. For Exp 1, the rate of polymerization was so high that 90% conversion was observed in 5 min and a full conversion was achieved in 30 min (Figure 5.2 (a), orange dots). There was no free radical involved in ROMP and the chain propagation was coordinated by transition metal center ( $[Ru]$ ).

At 25 °C, the conversion reached 100% after 30 min and it was difficult to use the data points to evaluate reaction kinetics due to mathematical difficulties (when  $x = 100\%$ ,  $\ln[1/(1-x)]$  has no physical meaning). We then repeated the same reaction at 0 °C to slow down the polymerization and facilitate the sampling procedure (Exp 2). For Exp 2, the monomer conversion was 57% at 10 min and 75% at 30 min. And 93% conversion was observed at 90 min. It was not surprising that a lower temperature led to a lower rate of polymerization because both the catalyst activation and chain propagation were largely slowed down at 0 °C. Importantly, in Exp 2 a pseudo first-order kinetic profile was observed as well (Figure 5.2 (b)), indicating a stable concentration of living species during the polymerization. Therefore the synthesized catalyst did appear to stay reactive after being activated in an aqueous environment. The water-soluble metathesis catalyst is expected to have similar reactivity and functional group compatibility as the Grubbs third-generation catalyst (G3) since they will generate identical propagating species.

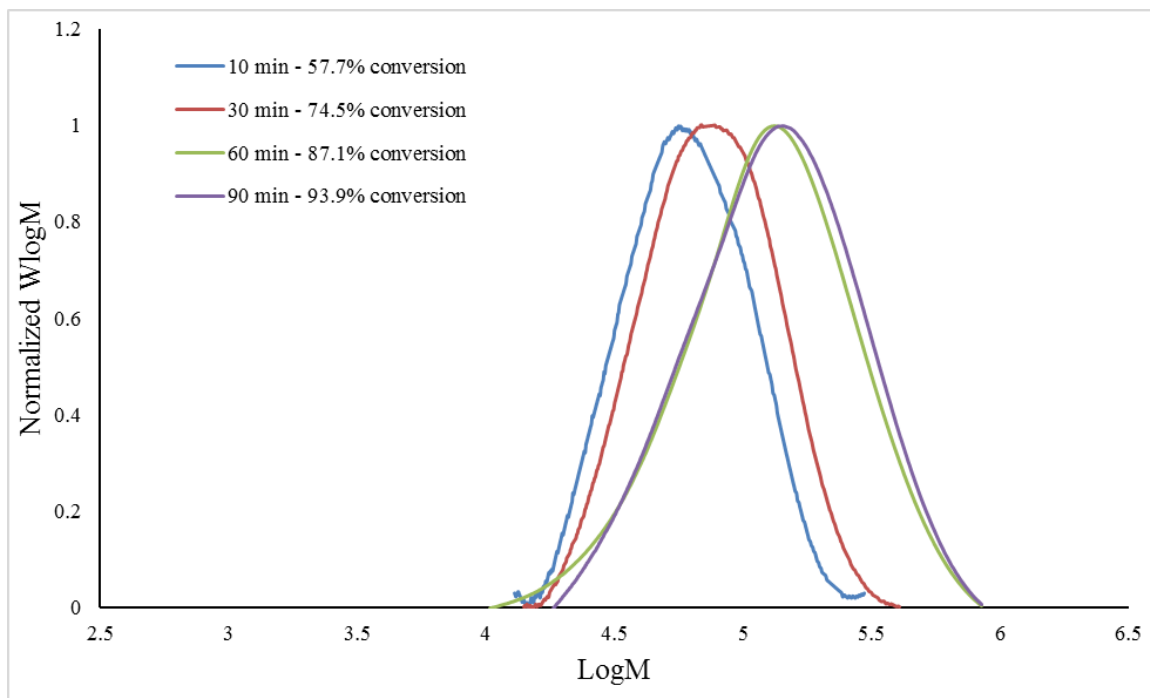
#### 5.5.4 Molecular weight

The number average molecular weight ( $M_n$ ) is a key indicator of the chain propagation during a living polymerization. For Exp 1, the number average molecular weight ( $M_n$ ) could reach 12900 g/mol at 100% conversion with a final dispersity ( $\mathcal{D}$ ) at 1.73, suggesting a very fast chain propagation at room temperature. For Exp 2, the  $M_n$  value increased from 52800 g/mol at 58% conversion to 112500 g/mol at 94% conversion (Figure 5.3). Further, the shift of GPC traces in Figure 5.4 indicated good livingness in the miniemulsion polymerization.



**Figure 5.3** Number average molecular weight ( $M_n$ ) and dispersity ( $\mathcal{D}$ ) plots for ROMP of norbornene (NB) in miniemulsion using PEGylated water-soluble metathesis catalyst.





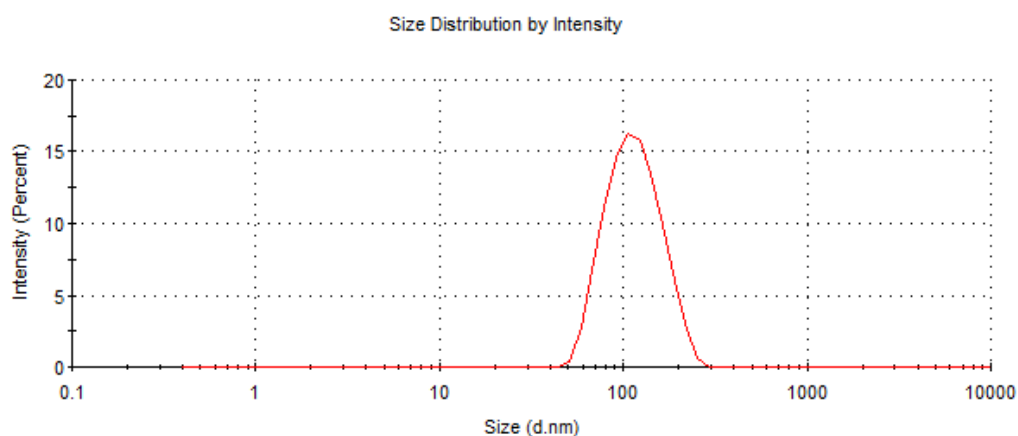
**Figure 5.4 The evolution of GPC traces (normalized height) with conversion for ROMP of NB in miniemulsion using PEGylated water-soluble catalyst.**

Figure 5.3 shows the experimental  $M_n$  increased with monomer conversion due to continuous chain growth. Initially the  $M_n$  values were slightly lower than the theoretical  $M_n$ . The differences are not large, and could be attributable to errors associated with the use of the Mark-Houwink parameters or potentially due to chain transfer from secondary metathesis during the polymerization.<sup>27</sup> Interestingly, when the monomer conversion was higher than 85%, the  $M_n$  value was higher than the theoretical value, suggesting that during a long period time of reaction the polymerization might encounter a loss of livingness.

### 5.5.5 Particle size distribution

The particle size distribution (PSD) from Exp 1 was given in Figure 5.5. A monomodal PSD was observed with an average particle size at 107 nm and the polydispersity index (PDI) of latex particles (PDI = 0.093) was very close to the PDI value of initial monomer droplets (PDI = 0.105). This agreed

with the mechanism of miniemulsion polymerization where the monomer droplets could keep their identity during polymerization without significant degradation or exchange kinetics involved.<sup>28</sup>



**Figure 5.5 Size distribution by intensity for polymer latex obtained from ROMP of norbornene (NB) in miniemulsion (Exp 1). Z-average parameter: 107 nm, PDI: 0.092.**

### 5.5.6 Effect of surfactants

The same experiments were also repeated with CTAB as surfactant in Exp 3 and Triton X-100 as surfactant in Exp 4. The selection of surfactants in miniemulsion ROMP may alter the reactivity of catalyst due to the potential interactions between the counter ions on the surfactants and transition metal center. Grubbs and coworkers noticed a possible halogen ligand exchanges around the ruthenium of Grubbs first generation catalyst and they preferred to use a chloride surfactant instead of bromide surfactant.<sup>29,30</sup> In our study, both CTAC and CTAB were used as surfactants with high conversion and the halogen exchange between the surfactants and catalyst had no significant effect on the final conversion. However, when using CTAB as surfactant, the molecular weight (237000 g/mol) obtained from Exp 3 was much higher than the theoretical value (100000 g/mol), which resulted from the partial loss of livingness.

The ionic and nonionic surfactants exhibited different abilities to stabilize the miniemulsion system. It was observed that the particle size was smaller with ionic stabilization (~ 105 nm for CTAC and CTAB) than with steric stabilization (228 nm for Triton X-100). The difference in the surfactant type also resulted in a broader particle size distribution (PDI) in a polymer latex stabilized by non-ionic surfactants.

## **5.6 Conclusion**

We conducted the ring opening metathesis polymerization of norbornene in miniemulsion using a PEGylated Ru-based catalyst. The water-soluble catalyst could polymerize norbornene rapidly in miniemulsion with high monomer conversion. The polymerization followed first-order kinetics with an excellent livingness. And the monomer miniemulsion was found to be stable with sufficient surfactant and costabilizer, which provided ideal environment for catalyst to initiate the polymerization with no coagulum. The particle size ranged from 100 to 300 nm with either ionic or non-ionic surfactants used. The scope of this study can be further extended to more specific applications by introducing functionalized norbornene derivatives as monomers.

## **5.7 Acknowledgements**

Financial support from the Ontario Research Chairs (MFC) programs, and from the Natural Sciences and Engineering Research Council of Canada is gratefully acknowledged.

## 5.8 References

- (1) Hoveyda, A. H.; Zhugralin, A. R. The Remarkable Metal-Catalysed Olefin Metathesis Reaction. *Nature* **2007**, *450* (7167), 243–251.
- (2) Nguyen, S. T.; Johnson, L. K.; Grubbs, R. H.; Ziller, J. W. Ring-Opening Metathesis Polymerization (ROMP) of Norbornene by a Group VIII Carbene Complex in Protic Media. *J. Am. Chem. Soc.* **1992**, *114* (10), 3974–3975.
- (3) Wathier, M.; Lakin, B. A.; Bansal, P. N.; Stoddart, S. S.; Snyder, B. D.; Grinstaff, M. W. A Large-Molecular-Weight Polyanion, Synthesized via Ring-Opening Metathesis Polymerization, as a Lubricant for Human Articular Cartilage. *J. Am. Chem. Soc.* **2013**, *135* (13), 4930–4933.
- (4) Haque, H. A.; Kakehi, S.; Hara, M.; Nagano, S.; Seki, T. High-Density Liquid-Crystalline Azobenzene Polymer Brush Attained by Surface-Initiated Ring-Opening Metathesis Polymerization. *Langmuir* **2013**, *29* (25), 7571–7575.
- (5) White, S. R.; Sottos, N. R.; Geubelle, P. H.; Moore, J. S.; Kessler, M. R.; Sriram, S. R.; Brown, E. N.; Viswanathan, S. Correction: Autonomic Healing of Polymer Composites. *Nature* **2002**, *415* (6873), 817–817.
- (6) Fishman, J. M.; Kiessling, L. L. Synthesis of Functionalizable and Degradable Polymers by Ring-Opening Metathesis Polymerization. *Angew. Chem. Int. Ed. Engl.* **2013**, *52*, 5061–5064.
- (7) Brumaghim, J. L.; Girolami, G. S. Ring-Opening Metathesis Polymerization of Norbornene by Cp\* 2 Os 2 Br 4 and Related Compounds. *Organometallics* **1999**, *18* (10), 1923–1929.
- (8) Ilker, M. F.; Schule, H.; Coughlin, E. B. Modular Norbornene Derivatives for the Preparation of Well-Defined Amphiphilic Polymers: Study of the Lipid Membrane Disruption Activities. *Macromolecules* **2004**, *37* (3), 694–700.
- (9) Sanford, M. S.; Love, J. A.; Grubbs, R. H. Mechanism and Activity of Ruthenium Olefin Metathesis Catalysts. *J. Am. Chem. Soc.* **2001**, *123* (27), 6543–6554.
- (10) Schork, F. J.; Luo, Y.; Smulders, W.; Russum, J. P.; Butté, A.; Fontenot, K. Miniemulsion

- Polymerization. *Adv. Polym. Sci.* **2005**, *175*, 129–255.
- (11) Smith, W. V.; Ewart, R. H. Kinetics of Emulsion Polymerization. *J. Chem. Phys.* **1948**, *16* (1948), 592.
- (12) Tiarks, F.; Landfester, K.; Antonietti, M. Preparation of Polymeric Nanocapsules by Miniemulsion Polymerization. *Langmuir* **2001**, *17* (3), 908–918.
- (13) Asua, J. M. Miniemulsion Polymerization. *Prog. Polym. Sci.* **2002**, *27* (7), 1283–1346.
- (14) Chern, C. S. Emulsion Polymerization Mechanisms and Kinetics. *Prog. Polym. Sci.* **2006**, *31* (5), 443–486.
- (15) Cunningham, M. F. Controlled/living Radical Polymerization in Aqueous Dispersed Systems. *Prog. Polym. Sci.* **2008**, *33* (4), 365–398.
- (16) Cunningham, M. F. Living/controlled Radical Polymerizations in Dispersed Phase Systems. *Prog. Polym. Sci.* **2002**, *27* (6), 1039–1067.
- (17) Rinehart, R. E.; Smith, H. P. The Emulsion Polymerization of the Norbornene Ring System Catalyzed by Noble Metal Compounds. *J. Polym. Sci. Part B Polym. Lett.* **1965**, *3* (12), 1049–1052.
- (18) Claverie, J. P.; Viala, S.; Maurel, V.; Novat, C. Ring-Opening Metathesis Polymerization in Emulsion. *Macromolecules* **2001**, *34* (3), 382–388.
- (19) Quémener, D.; Chemtob, A.; Héroguez, V.; Gnanou, Y. Synthesis of Latex Particles by Ring-Opening Metathesis Polymerization. *Polymer (Guildf)*. **2005**, *46* (4), 1067–1075.
- (20) Breitenkamp, K.; Emrick, T. Amphiphilic Ruthenium Benzylidene Metathesis Catalyst with PEG-Substituted Pyridine Ligands. *J. Polym. Sci. Part A Polym. Chem.* **2005**, *43* (22), 5715–5721.
- (21) Samanta, D.; Kratz, K.; Zhang, X.; Emrick, T. A Synthesis of PEG- and Phosphorylcholine-Substituted Pyridines to Afford Water-Soluble Ruthenium Benzylidene Metathesis Catalysts. *Macromolecules* **2008**, *41* (3), 530–532.
- (22) Hamielec, A. E.; Ouano, A. C. Generalized Universal Molecular Weight Calibration Parameter in GPC. *J. Liq. Chromatogr.* **1978**, *1* (1), 111–120.

- (23) Patil, A. O.; Zushma, S.; Stibrany, R. T.; Rucker, S. P.; Wheeler, L. M. Vinyl-Type Polymerization of Norbornene by nickel(II) Bisbenzimidazole Catalysts. *J. Polym. Sci. Part A Polym. Chem.* **2003**, *41* (13), 2095–2106.
- (24) Voorhees, P. W. The Theory of Ostwald Ripening. *J. Stat. Phys.* **1985**, *38*, 231–252.
- (25) Capek, I. Degradation of Kinetically-Stable O/w Emulsions. *Adv. Colloid Interface Sci.* **2004**, *107* (2-3), 125–155.
- (26) Rule, J. D.; Moore, J. S. ROMP Reactivity of E Ndo - and E Xo -Dicyclopentadiene. *Macromolecules* **2002**, *35* (21), 7878–7882.
- (27) Chen, Z.-R.; Claverie, J. P.; Grubbs, R. H.; Kornfield, J. a. Modeling Ring-Chain Equilibria in Ring-Opening Polymerization of Cycloolefins. *Macromolecules* **1995**, *28*, 2147–2154.
- (28) Landfester, K.; Bechthold, N.; Förster, S.; Antonietti, M. Evidence for the Preservation of the Particle Identity in Miniemulsion Polymerization. *Macromol. Rapid Commun.* **1999**, *20* (2), 81–84.
- (29) Lynn, D. M.; Kanaoka, S.; Grubbs, R. H. Living Ring-Opening Metathesis Polymerization in Aqueous Media Catalyzed by Well-Defined Ruthenium Carbene Complexes. *J. Am. Chem. Soc.* **1996**, *118* (4), 784–790.
- (30) Lynn, D. M.; Mohr, B.; Grubbs, R. H.; Henling, L. M.; Day, M. W. Water-Soluble Ru Alkylidenes: Synthesis, Characterization, and Application to Olefin Metathesis in Protic Solvents. *J. Am. Chem. Soc.* **2000**, *122* (2), 6601–6609.

## 5.9 Supporting Information

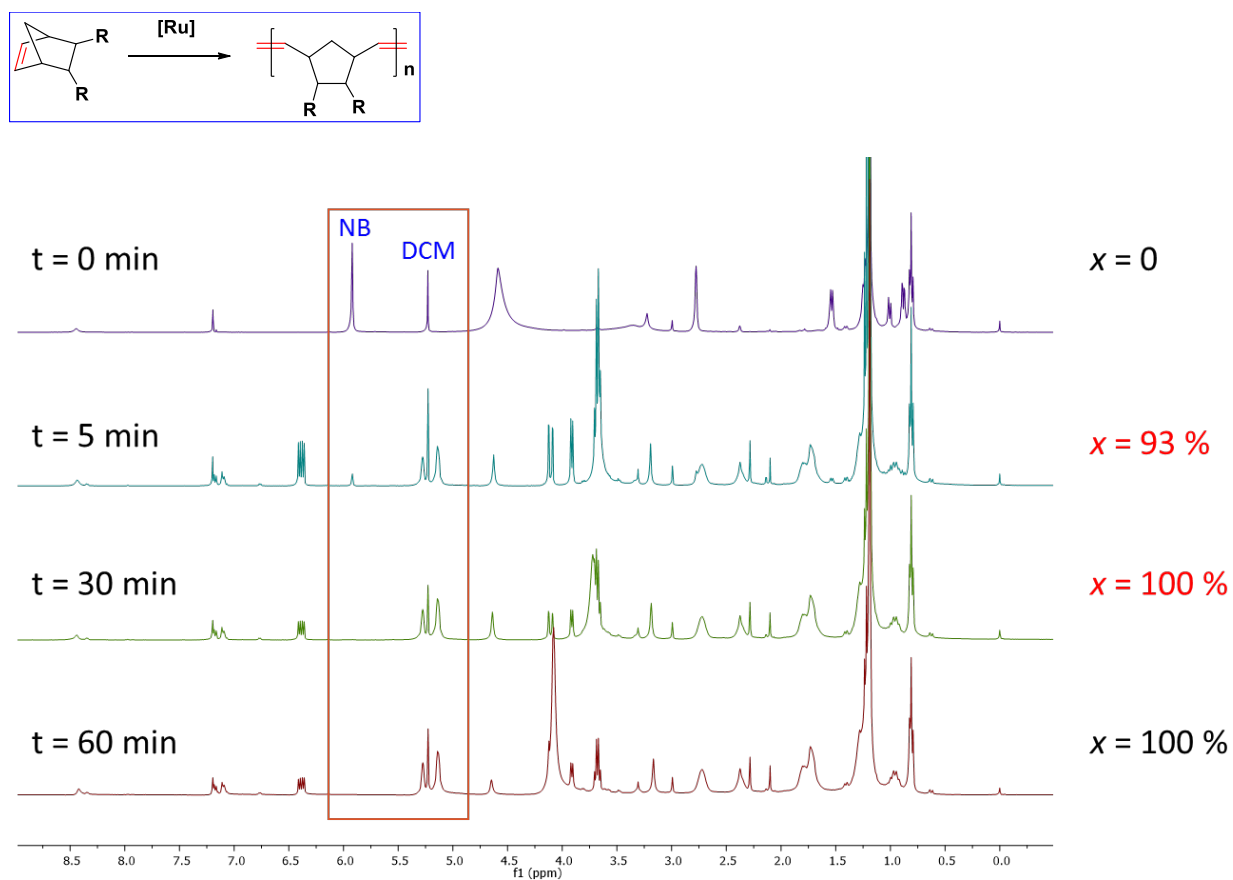
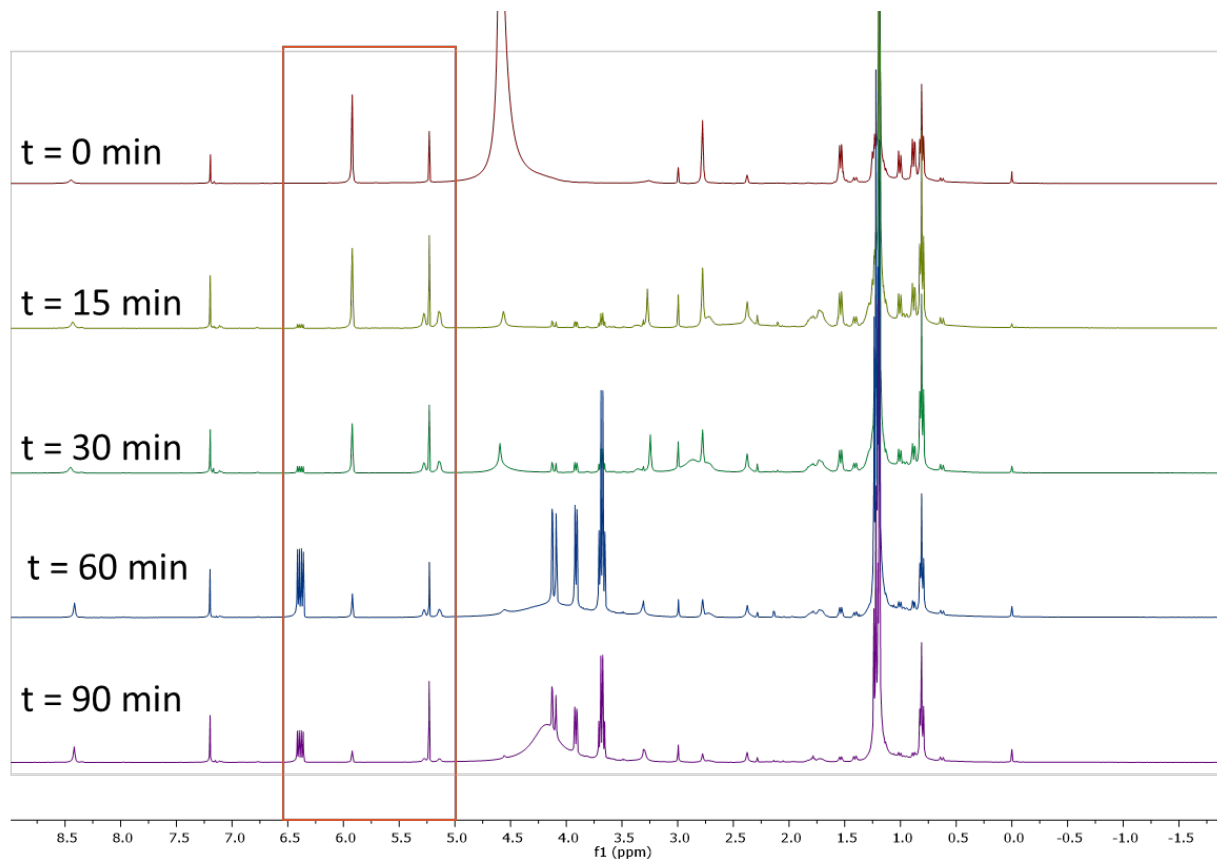
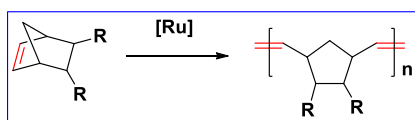


Figure S1.  $^1\text{H NMR}$  for ROMP of NB in miniemulsion using CTAC as surfactant (Exp 1).

Conditions: RT, norbornene as monomer,  $[\text{Monomer}]/[\text{Catalyst}] = 1000:1$ , DD/NB/Surfactant/ $\text{H}_2\text{O}$  = 0.125 g/1.25 g/0.125 g/25 g (0.74 mmol/11.6 mmol/0.39 mmol/1388.89 mmol). NMR samples were prepared by micro-scale extraction from 0.5 mL product into 1 mL  $\text{CDCl}_3$ .



**Figure S2.  $^1\text{H}$  NMR for ROMP of NB in miniemulsion using CTAC as surfactant (Exp 2).**

**Conditions:  $0^\circ\text{C}$  (ice bath), norbornene as monomer,  $[\text{Monomer}]/[\text{Catalyst}] = 1000:1$ ,**

**$\text{DD/NB/Surfactant}/\text{H}_2\text{O} = 0.125\text{ g}/1.25\text{ g}/0.125\text{ g}/25\text{ g}$  (0.74 mmol/11.6 mmol/0.39 mmol/1388.89**

**mmol). NMR samples were prepared by micro-scale extraction from 0.5 mL product into 1 mL**

**$\text{CDCl}_3$ .**



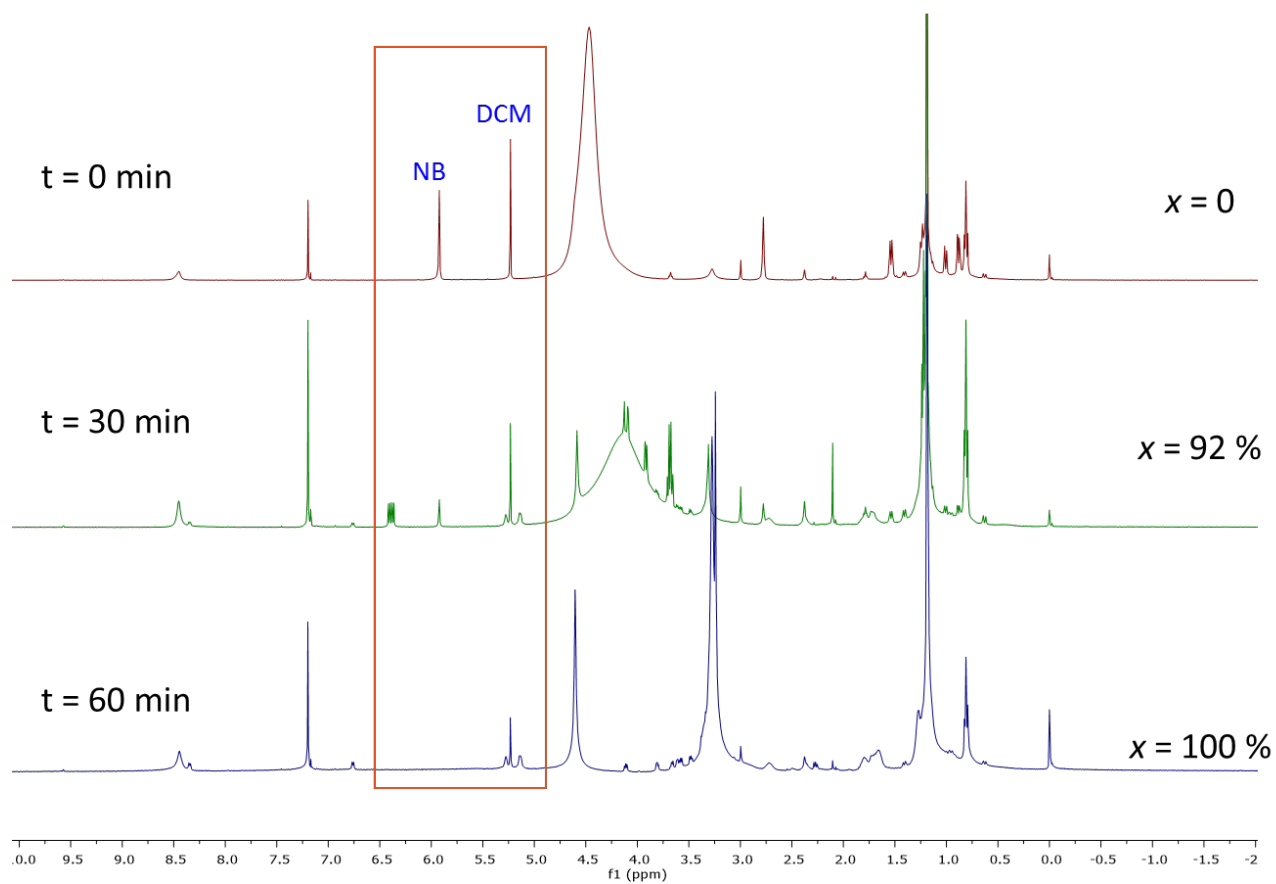
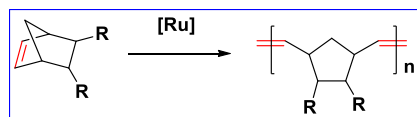


**Figure S3.**  $^1\text{H}$  NMR for ROMP of NB in miniemulsion using CTAB as surfactant (Exp 3).

**Conditions:** RT, norbornene as monomer,  $[\text{Monomer}]/[\text{Catalyst}] = 1000:1$ .

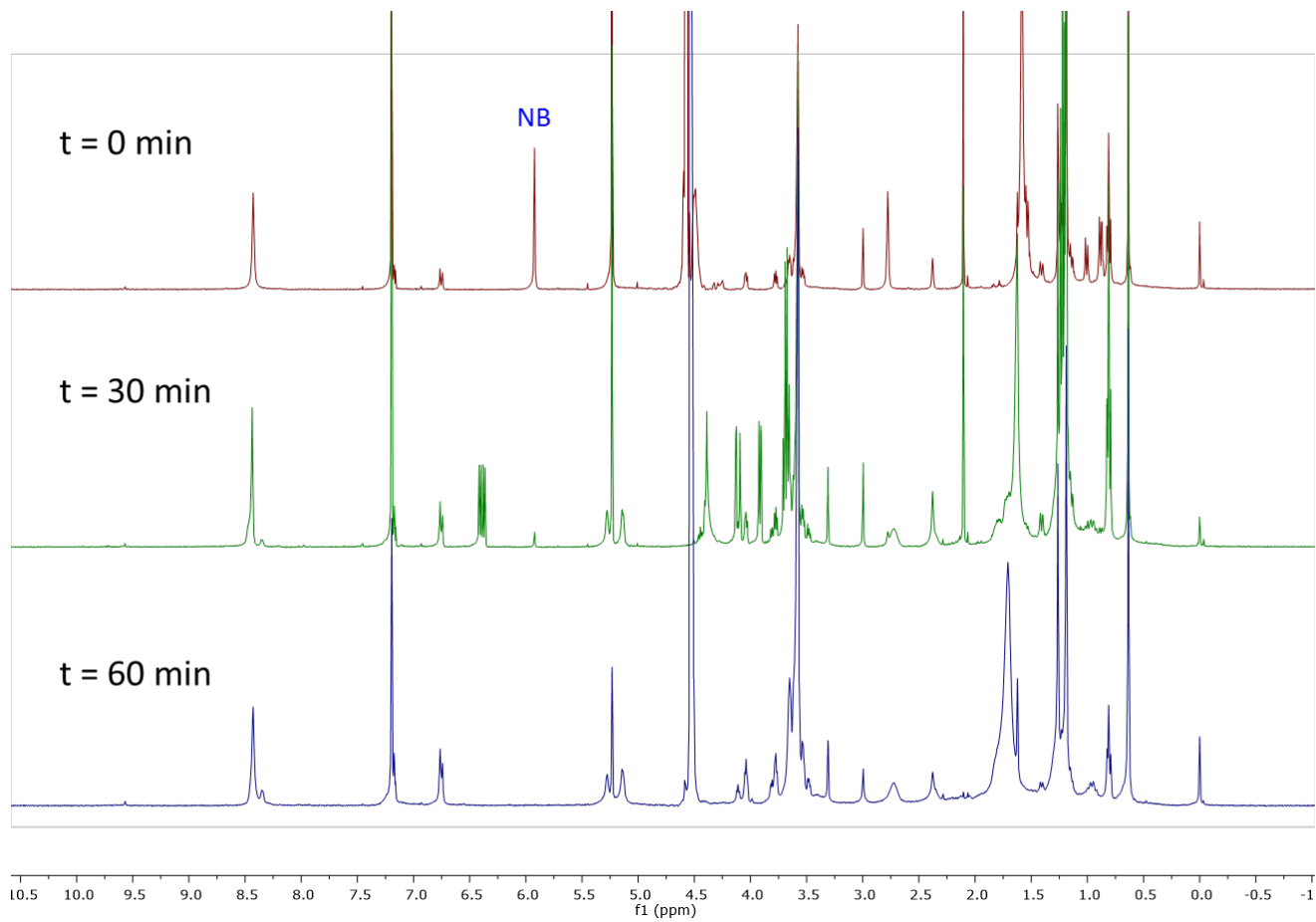
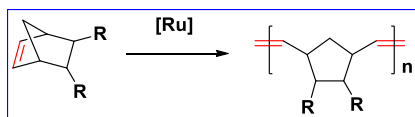


**Figure S4.  $^1\text{H}$  NMR for ROMP of COD in miniemulsion using Triton X-100 as surfactant.**

**Conditions: RT, norbornene as monomer, [Monomer]/[Catalyst] = 1000:1.**

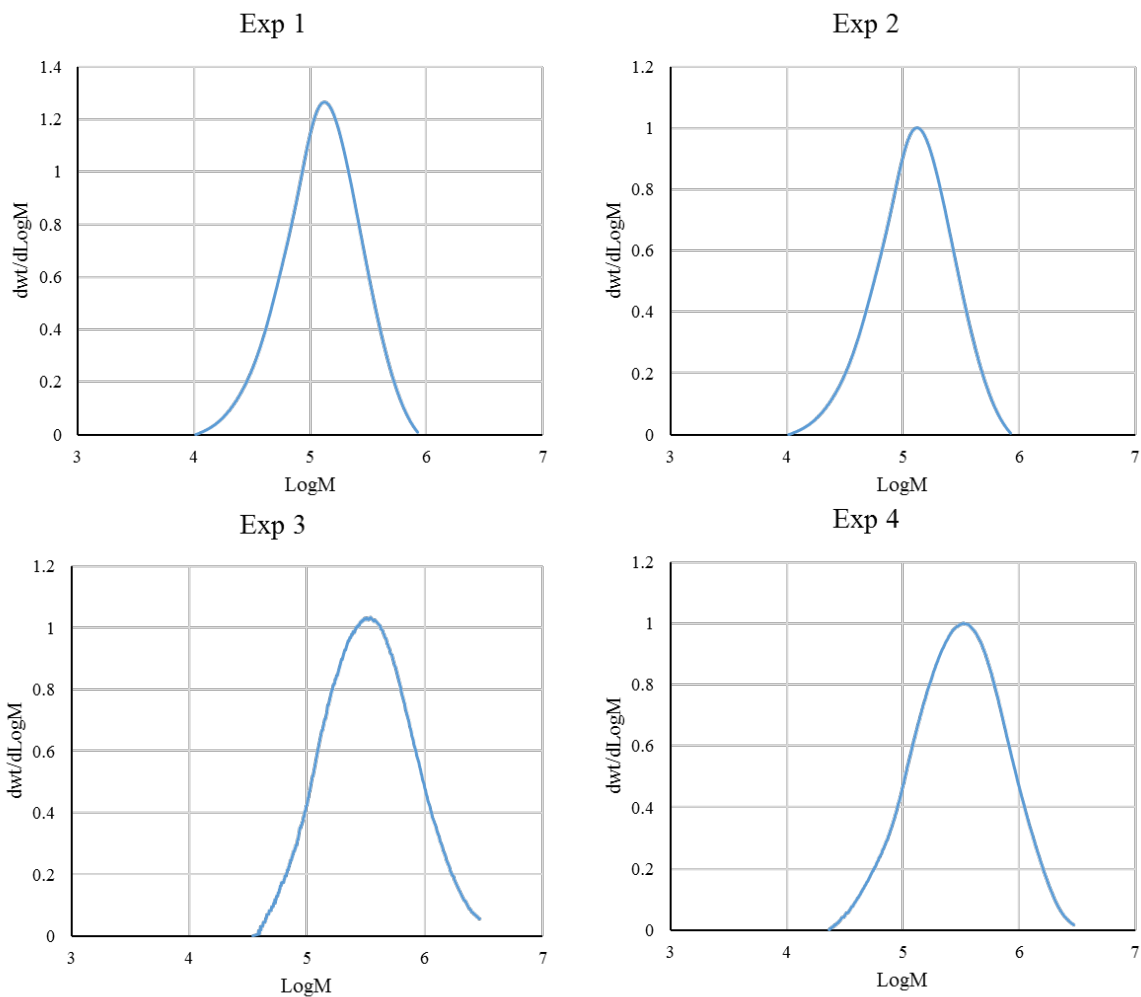


**Figure S5. GPC traces of polymer products obtained from Exp 1-4 at 60 min.**

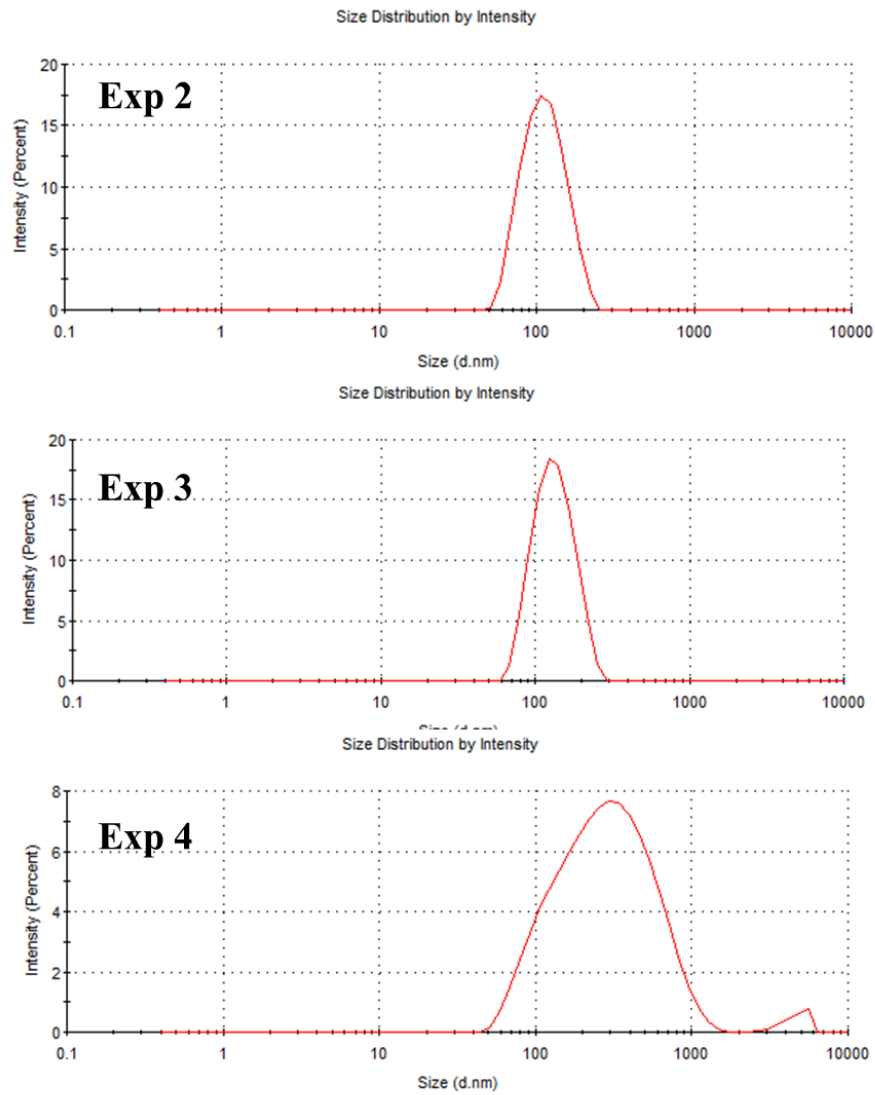


**Figure S6. Particle size distribution (PSD) by intensity by DLS for latex particles obtained from Exp 2-4.**

## Chapter 6 Conclusions and Recommendations for Future Work

### 6.1 Conclusions

In this work, we demonstrated that water could be introduced as the continuous phase to polymerize cyclic olefins by ROMP in miniemulsion. Using a PEGylated Ru-based metathesis catalyst we showed that both 1,5-cyclooctadiene (COD) and norbornene (NB) could be polymerized rapidly in miniemulsion with high monomer conversion.  $^1\text{H}$  NMR showed the catalyst with PEG-tagged pyridines was stable and reactive in water, although it was very sensitive to oxygen.

At room temperature, the ROMP of COD in miniemulsion could reach  $\sim 100\%$  conversion in 1 hour.  $^1\text{H}$  NMR revealed first order kinetics with a stable concentration of living species ( $[Ru]$ ). The livingness of ROMP in miniemulsion was also demonstrated by the increase of number average molecular weight ( $M_n$ ) and the shift of entire GPC traces to higher values with conversion. The particle size of polybutadiene (PB) latexes ranged from 100 to 300 nm with either ionic or non-ionic surfactants used. These results encouraged us to use a lower catalyst loading (0.1 mol% to monomer) and a higher monomer content (20 wt% to water), both of which were achieved with 100% conversion. When using norbornene (NB) as monomer, a faster rate of polymerization was observed and the monomer conversion could reach 100% in 10 min at room temperature. At  $0^\circ\text{C}$ , the monomer conversion could reach 93% in 90 min. Kinetic studies revealed first-order kinetics with excellent livingness as confirmed by the shift of gel permeation chromatograph (GPC) traces. Depending on the surfactants used, the polynorbornene particle sizes ranged from 100 to 300 nm with monomodal distributions.

In all the experiments, the miniemulsion polymerization was initiated by directly adding the water-soluble catalyst into the monomer miniemulsion. Using the recipe provided in our study, the obtained COD or NB miniemulsion was found to be stable with sufficient surfactant and costabilizer, which provided an ideal environment for metathesis catalyst to initiate the polymerization with no coagulum. The

mini-emulsion polymerization followed droplet nucleation mechanism with no monomer diffusion necessarily involved, which made this strategy very promising when polymerizing hydrophobic monomers. Furthermore, multiple experiments were run by using different surfactants (CTAC, CTAB, and Triton X-100) and the type of surfactants resulted in different molecular weights and particle sizes. Both CTAC and CTAB were used as surfactants with full conversion and the halogen exchange between the surfactants and catalyst had no significant effect on the final conversion. However a broader particle size distribution ( $PDI > 0.1$ ) was observed in polymer latexes stabilized by non-ionic surfactants.

## **6.2 Recommendations for future work**

The development of metathesis catalyst is always the key step throughout the research of olefin metathesis. The dissociation of ligands and the interaction between transition metal and cyclic olefins is critical during the initiation stage of ROMP. We would recommend more research efforts on the development of metathesis catalysts that can be used in emulsion or mini-emulsion systems with elevated activity and tolerance.

In Chapter 4, we demonstrated a good control of polymerization when conducting mini-emulsion polymerization. The complexity of a heterogeneous system like emulsion or mini-emulsion made it difficult to fully understand the reaction kinetics and nucleation mechanism. This is especially true when dealing with a transition-metal mediated non-radical polymerization like ROMP. Clearly, more in-depth knowledge is needed here to fully understand the side reactions involved in ROMP such as chain transfer and how to avoid side reactions (or how to take advantage of them). We showed that a larger average particle size was obtained when increasing the solid content of mini-emulsion emulsion system. It would also be interesting to investigate the effect of surfactant on particle sizes of final products when the control of particle size is critical for industrial application. And a higher surfactant to monomer ratio will be required if the solid content goes beyond 20 wt%.

In Chapter 5, we described the ROMP of NB in an aqueous dispersed system, which extended our research to a broader range of ROMP monomers. However no attention was given to introducing functional monomers with more sophisticated structures and properties. Thus we would recommend more cyclic olefins especially norbornene derivatives be introduced to our miniemulsion system. For instance (Figure 6.1), a 2,3-disubstituted-7-alkylidene norborn-2-ene derivative (monomer 1) with hydrophilic character can be added into the current ROMP process to yield polymer chains with spaced hydrophilic and hydrophobic groups.<sup>1</sup> An *exo,exo*-7-oxabicyclo[2.2.1]hept-5-ene-2,3-di(*N,N*-dimethyl)amino ethanolato dicarboxylate (monomer 2) can be polymerized to build blocks for functional material applications.<sup>2</sup> The incorporation of other functional groups, like –OH group in 5-hydroxyl-1-cyclooctene (monomer 3) and halogen group in 5-bromo-1-cyclooctene (monomer 4) can be potentially achieved by ROMP as well.<sup>3</sup>

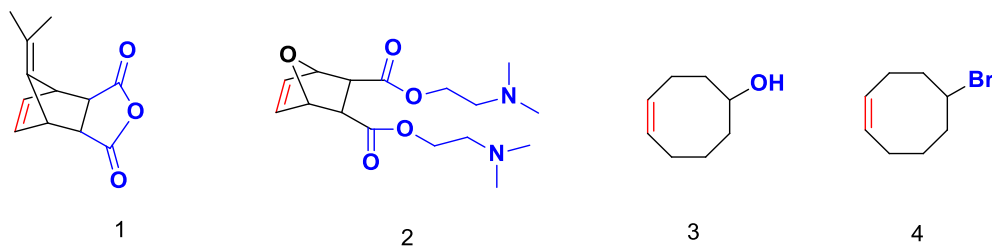


**Figure 6.1 Functional cyclic olefins for ROMP**

Importantly, conventional emulsion technique is more popular in industry compared to miniemulsion polymerization. Thus the next step of this study is to establish the conditions at which ROMP can be conducted in a conventional emulsion system. In emulsion polymerization, if the nucleation takes place in micelles or water phase, a permanent solubility of the catalyst in water can be an asset to largely reduce the probability of catalyst entering into monomer droplets. This approach is helpful when the monomer used is somewhat soluble in water and cannot form a very stable miniemulsion. Additionally, the current

procedure can further be simplified because sonication and costabilizer are not necessary in an emulsion polymerization process.

### 6.3 References

- (1) Ilker, M. F.; Schule, H.; Coughlin, E. B. Modular Norbornene Derivatives for the Preparation of Well-Defined Amphiphilic Polymers: Study of the Lipid Membrane Disruption Activities. *Macromolecules* **2004**, *37* (3), 694–700.
- (2) Alfred, S. F.; Lienkamp, K.; Madkour, A. E.; Tew, G. N. Water-Soluble ROMP Polymers from Amine-Functionalized Norbornenes. *J. Polym. Sci. Part A Polym. Chem.* **2008**, *46* (19), 6672–6676.
- (3) Hillmyer, M. A.; Laredo, W. R.; Grubbs, R. H. Ring-Opening Metathesis Polymerization of Functionalized Cyclooctenes by a Ruthenium-Based Metathesis Catalyst. *Macromolecules* **1995**, *28* (18), 6311–6316.



## Appendix A Preparation of monomer miniemulsion

Early attempts and experimental results for preparing stable monomer miniemulsion are reported as below.

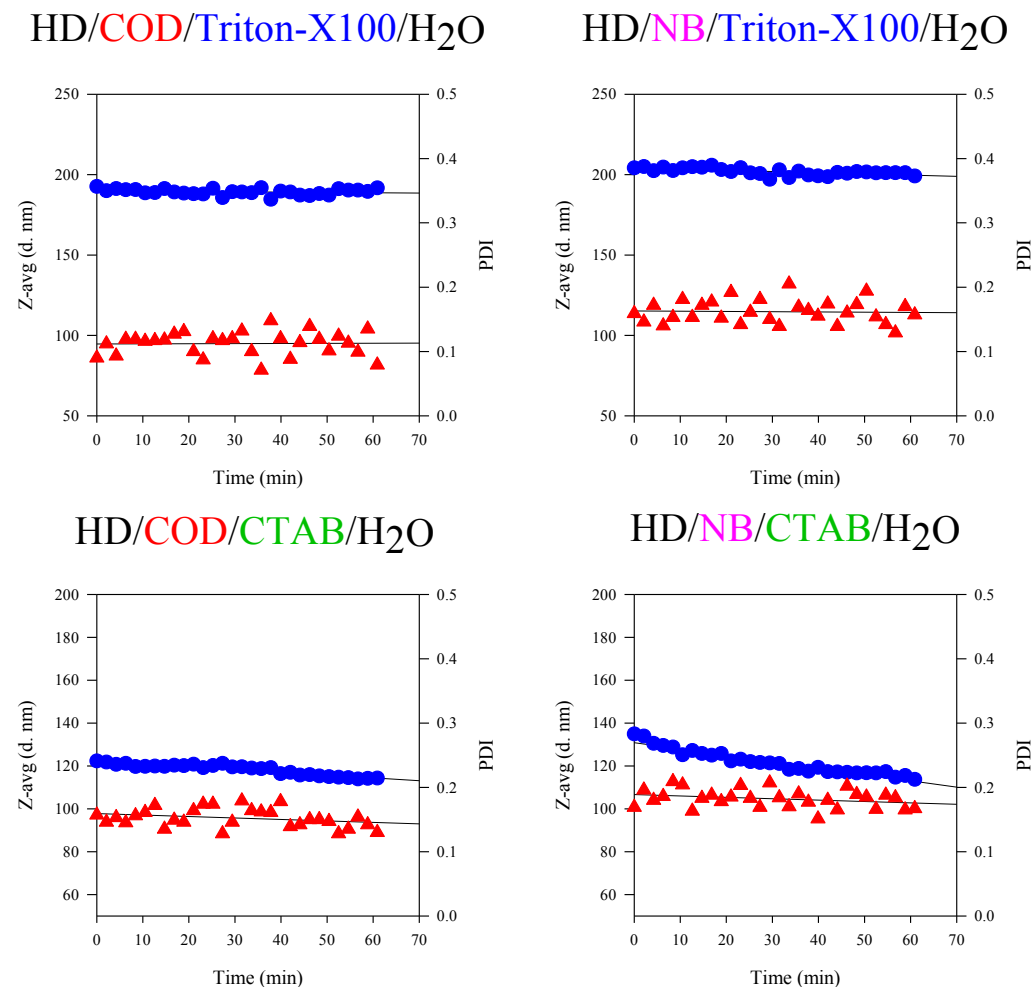


**Figure A1. Z-avg diameter vs time and PDI vs time for monomer miniemulsions with various monomers and surfactants. Recipes: HD/Monomer/Surfactant/H<sub>2</sub>O = 0.05 g/0.5 g/0.05 g/5 g.**

**Sonication at 15 watt for 15 min in ice bath. Each sample was diluted in water (0.15mL in 1.5 mL) prior to DLS measurement.**

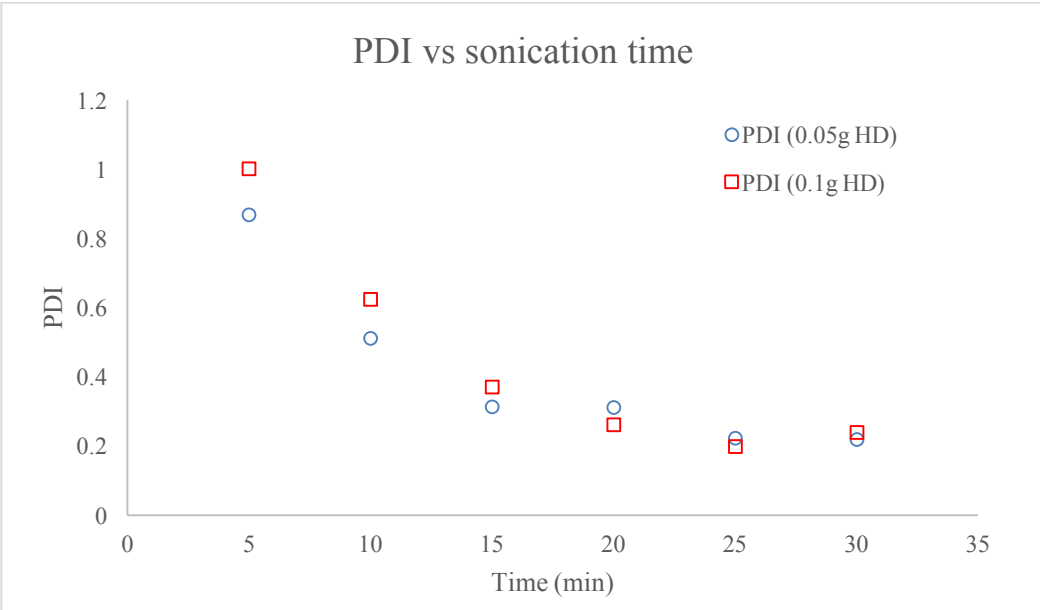
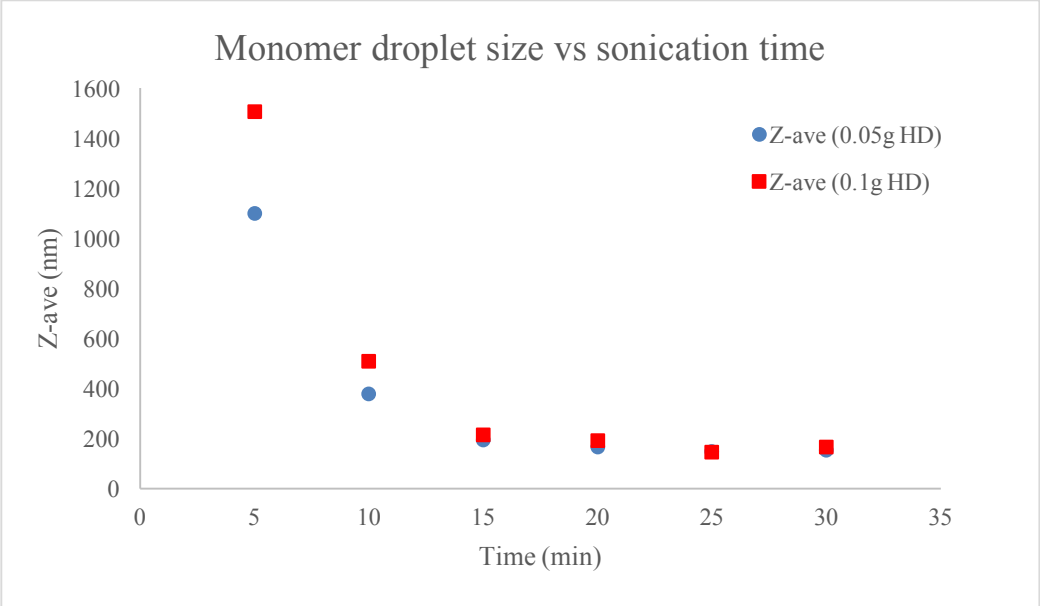


**Figure A2. Evolution of monomer droplet size (up) and PDI (bottom) versus sonication time in a bath sonicator.  $\text{H}_2\text{O}/\text{CTACl}/\text{Monomer} = 5 \text{ g}/0.05\text{g}/0.5\text{g}$ .  $[\text{CTACl}] = 31.3 \text{ mM}$ ,  $[\text{COD}] = 926 \text{ mM}$ . Hexadecane (co-stabilizer) was added at 0.05g (10 wt% of monomer) and 0.1g (20 wt% of monomer) respectively to compare the difference in colloidal behavior.**

## Appendix B Experimental results for ROMP with the new catalyst

Chapter 4 highlighted the importance of air-free condition to run ROMP successfully in miniemulsion. As a comparison, the experimental results at the early stage are reported as below.

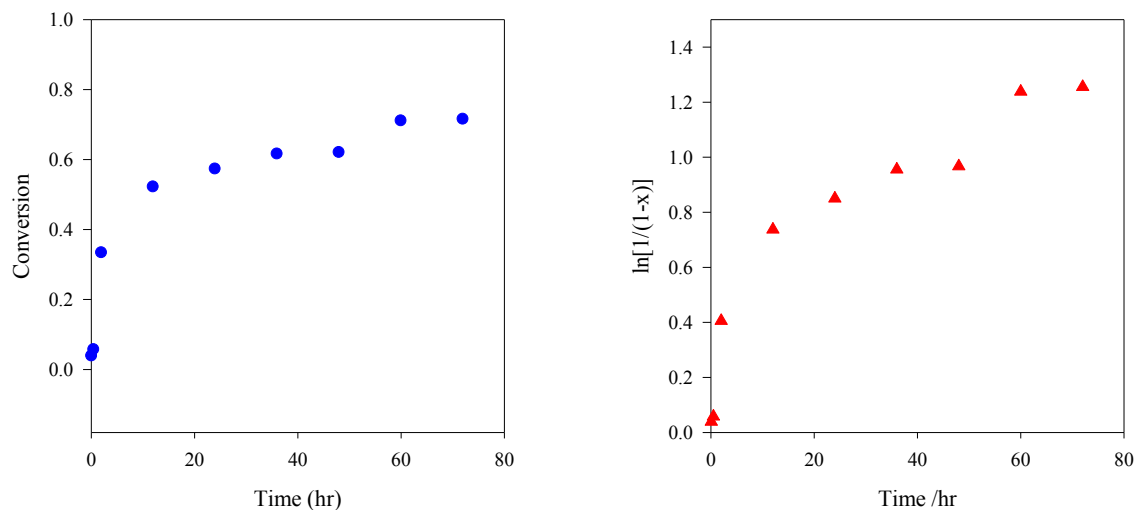


**Figure B1. Conversion and  $\ln[1/(1-x)]$  plots for miniemulsion ROMP of COD ( $x$  is conversion).**

**[monomer]/[catalyst]=500:1, HD/Monomer/Triton X-100/H<sub>2</sub>O = 0.22 mmol/4.6 mmol/0.08 mmol/280 mmol, 25 °C.**

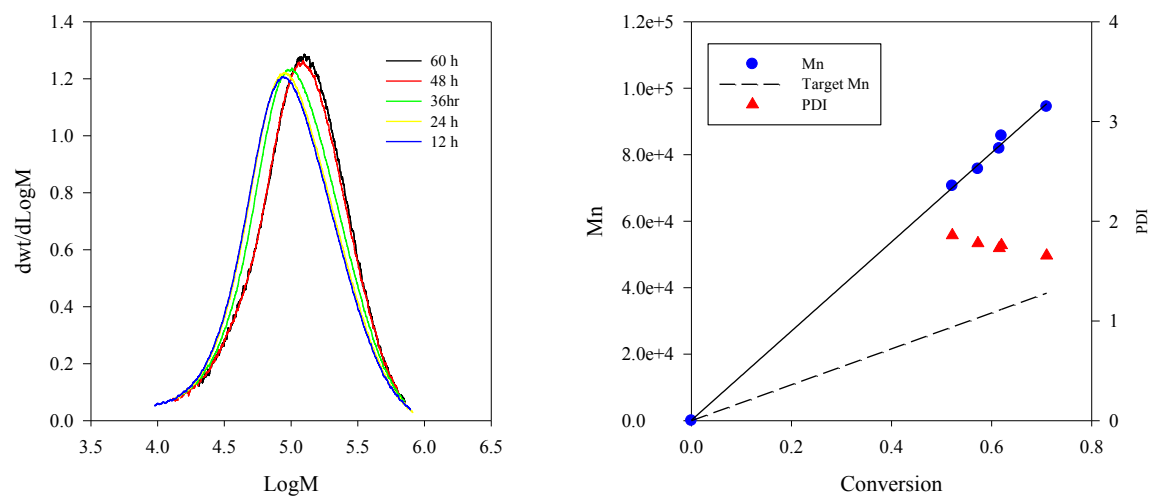


**Figure B2. Molecular weight distribution (MWD), Mn and PDI profiles for miniemulsion ROMP.**